

Anion transport and binding properties of *N,N'*-(phenylmethylene)dibenzamide based receptors

Harriet J. Clarke, Wim Van Rossom, Peter N. Horton, Mark E. Light and Philip A. Gale*

Chemistry, University of Southampton, Southampton SO17 1BJ, UK

Table of Contents

1.0 General Remarks	2
2.0 Synthesis	3
2.1 <i>N,N'</i> -(phenylmethylene)dibenzamide (1).....	3
2.2 <i>N,N'</i> -(phenylmethylene)bis(4-nitrobenzamide) (2)	3
2.3 <i>N,N'</i> -((4-(trifluoromethyl)phenyl)methylene)bis(4-nitrobenzamide) (3)	3
2.4 <i>N,N'</i> -((3,5-bis(trifluoromethyl)phenyl)methylene)bis(4-nitrobenzamide) (4)	4
2.5 <i>N,N'</i> -(phenylmethylene)bis(3,5-bis(trifluoromethyl)benzamide) (5)	4
2.6 <i>N,N'</i> -((4-(trifluoromethyl)phenyl)methylene)bis(3,5-bis(trifluoromethyl)benzamide) (6)	4
2.7 <i>N,N'</i> -(phenylmethylene)bis(2,3,4,5,6-pentafluorobenzamide) (7).....	5
3.0 NMR Spectra DMSO- <i>d</i> ₆	6
4.0 HRMS	13
5.0 Single Crystal Xray Diffraction-.....	17
6.0 Transport Assays.....	19
6.1 Vesicle Preparation	19
6.2 Cl ⁻ /NO ₃ ⁻ Assay	19
6.3 Hill Plots	19
6.4 Cl ⁻ /HCO ₃ ⁻ Assay	21
6.5 Cholesterol assay	22
6.6 M ⁺ /Cl ⁻ Symport assay	23
6.7 U-tube Test.....	23
6.8 Electrode calibration and conversion of raw data	24
7.0 Proton NMR titrations.....	25
7.1 Titrations in DMSO- <i>d</i> ₆ /0.5% H ₂ O	25
7.2 Titrations in 59.75% MeCN- <i>d</i> ₃ / 39.75% DMSO- <i>d</i> ₆ /0.5% H ₂ O	36
8.0 NMR dilution studies.....	47
9.0 References.....	51

1.0 General Remarks

All solvents and starting materials were purchased from commercially available suppliers and were used without further purification unless stated otherwise.

Melting point analyses were carried out using a Barnstead Electrothermal IA9100 melting point machine. ^1H NMR (400 MHz), ^{13}C { ^1H } NMR (101 MHz) spectra were determined on a Bruker AVII400 spectrometer. Chemical shifts (δ) were reported in parts per million (ppm) and calibrated using the residual solvent peak for DMSO- d_6 δ =2.50 ppm for ^1H NMR and δ =39.51 ppm for ^{13}C NMR. Spin multiplicities were abbreviated as follows s=singlet, d=doublet, t=triplet, q=quartet, m=multiplet and br=broad.

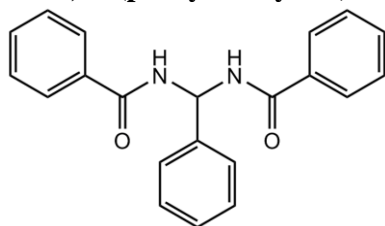
HRMS samples were analysed using a MaXis (Bruker Daltonics, Bremen, Germany) mass spectrometer equipped with a Time of Flight (TOF) analyser. Samples were introduced to the mass spectrometer via a Dionex Ultimate 3000 autosampler and uHPLC pump. Gradient 20% acetonitrile (0.2% formic acid) to 100% acetonitrile (0.2% formic acid) in five minutes at 0.6 mL min. Column, Acquity UPLC BEH C18 (Waters) 1.7 micron 50 x 2.1mm. High resolution mass spectra were recorded using positive/negative ion electrospray ionisation.

X-ray data was collected on a Rigaku AFC 12 diffractometer mounted on Rigaku FR-E+ Super Bright High Flux rotating anode CCD diffractometer equipped with VariMax high flux (HF) optics and Saturn 724+ CCD detector.¹

During transport assays the chloride concentration was measured using an Accumet chloride-selective electrode. Vesicles were made of POPC lipid (1-palmitoyl-2-oleoyl-sn-glycero-3-phosphocholine) stored as 1 g in 35 mL chloroform at -20°C.

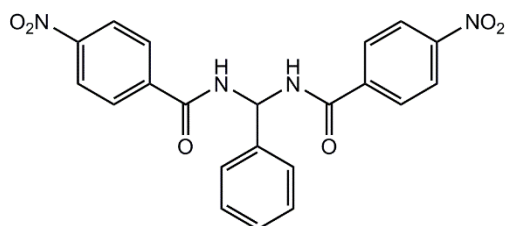
2.0 Synthesis

2.1 N,N'-(phenylmethylene)dibenzamide (1)



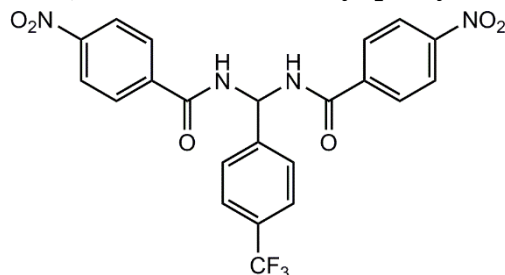
*General procedure adapted from the literature*²- Benzamide (476 mg, 3.9 mmol) and benzaldehyde (203 μ L, 2 mmol) were dissolved in dry DMF (8 mL). TMSCl (507 μ L, 4 mmol) was added as a catalyst and was stirred at 50 °C for 18 hours under nitrogen. A white precipitate was formed with the addition of a few drops of water and was purified by stirring with diethyl ether for 30 min. The product was isolated using vacuum filtration. Yield 31%; m.p. 218.0-220.0°C. ¹H NMR (400 MHz, DMSO-*d*₆) δ ppm 9.05 (d, *J*=7.80 Hz, 2 H), 7.89 - 7.96 (m, 4 H), 7.53 - 7.62 (m, 2 H), 7.47 - 7.51 (m, 6 H), 7.40 (t, *J*=7.40 Hz, 2 H), 7.32 (t, *J*=7.40 Hz, 1 H), 7.05 (t, *J*=7.80 Hz, 1 H). ¹³C NMR (101 MHz, DMSO-*d*₆) δ ppm 166.0 (CO), 140.8 (ArC), 134.3 (ArC), 132.0 (ArCH), 128.8 (ArCH), 128.8 (ArCH), 128.1 (ArCH), 128.0 (ArCH), 127.0 (ArCH), 59.2 (CH). LR-MS ESI⁺ (*m/z*): 353 [M+Na⁺]. HR-MS ESI⁺ (*m/z*): Calc. C₂₁H₁₈N₂NaO₂ 353.1260 [M+Na⁺]. Meas. 353.1255 [M+Na⁺]. Diff. (ppm) 0.0005.

2.2 N,N'-(phenylmethylene)bis(4-nitrobenzamide) (2)



Using the *general procedure* with 4- nitrobenzamide (662 mg, 3.9 mmol), benzaldehyde (203 μ L, 2 mmol) and TMSCl (507 μ L, 4 mmol). Yield 44%; m.p. 253.1-254.4 °C. ¹H NMR (400 MHz, DMSO-*d*₆) δ ppm 9.53 (d, *J*=7.21 Hz, 2 H), 8.33 (d, *J*=8.68 Hz, 4 H), 8.16 (d, *J*=8.68 Hz, 4 H), 7.52 (d, *J*=7.36 Hz, 2 H), 7.42 (t, *J*=7.38 Hz, 2 H), 7.36-7.37 (m, 1 H), 7.00 (t, *J*=7.27 Hz, 1 H). ¹³C NMR (101 MHz, DMSO-*d*₆) δ ppm 164.8 (CO), 149.7 (ArC), 140.0 (ArC), 139.6 (ArC), 129.7 (ArCH), 128.8 (ArCH), 128.4 (ArCH), 127.3 (ArCH), 123.9 (ArCH), 59.9 (CH). LR-MS ESI⁺ (*m/z*): 421 [M+H⁺]. HR-MS ESI⁺ (*m/z*): Calc. C₂₁H₁₆N₄NaO₆ 443.0962 [M+Na⁺]. Meas. 443.0969 [M+Na⁺]. Diff. (ppm) 0.0007.

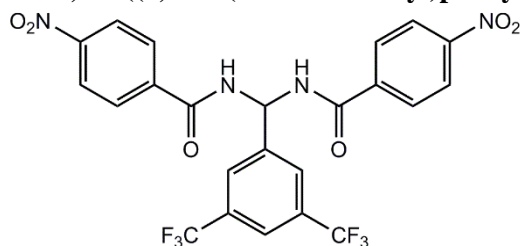
2.3 N,N'-((4-(trifluoromethyl)phenyl)methylene)bis(4-nitrobenzamide) (3)



Using the *general procedure* with 4-nitrobenzamide (340 mg, 2 mmol), 4 (trifluoromethyl)benzaldehyde (85 μ L, 0.5 mmol) and TMSCl (200 μ L, 1 mmol). Yield 42%; m.p. 280.0-281.9 °C. ¹H NMR (400 MHz, DMSO-*d*₆) δ ppm 9.61 (d, *J*=7.09 Hz, 2 H), 8.35 (d, *J*=8.86 Hz, 4 H), 8.17 (d, *J*=8.86 Hz, 4 H), 7.79 (d, *J*=8.36 Hz, 2 H), 7.74 (d, *J*=8.36 Hz, 2 H), 7.04 (t, *J*=7.09 Hz, 1 H). ¹³C NMR (101 MHz, DMSO-*d*₆) δ ppm 165.0 (CO), 149.7 (ArC), 144.1 (ArC), 139.8 (ArC), 129.7 (ArCH), 129.1 (q, CF₃), 128.2 (ArCH), 125.7 (ArC), 123.9 (ArCH), 123.3 (ArCH), 59.7 (CH).

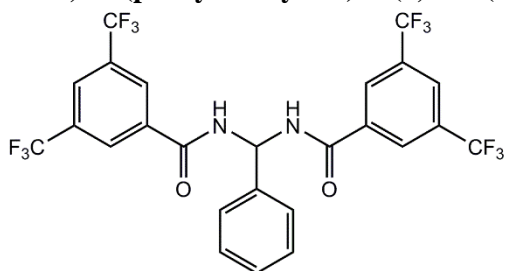
LR-MS ESI⁺ (*m/z*): 489 [M+H⁺]. HR-MS ESI⁺-(*m/z*): Calc. C₂₂H₁₅F₃N₄NaO₆ 511.0836 [M+Na⁺]. Meas. 511.0845 [M+Na⁺]. Diff. (ppm) 0.0009.

2.4 N, N'-((3,5-bis(trifluoromethyl)phenyl)methylene)bis(4-nitrobenzamide) (4)



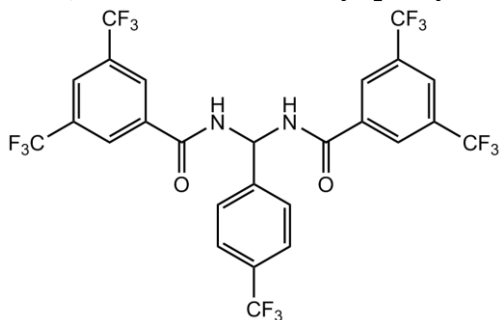
Using the *general procedure* with 4-nitrobenzamide (1.008 g, 6 mmol), 3,5-bis(trifluoromethyl)benzaldehyde (500 μ L, 3 mmol) and TMSCl (770 μ L, 6 mmol) in 10 mL DMF. Yield 81 %; m.p. 283.2-285.1 °C. ¹H NMR (400 MHz, DMSO-*d*₆) δ ppm 9.68 (br d, *J*=6.85 Hz, 2 H), 8.35 (br d, *J*=8.56 Hz, 4 H), 8.26 (s, 2 H), 8.15 (br d, *J*=8.44 Hz, 5 H)^a, 7.09 (br t, *J*=6.66 Hz, 1 H). ¹³C NMR (101 MHz, DMSO-*d*₆) δ ppm 165.2 (CO), 149.8 (ArC), 142.8 (ArC), 139.6 (ArC), 130.8 (q, CF₃), 129.7 (ArCH), 128.6 (ArC), 124.0 (ArCH), 122.6 (ArCH), 122.4 (ArCH), 59.7 (CH). LR-MS ESI⁺ (*m/z*): 555[M+H⁺]. HR-MS ESI⁺-(*m/z*): Calc. C₂₃H₁₄F₆N₄NaO₆ 579.0710 [M+Na⁺]. Meas. 579.0715 [M+Na⁺]. Diff. (ppm) 0.0005.^a two overlapping signals singlet overlapping a doublet.

2.5 N, N'-(phenylmethylene)bis(3,5-bis(trifluoromethyl)benzamide) (5)



Using the *general procedure* with 3,5-bis(trifluoromethyl)benzamide (600 mg, 2.3 mmol), benzaldehyde (138 μ L, 1.2 mmol) and TMSCl (296 μ L, 2.3 mmol) in 10 mL DMF. Recrystallized from EtOAc to give white powder product. Yield 66 %; m.p. 257.1-259 °C. ¹H NMR (400 MHz, DMSO-*d*₆) δ ppm 9.73 (d, *J*=7.12 Hz, 2 H), 8.60 (s, 4 H), 8.35 (s, 2 H), 7.56 (d, *J*=7.34 Hz, 2 H), 7.44 (t, *J*=7.34 Hz, 2H) 7.36 - 7.40 (m, 1 H), 7.06 (t, *J*=6.97 Hz, 1 H). ¹³C NMR (101 MHz, DMSO-*d*₆) δ ppm 163.6 (CO), 139.1 (ArC), 136.4 (ArC), 130.9 (q, CF₃), 129.0 (br s, ArC), 128.6 (ArCH), 127.4 (ArCH), 125.6 (br s, ArCH), 124.9 (ArCH), 122.2 (ArCH), 60.3 (CH). LR-MS ESI⁺ (*m/z*): 602 [M+H⁺]. HR-MS ESI⁺-(*m/z*): Calc. C₂₅H₁₅F₁₂N₂O₂ 603.0936 [M+H⁺]. Meas. 603.927 [M+H⁺]. Diff. (ppm) 0.0009.

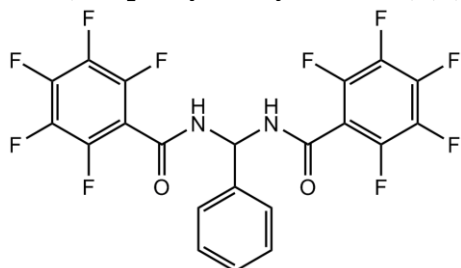
2.6 N,N'-((4-(trifluoromethyl)phenyl)methylene)bis(3,5-bis(trifluoromethyl)benzamide) (6)



Using the *general procedure* with 3,5-bis(trifluoromethyl)benzamide (1.03 mg, 4 mmol), 4-(trifluoromethyl) benzaldehyde (272 μ L, 2 mmol) and TMSCl (507 μ L, 4 mmol). Yield 8 %; m.p. 269.0-270.0 °C. ¹H NMR (400 MHz, DMSO-*d*₆) δ ppm 9.82 (d, *J*=6.96 Hz, 2 H), 8.60 (s, 4 H), 8.39 (s, 2 H), 7.77 - 7.86 (m, 4 H), 7.09 (t, *J*=6.86 Hz, 1 H). ¹³C NMR (101 MHz, DMSO-*d*₆) δ ppm 163.7 (CO),

143.7 (ArC), 136.2 (ArC), 130.9 (q, CF₃), 129.0 (br s, ArC), 128.4 (ArCH), 127.6 (ArC), 125.8 (m, CF₃), 124.9 (ArCH), 122.2 (ArCH), 119.5 (ArCH), 60.0 (CH). LR-MS ESI⁻ (*m/z*): 669 [M-H⁺]. HR-MS ESI⁺-(*m/z*): Calc. C₂₆H₁₄N₂O₂F₁₅ 671.0810 [M+H⁺]. Meas. 671.0806 [M+H⁺]. Diff. (ppm) 0.0004.

2.7 N,N'-(phenylmethylene)bis(2,3,4,5,6-pentafluorobenzamide) (7)



2,3,4,5,6-Pentafluorobenzamide (842 mg, 4 mmol) and benzaldehyde (203 μ L, 2 mmol) were dissolved in dry toluene (5 mL). ZnCl₂ (~5 mg) was added as a catalyst and was refluxed for 24 hours under nitrogen. A white precipitate was formed over time and the product was isolated using hot vacuum filtration washing with diethyl ether. Yield 20 %; m.p. 253.0-256.0 °C. ¹H NMR (400 MHz, DMSO-*d*₆) δ ppm 9.95 (d, *J*=7.96 Hz, 2 H), 7.46 - 7.48 (m, 4 H), 7.38 - 7.42 (m, 1 H), 6.90 (t, *J*=7.94 Hz, 1 H). ¹³C NMR (101 MHz, DMSO-*d*₆) δ ppm 156.7 (CO), 144.9 (ArC), 142.5 (ArC), 140.5 (ArC) 138.6 (ArC), 138.2 (ArC), 136.2 (ArC), 129.1 (ArCH), 128.9 (ArCH), 126.7 (ArCH), 112.5 (ArC), 58.6 (CH) LR-MS ESI⁻ (*m/z*): 553 [M+Na⁺]. HR-MS ESI⁺-(*m/z*): Calc C₂₁H₉O₂N₂F₁₀ 511.0499 [M+H⁺]. Meas 511.0511 [M+H⁺], Calc. C₂₁H₈O₂N₂NaF₁₀ 533.0318 [M+Na⁺]. Meas. 533.0330 [M+Na⁺]. Diff. (ppm) 0.0012.

3.0 NMR Spectra DMSO-*d*₆

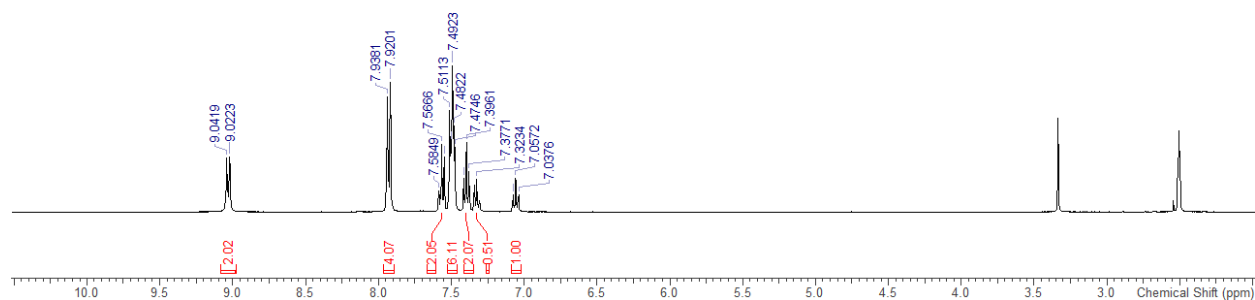


Figure S3.1- ¹H NMR spectrum receptor 1.

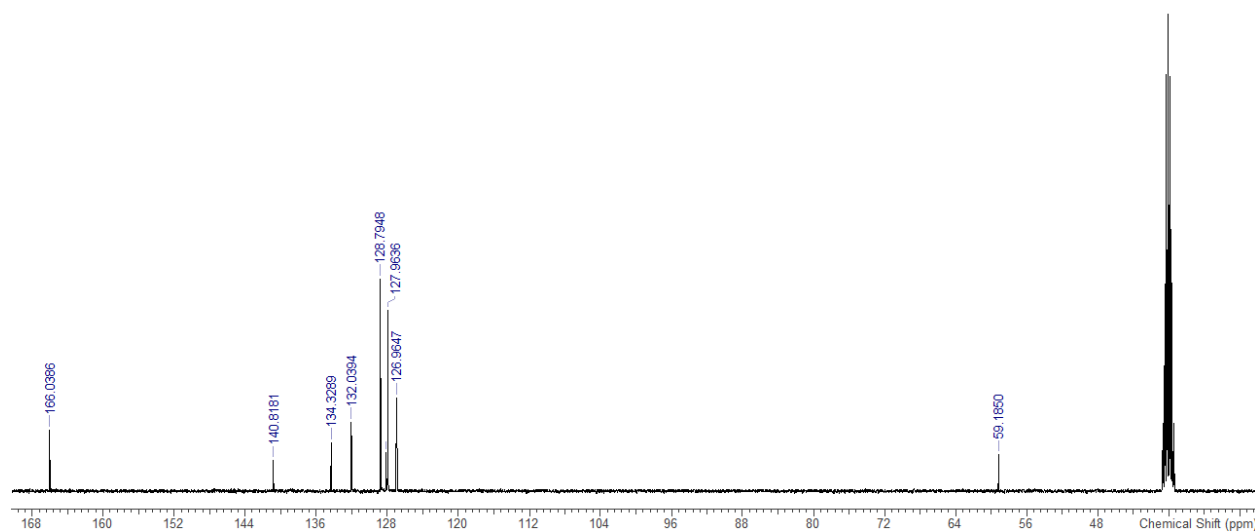


Figure S3.2- ¹³C NMR spectrum receptor 1.

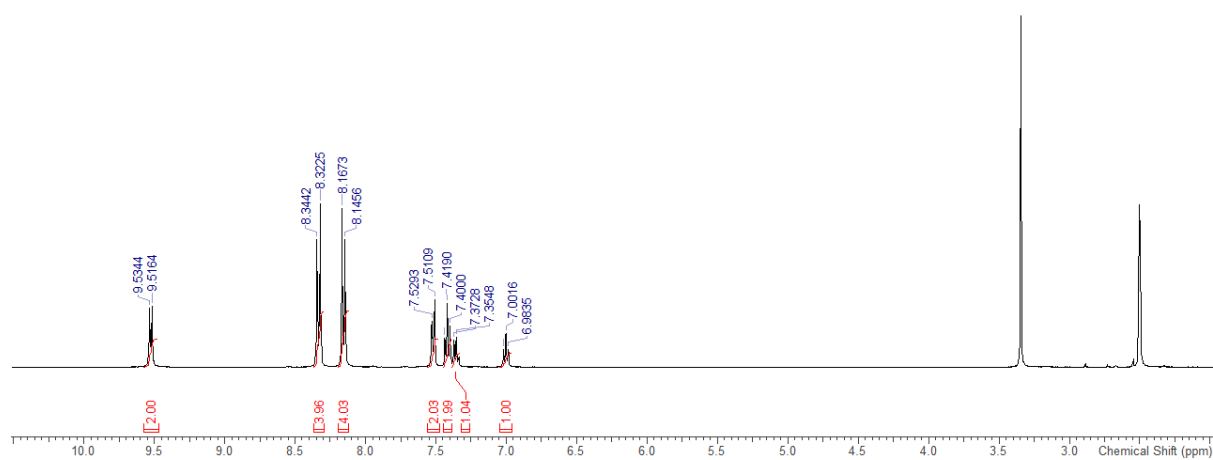


Figure S3.3- ¹H NMR spectrum receptor **2**.

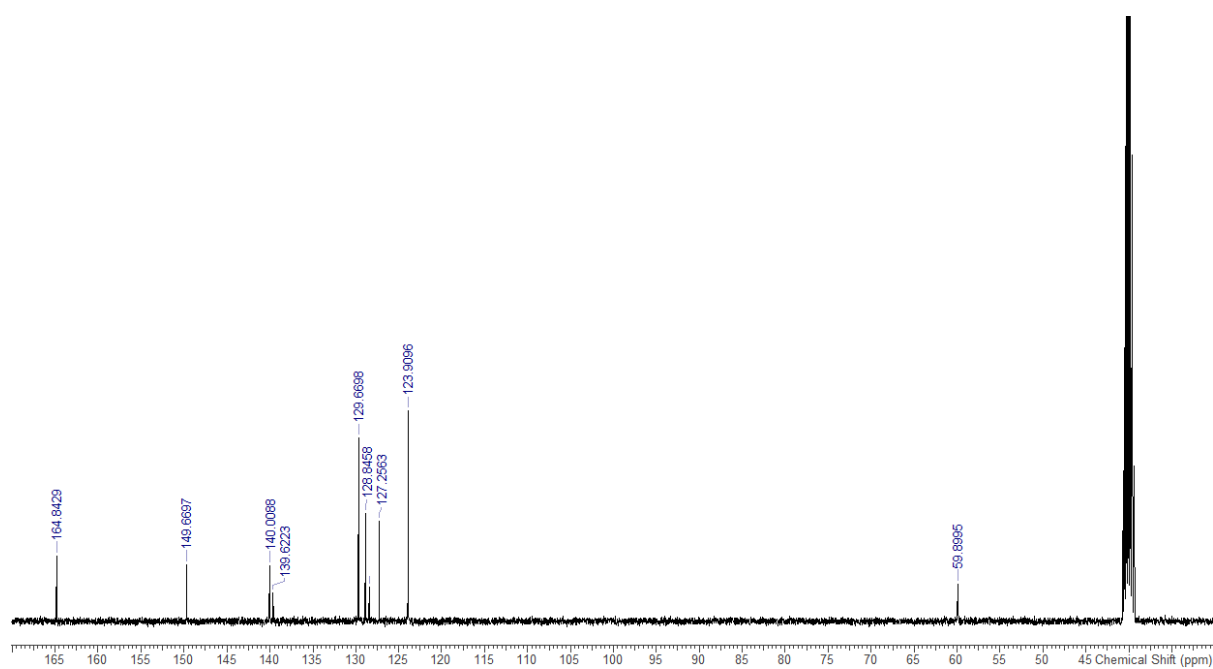


Figure S3.4- ¹³C NMR spectrum receptor **2**.

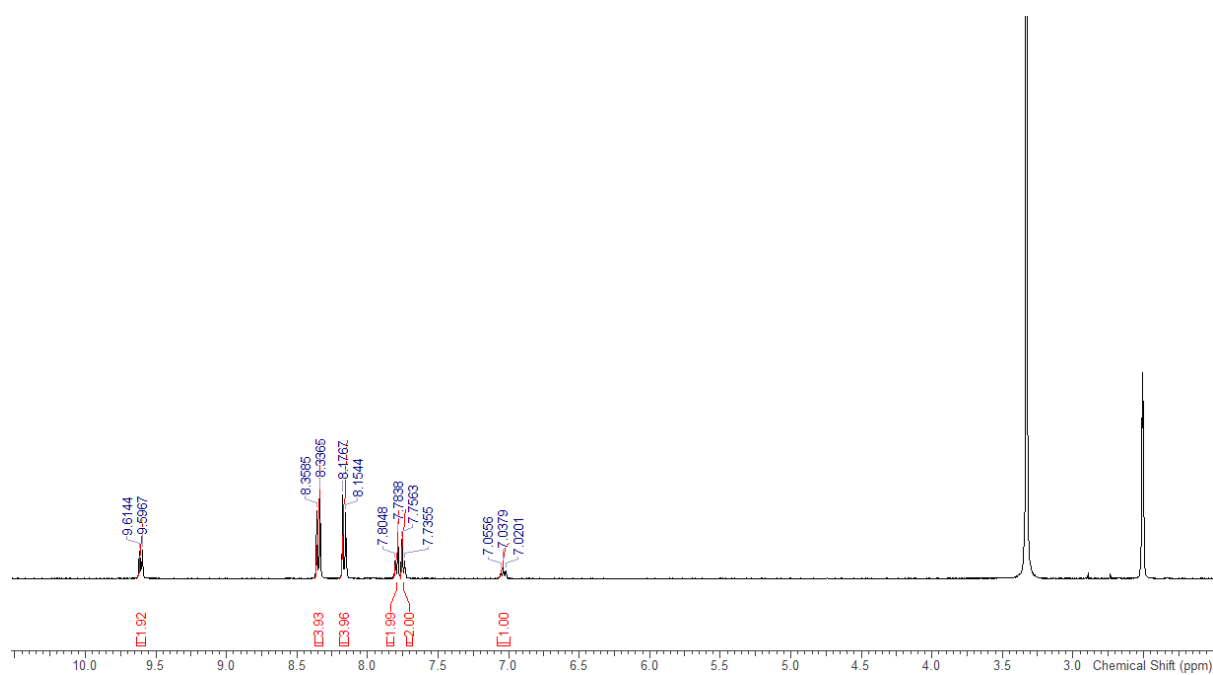


Figure S3.5- ¹H NMR spectrum receptor **3**.

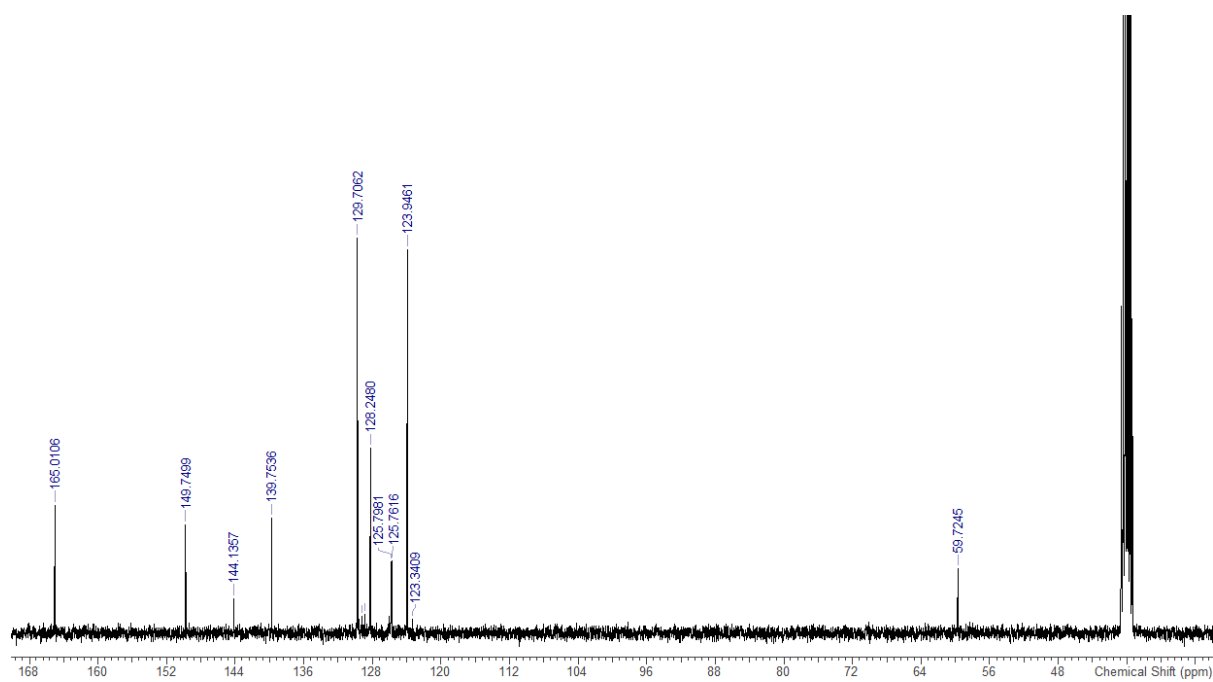


Figure S3.6- ¹³C NMR spectrum receptor **3**.

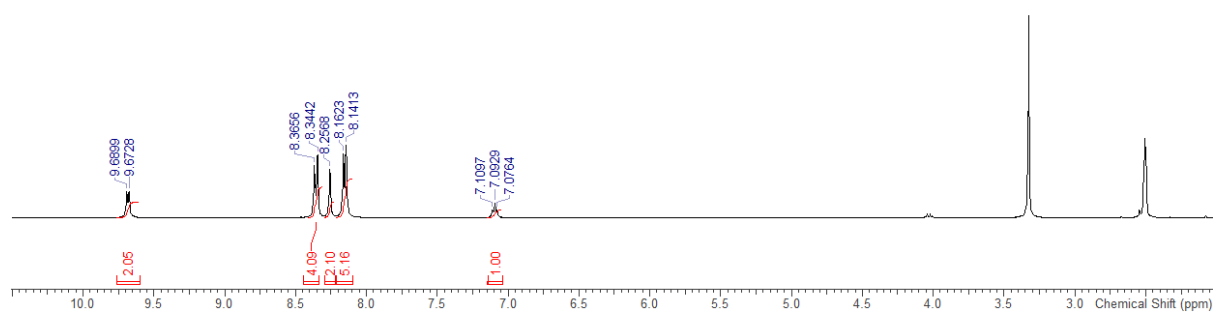


Figure S3.7- ¹H NMR spectrum receptor 4.

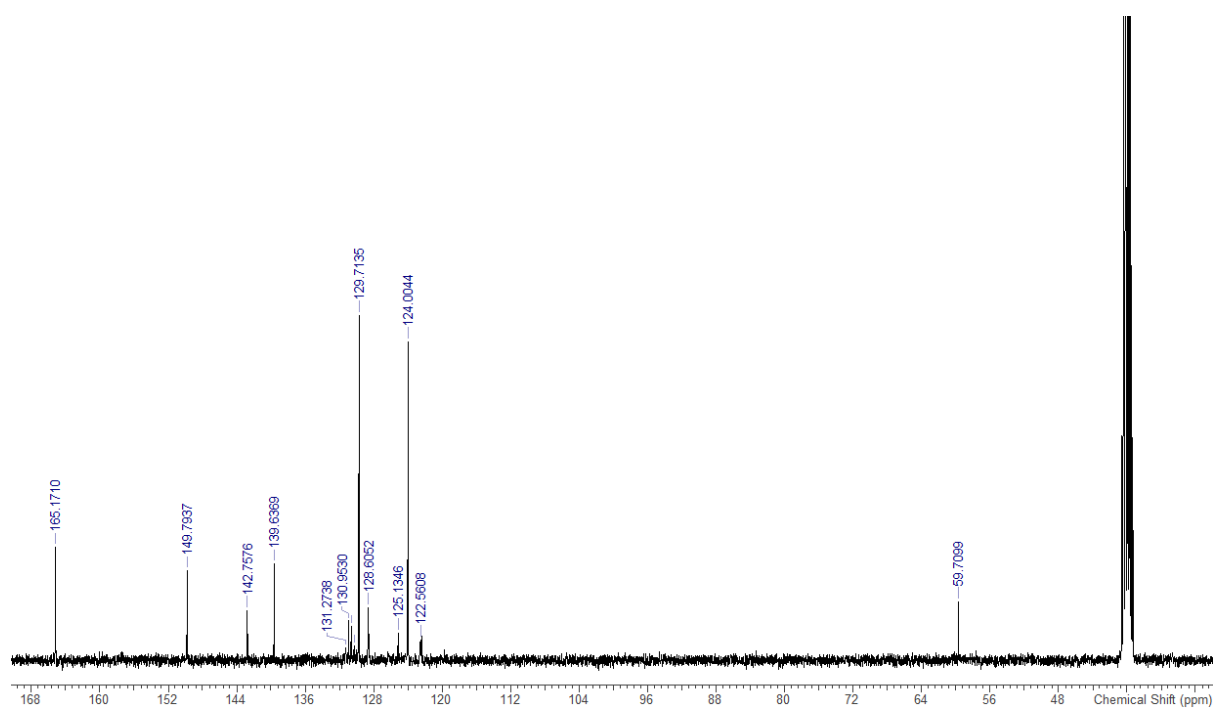


Figure S3.8- ¹³C NMR spectrum receptor 4.

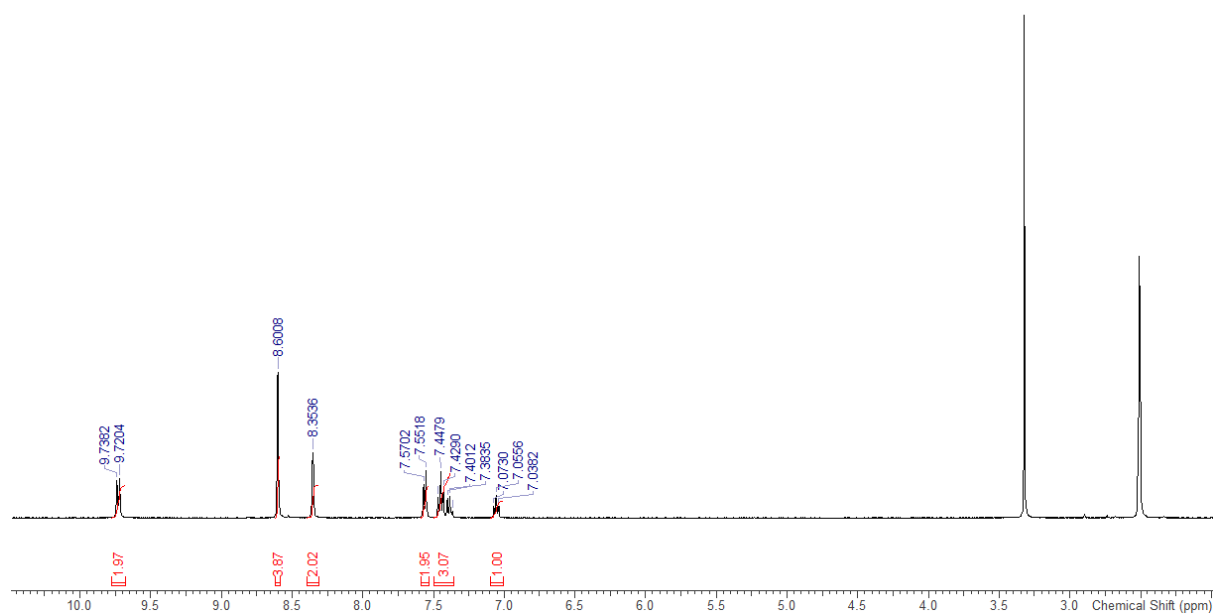


Figure S3.9- ¹H NMR spectrum receptor **5**.

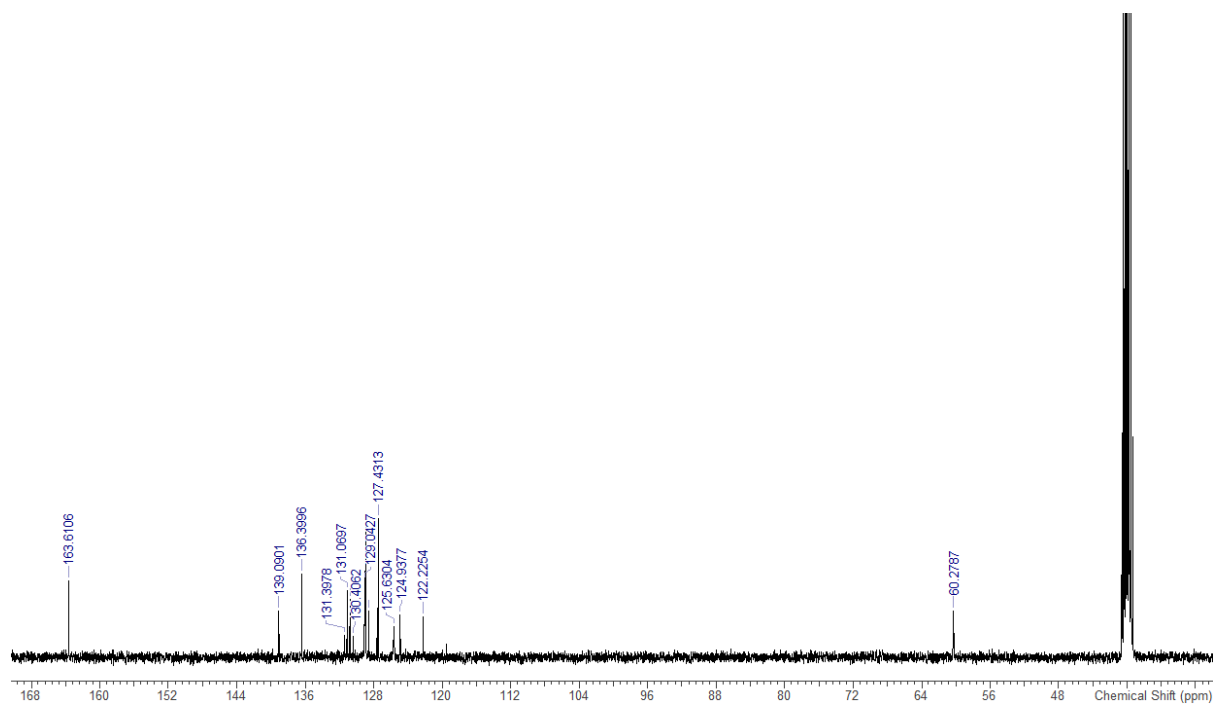


Figure S3.10- ¹³C NMR spectrum receptor **5**.

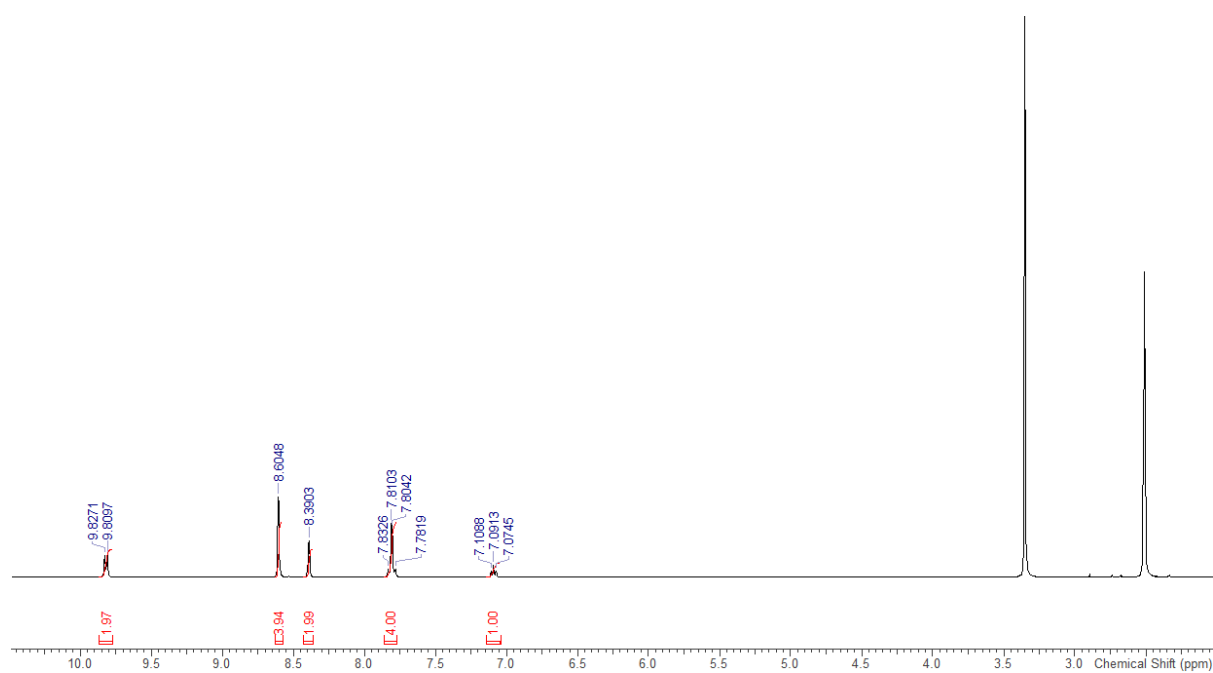


Figure S3.11- ¹H NMR spectrum receptor **6**.

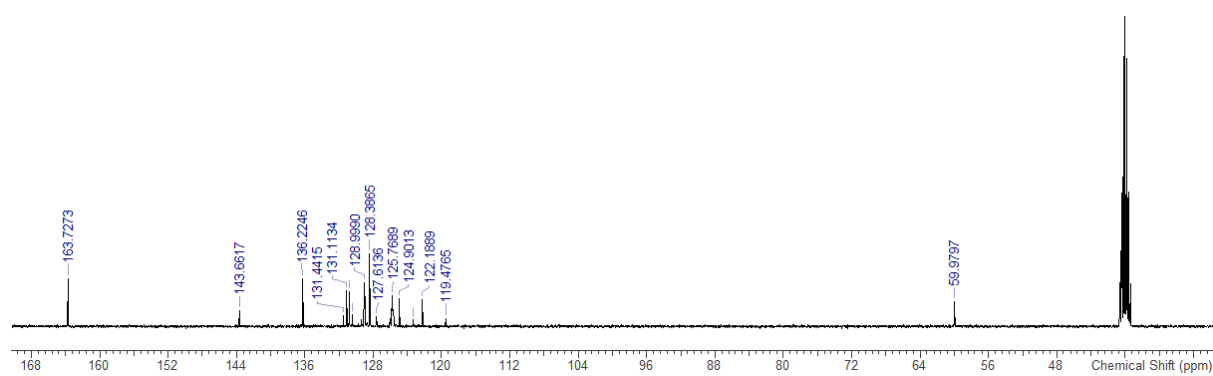


Figure S3.12- ¹³C NMR spectrum receptor **6**.

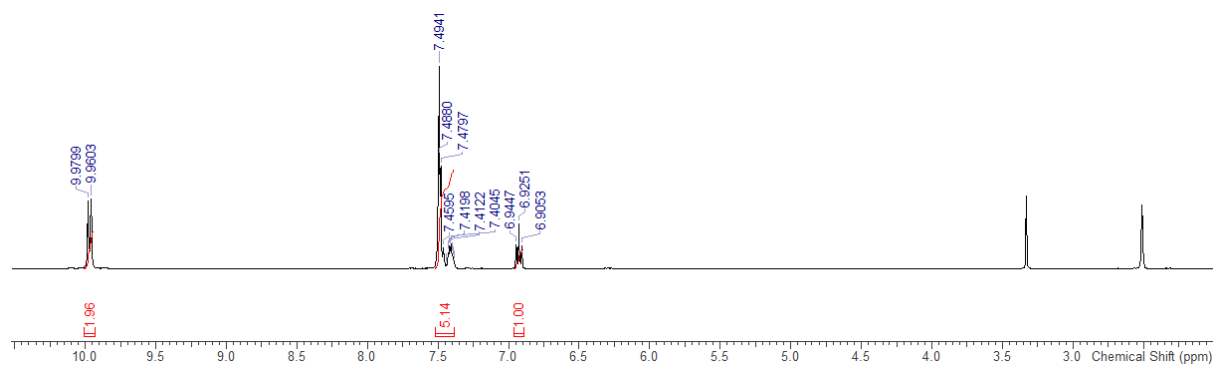


Figure S3.13- ¹H NMR spectrum receptor **7**.

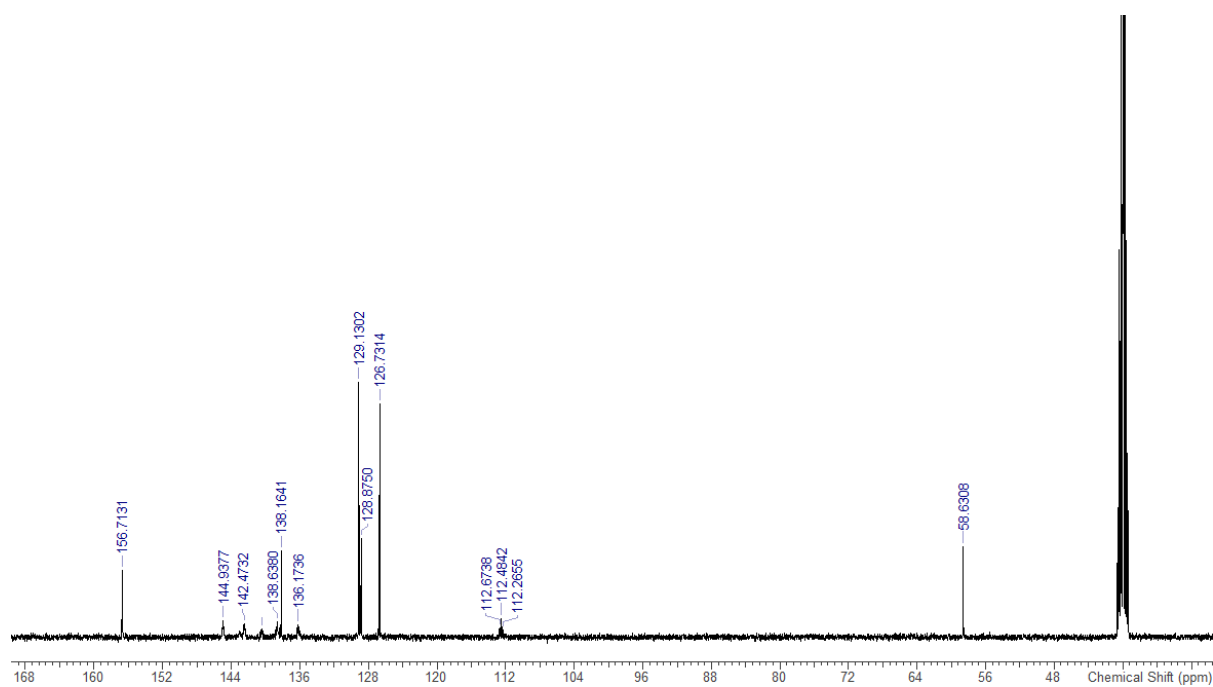


Figure S3.14- ¹³C NMR spectrum receptor **7**.

4.0 HRMS

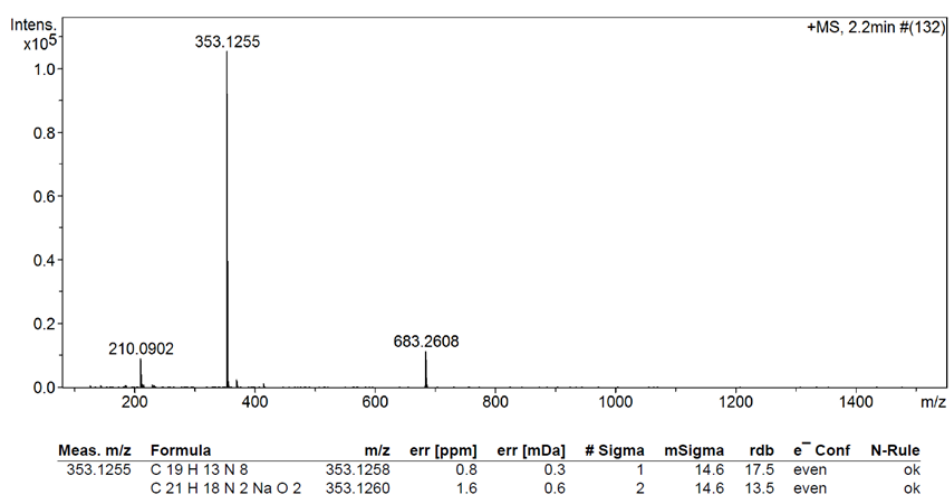


Figure S4.1- HRMS for receptor 1.

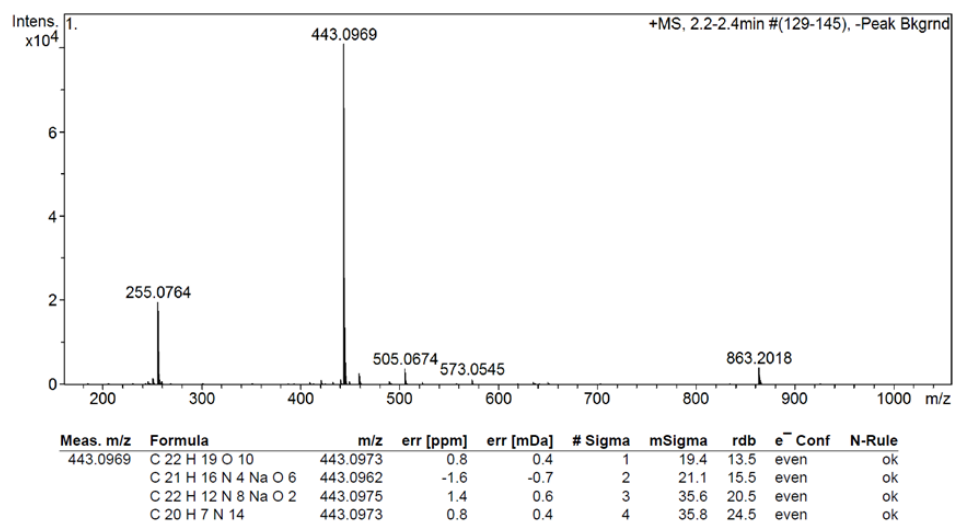


Figure S4.2- HRMS for receptor 2.

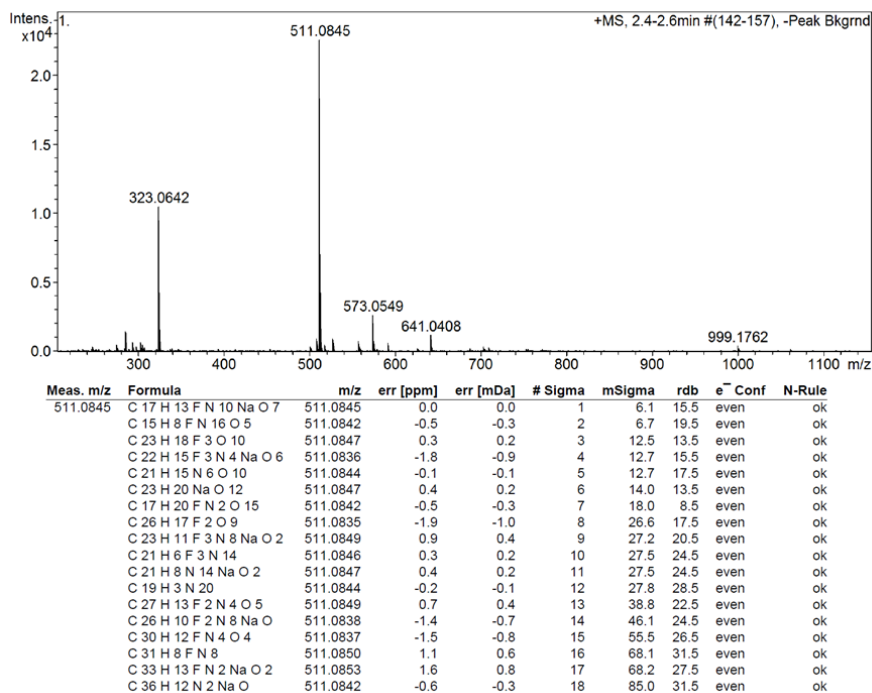


Figure S4.3- HRMS for receptor 3.

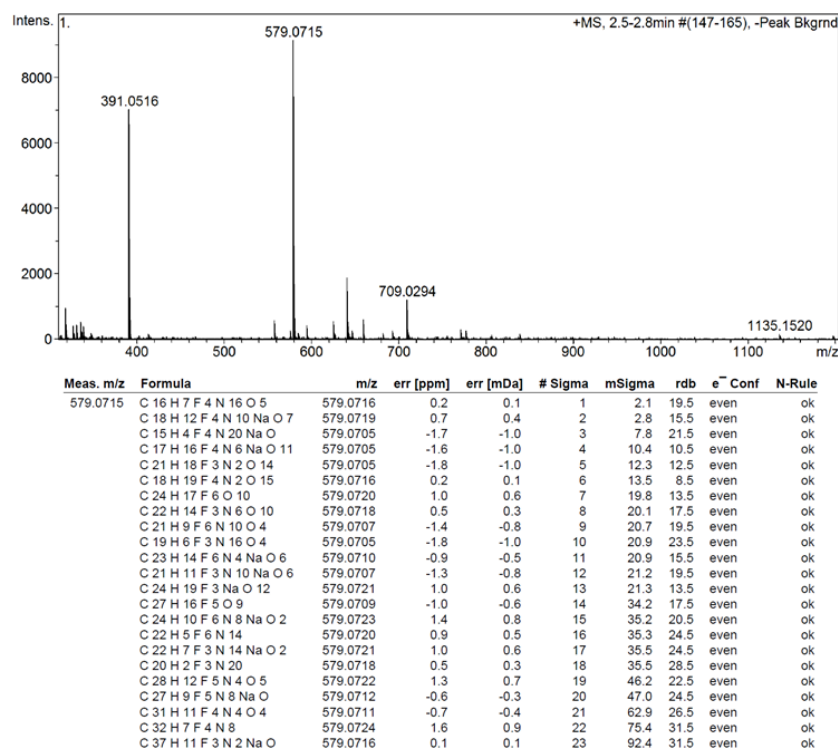


Figure S4.4- HRMS for receptor 4.

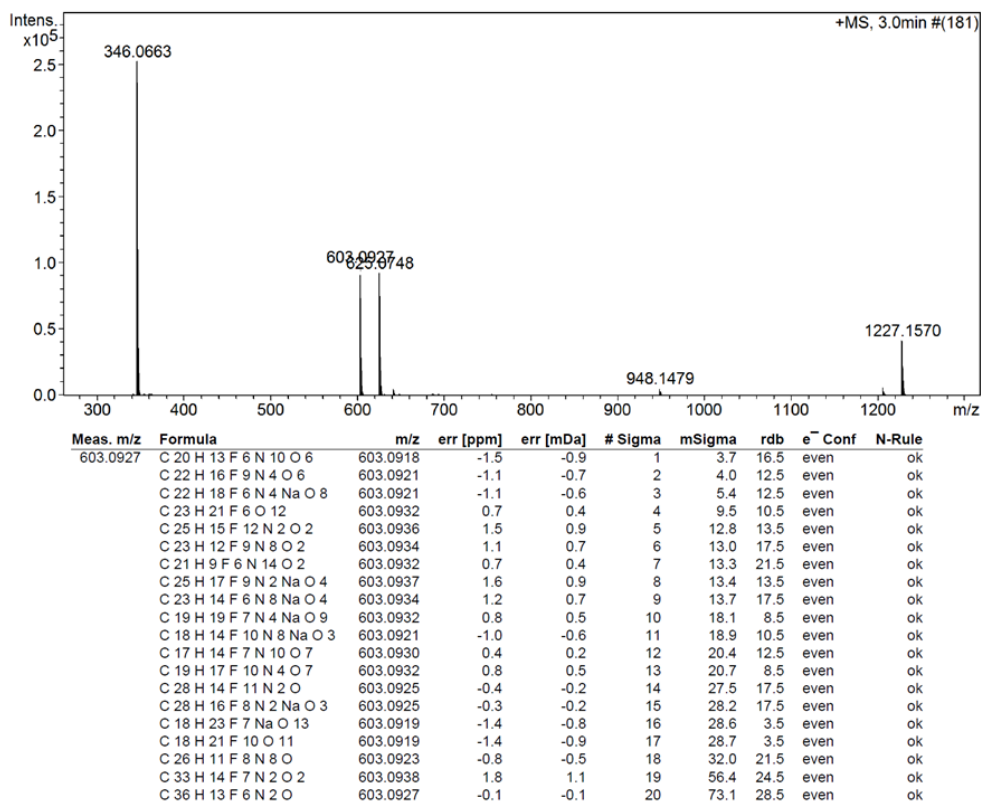


Figure S4.5- HRMS for receptor 5.

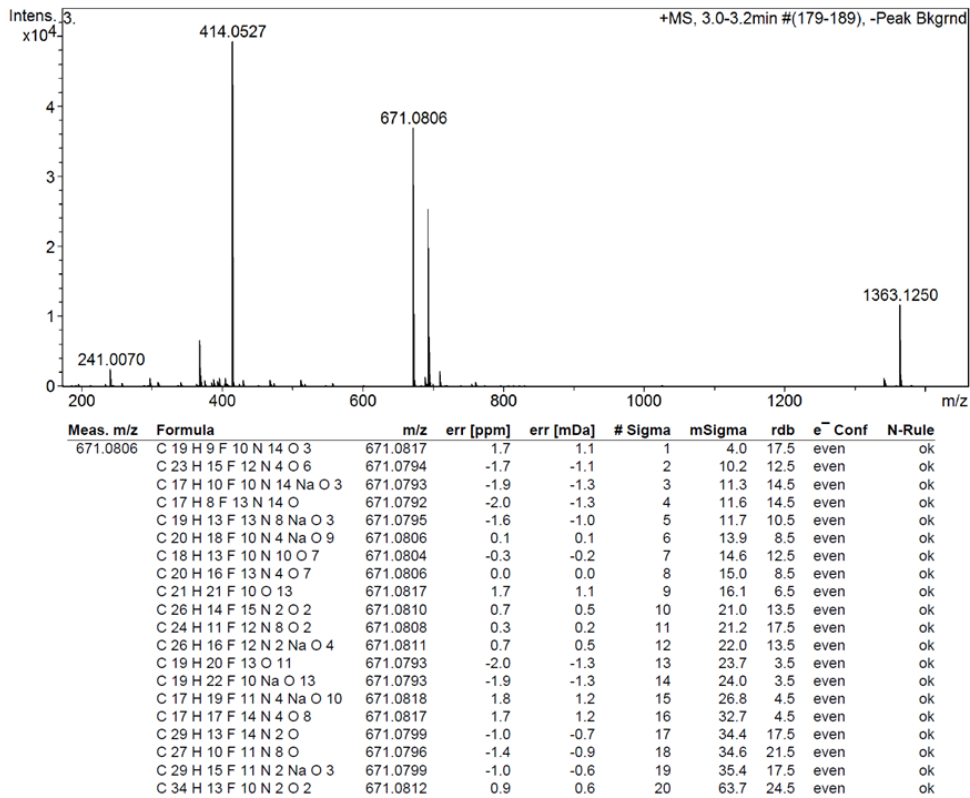
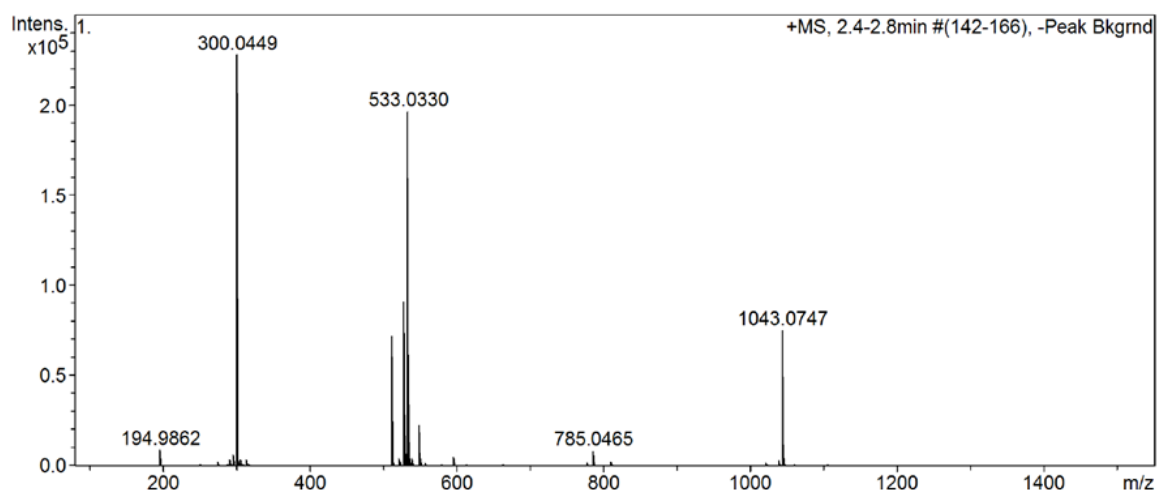


Figure S4.6- HRMS for receptor 6.



Meas. m/z	Formula	m/z	err [ppm]	err [mDa]	# Sigma	mSigma	rdb	e ⁻ Conf	N-Rule
511.0511	C ₁₄ H ₄ F ₅ N ₁₄ O ₃	511.0505	-1.2	-0.6	1	2.8	17.5	even	ok
	C ₁₆ H ₇ F ₈ N ₈ O ₃	511.0508	-0.7	-0.4	2	3.1	13.5	even	ok
	C ₁₆ H ₉ F ₅ N ₈ NaO ₅	511.0508	-0.6	-0.3	3	3.9	13.5	even	ok
	C ₁₈ H ₁₂ F ₈ N ₂ NaO ₅	511.0511	-0.1	-0.1	4	4.2	9.5	even	ok
	C ₁₇ H ₁₂ F ₅ N ₄ O ₉	511.0519	1.5	0.8	5	8.7	11.5	even	ok
	C ₁₉ H ₈ F ₈ N ₆ NaO	511.0524	2.5	1.3	6	11.4	14.5	even	ok
	C ₁₇ H ₅ F ₅ N ₁₂ NaO	511.0522	2.0	1.0	7	11.7	18.5	even	ok
	C ₂₁ H ₉ F ₁₀ N ₂ O ₂	511.0499	-2.5	-1.3	8	15.6	13.5	even	ok
	C ₁₉ H ₆ F ₇ N ₈ O ₂	511.0496	-2.9	-1.5	9	15.9	17.5	even	ok
	C ₂₁ H ₁₁ F ₇ N ₂ NaO ₄	511.0499	-2.4	-1.2	10	16.2	13.5	even	ok
	C ₁₆ H ₁₆ F ₅ O ₁₃	511.0506	-1.1	-0.6	11	17.2	6.5	even	ok
	C ₁₃ H ₁₀ F ₆ N ₈ NaO ₆	511.0520	1.6	0.8	12	21.8	9.5	even	ok
	C ₁₃ H ₈ F ₉ N ₈ O ₄	511.0519	1.6	0.8	13	21.9	9.5	even	ok
	C ₁₅ H ₁₃ F ₉ N ₂ NaO ₆	511.0522	2.1	1.1	14	22.1	5.5	even	ok
	C ₂₃ H ₁₀ F ₇ N ₂ O ₄	511.0523	2.3	1.2	15	29.0	16.5	even	ok
	C ₂₄ H ₁₀ F ₁₀ Na	511.0515	0.7	0.4	16	30.1	14.5	even	ok
	C ₂₂ H ₇ F ₇ N ₆ Na	511.0513	0.2	0.1	17	30.4	18.5	even	ok
	C ₁₃ H ₁₇ F ₆ O ₁₄	511.0517	1.1	0.6	18	31.8	2.5	even	ok
	C ₂₆ H ₉ F ₆ N ₂ O ₃	511.0512	0.1	0.0	19	48.1	20.5	even	ok
	C ₂₉ H ₈ F ₅ N ₂ O ₂	511.0500	-2.1	-1.1	20	58.4	24.5	even	ok
	C ₃₂ H ₉ F ₅ Na	511.0517	1.0	0.5	21	71.1	25.5	even	ok
533.0330	C ₁₄ H ₃ F ₅ N ₁₄ NaO ₃	533.0325	-0.9	-0.5	1	4.1	17.5	even	ok
	C ₁₆ H ₆ F ₈ N ₈ NaO ₃	533.0327	-0.5	-0.3	2	4.4	13.5	even	ok
	C ₁₄ H ₈ F ₈ N ₁₄ O	533.0325	-1.0	-0.5	3	4.9	17.5	even	ok
	C ₁₅ H ₆ F ₅ N ₁₀ O ₇	533.0336	1.1	0.6	4	8.3	15.5	even	ok
	C ₁₇ H ₉ F ₈ N ₄ O ₇	533.0338	1.5	0.8	5	8.6	11.5	even	ok
	C ₁₇ H ₁₁ F ₅ N ₄ NaO ₉	533.0338	1.6	0.9	6	10.3	11.5	even	ok
	C ₁₉ H ₃ F ₁₀ N ₈	533.0316	-2.7	-1.4	7	14.5	17.5	even	ok
	C ₂₁ H ₈ F ₁₀ N ₂ NaO ₂	533.0318	-2.2	-1.2	8	14.7	13.5	even	ok
	C ₂₀ H ₈ F ₇ N ₄ O ₆	533.0327	-0.6	-0.3	9	14.7	15.5	even	ok
	C ₁₉ H ₅ F ₇ N ₈ NaO ₂	533.0316	-2.6	-1.4	10	15.0	17.5	even	ok
	C ₁₆ H ₁₃ F ₈ O ₁₁	533.0325	-1.0	-0.5	11	17.9	6.5	even	ok
	C ₁₆ H ₁₅ F ₅ NaO ₁₃	533.0325	-0.9	-0.5	12	18.5	6.5	even	ok
	C ₁₅ H ₁₀ F ₈ N ₄ NaO ₇	533.0314	-3.0	-1.6	13	19.4	8.5	even	ok
	C ₁₄ H ₁₀ F ₅ N ₆ O ₁₁	533.0322	-1.4	-0.8	14	20.3	10.5	even	ok
	C ₁₃ H ₇ F ₉ N ₈ NaO ₄	533.0339	1.7	0.9	15	23.1	9.5	even	ok
	C ₂₃ H ₇ F ₁₀ N ₂ O ₂	533.0342	2.3	1.3	16	27.5	16.5	even	ok
	C ₂₁ H ₄ F ₇ N ₈ O ₂	533.0340	1.9	1.0	17	27.8	20.5	even	ok
	C ₂₃ H ₉ F ₇ N ₂ NaO ₄	533.0343	2.4	1.3	18	28.2	16.5	even	ok
	C ₁₃ H ₁₆ F ₆ NaO ₁₄	533.0336	1.2	0.7	19	33.0	2.5	even	ok
	C ₂₃ H ₇ F ₆ N ₄ O ₅	533.0315	-2.8	-1.5	20	33.0	19.5	even	ok
	C ₁₃ H ₁₄ F ₉ O ₁₂	533.0336	1.2	0.6	21	38.0	2.5	even	ok
	C ₂₆ H ₆ F ₉ N ₂ O	533.0331	0.2	0.1	22	46.4	20.5	even	ok
	C ₂₄ H ₃ F ₆ N ₈ O	533.0329	-0.2	-0.1	23	46.6	24.5	even	ok
	C ₂₆ H ₈ F ₆ N ₂ NaO ₃	533.0331	0.3	0.1	24	47.2	20.5	even	ok
	C ₂₉ H ₅ F ₈ N ₂	533.0320	-1.9	-1.0	25	57.1	24.5	even	ok
	C ₂₇ H ₂ F ₅ N ₈	533.0317	-2.4	-1.3	26	57.3	28.5	even	ok
	C ₂₉ H ₇ F ₅ N ₂ NaO ₂	533.0320	-1.9	-1.0	27	57.6	24.5	even	ok
	C ₃₁ H ₆ F ₅ N ₂ O ₂	533.0344	2.6	1.4	28	69.0	27.5	even	ok

Figure S4.7- HRMS for receptor 7.

5.0 Single Crystal Xray Diffraction-

Diffractometer: *Rigaku AFC12* goniometer equipped with an enhanced sensitivity (HG) *Saturn724+* detector mounted at the window of an *FR-E+ SuperBright* molybdenum rotating anode generator with *VHF Varimax* optics (70 μ m focus). **Cell determination and data collection:** *CrystalClear-SM Expert 3.1 b27* (Rigaku, 2013). **Data reduction, cell refinement and absorption correction:** *CrystalClear-SM Expert 3.1 b 27* (Rigaku, 2013). **Structure solution:** *SUPERFLIP* (Palatinus, L. & Chapuis, G. (2007). *J. Appl. Cryst.* 40, 786-790). **Structure refinement:** *SHELXL-2013* (Sheldrick, G.M. (2008). *Acta Cryst. A* 64, 112-122). **Graphics:** *ORTEP3 for Windows* (L. J. Farrugia, *J. Appl. Crystallogr.* 1997, 30, 565

Table S5.1. Crystal data and structure refinement for receptor **2** **CCDC-1053071**.

Empirical formula	$C_{21}H_{16}N_4O_6$	
Formula weight	420.38	
Temperature	100(2) K	
Wavelength	0.71075 Å	
Crystal system	Orthorhombic	
Space group	<i>Pnma</i>	
Unit cell dimensions	$a = 16.5475(11)$ Å	$\alpha = 90^\circ$
	$b = 22.8442(16)$ Å	$\beta = 90^\circ$
	$c = 4.9997(4)$ Å	$\gamma = 90^\circ$
Volume	1890.0(2) Å ³	
<i>Z</i>	4	
Density (calculated)	1.477 Mg / m ³	
Absorption coefficient	0.111 mm ⁻¹	
<i>F</i> (000)	872	
Crystal size	0.100 × 0.070 × 0.030 mm ³	
θ range for data collection	3.040 – 27.466°	
Index ranges	$-21 \leq h \leq 21, -28 \leq k \leq 29, -4 \leq l \leq 6$	
Reflections collected	10813	
Independent reflections	2216 [$R_{int} = 0.0355$]	
Data / restraints / parameters	2216 / 0 / 145	
Goodness-of-fit on F^2	1.026	
Final <i>R</i> indices [$F^2 > 2\sigma(F^2)$]	$R1 = 0.0365, wR2 = 0.0926$	
<i>R</i> indices (all data)	$R1 = 0.0463, wR2 = 0.0982$	

Diffraction: *Rigaku AFC12* goniometer equipped with an enhanced sensitivity (HG) *Saturn724+* detector mounted at the window of an *FR-E+ SuperBright* molybdenum rotating anode generator with *HF Varimax* optics (70 μ m focus). **Cell determination and data collection:** *CrystalClear-SM Expert 3.1 b27* (Rigaku, 2013). **Data reduction, cell refinement and absorption correction:** *CrysAlisPro*, Agilent Technologies, Version 1.171.37.35 **Structure solution:** *ShelXT* (2015) (Sheldrick, G.M. (2015). *Acta Cryst. A* 71, 3-8.) **Structure refinement:** *ShelXL* (2008) (Sheldrick, G.M. (2008). *Acta Cryst. A* 64, 112-122.) **Graphics:** The *PyMOL* Molecular Graphics System, Version 1.7.4 Schrödinger, LLC.

Table S5.2. Crystal data and structure refinement for receptor **6** **CCDC-1053070**.

Empirical formula	C ₂₆ H ₁₃ F ₁₅ N ₂ O ₂
Formula weight	670.38
Temperature/K	100(2)
Crystal system	orthorhombic
Space group	Pnma
a/Å	9.7085(2)
b/Å	26.9582(10)
c/Å	10.0203(2)
α /°	90
β /°	90
γ /°	90
Volume/Å ³	2622.53(12)
Z	4
ρ_{calc} /cm ³	1.698
μ /mm ⁻¹	0.181
F(000)	1336.0
Crystal size/mm ³	0.3 × 0.08 × 0.03
Radiation	MoK α (λ = 0.71073)
Θ range for data collection/°	4.336 to 63.986
Index ranges	-14 ≤ h ≤ 14, -26 ≤ k ≤ 39, -14 ≤ l ≤ 13
Reflections collected	16362
Independent reflections	4347 [R_{int} = 0.0253]
Data/restraints/parameters	4347/0/215
Goodness-of-fit on F ²	1.082
Final R indexes [$I \geq 2\sigma(I)$]	R_1 = 0.0483, wR_2 = 0.1294
Final R indexes [all data]	R_1 = 0.0581, wR_2 = 0.1431

6.0 Transport Assays

6.1 Vesicle Preparation

Unilamellar vesicles were prepared according to previous literature methods.³⁻⁵ Under reduced pressure, a lipid film of 1 palmitoyl-2-oleoyl-sn-glycero-3-phosphocholine (POPC) was formed from a chloroform solution. The film was dried under vacuum for 4+ hours. The lipid film was rehydrated using the corresponding metal chloride salt (generally 489 mM MCl, buffered to pH 7.2 using 5 mM sodium phosphate salts) in a vortex. The lipid suspension was subjected to 9 freeze thaw cycles and was left to age at room temperature for 30 min. The suspension was extruded 25 times through a 200 nm polycarbonate membrane, this results in unilamellar vesicles which were then dialysed in the corresponding external solution to remove any unencapsulated metal salts.

6.2 Cl⁻/NO₃⁻ Assay

POPC unilamellar vesicles containing NaCl (489 mM buffered to pH 7.2 using 5 mM sodium phosphate salts) were suspended in NaNO₃ (489 mM buffered to pH 7.2 using 5 mM sodium phosphate salts) to make a lipid concentration per sample of 1 mM. A DMSO solution of the receptor was added to commence the experiment, the chloride efflux was monitored using a chloride selective electrode. After 5 mins the vesicles were lysed using 50 μ L of polyoxyethylene (8) lauryl ether and after 7 mins a final chloride efflux reading was taken, this was used as 100 % chloride efflux and the rest of the readings were calibrated to this.

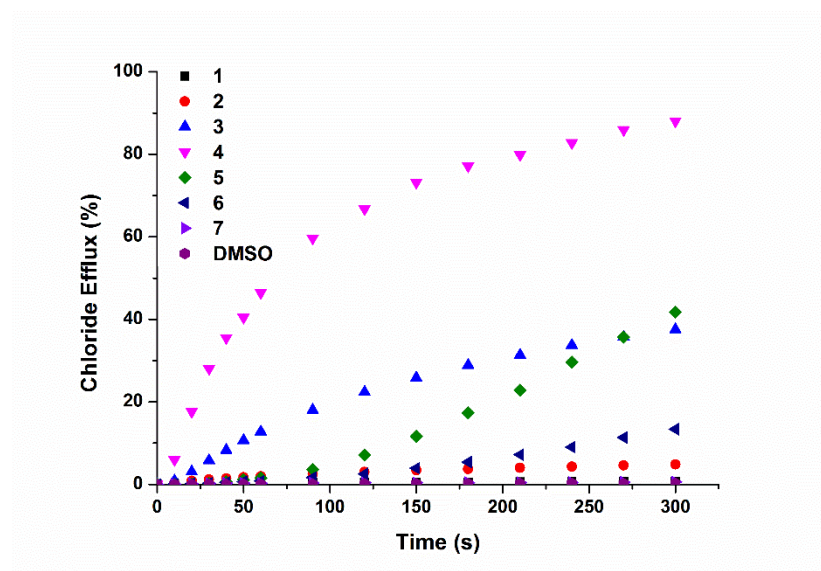


Figure S6.2.1- Chloride efflux facilitated by 1–7 at 2 mol% loading (with respect to lipid) from POPC vesicles containing 489 mM NaCl buffered to pH 7.2 with 5 mM sodium phosphate salts suspended in 489mM NaNO₃ buffered to pH 7.2 with sodium phosphate salts. To end the experiment detergent was added to lyse the vesicles and this final chloride efflux was used as 100 % to calibrate the ion selective electrode. Each point is an average of three runs.

6.3 Hill Plots

Cl⁻/NO₃⁻ assay was performed at varying concentrations of receptor. From this, the % chloride efflux at 270 s was plotted as a function of the receptors concentration, this data is then fitted to the Hill equation⁶ using origin 9.0.

$$y = V_{max} \frac{x^n}{k^n + x^n}$$

Where x = receptor concentration, y = % chloride efflux at 270 s, V_{max} = the maximum chloride efflux possible (fixed to 100%), n is the Hill coefficient and k is the receptor concentration needed to reach $\frac{V_{max}}{2}$ in this case $k = EC_{50}$.

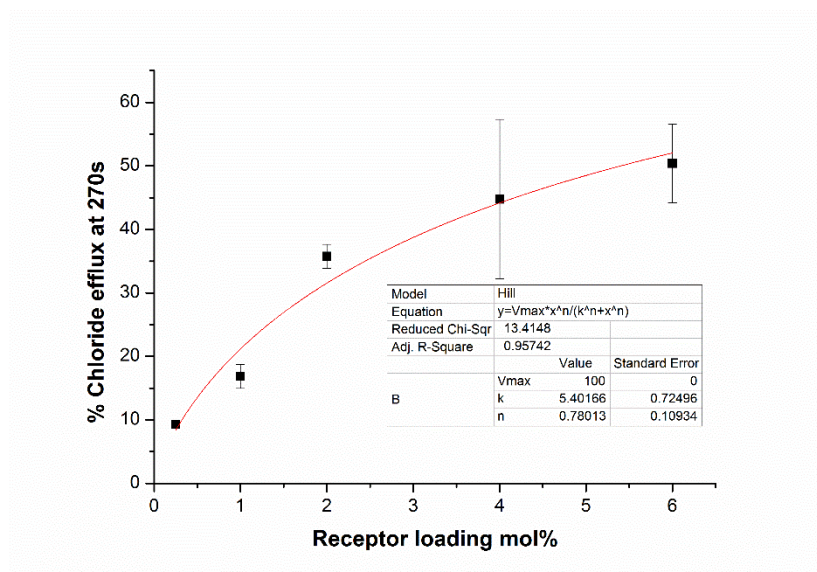


Figure S6.3.1- Hill plot for receptor **3**. $EC_{50}=5.40$ mol% $n=0.78$.

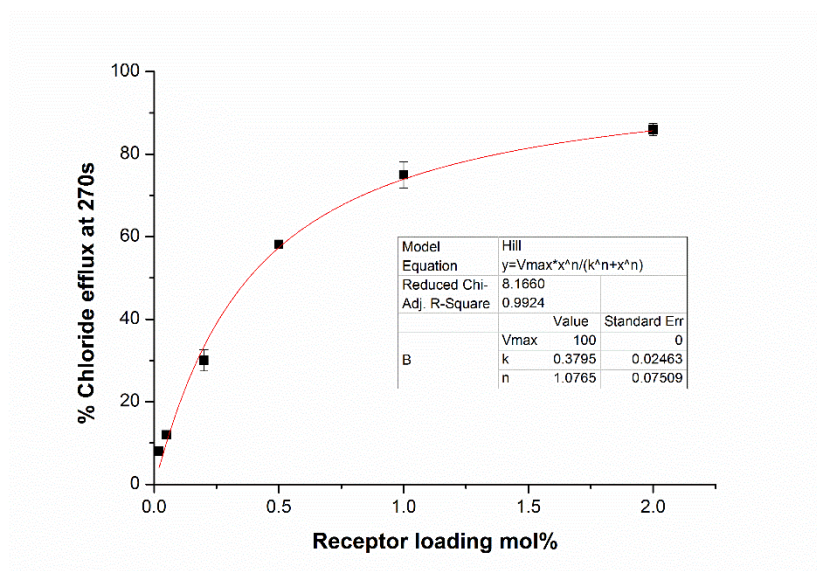


Figure S6.3.2- Hill plot for receptor **4**. $EC_{50}=0.38$ mol% $n=1.07$.

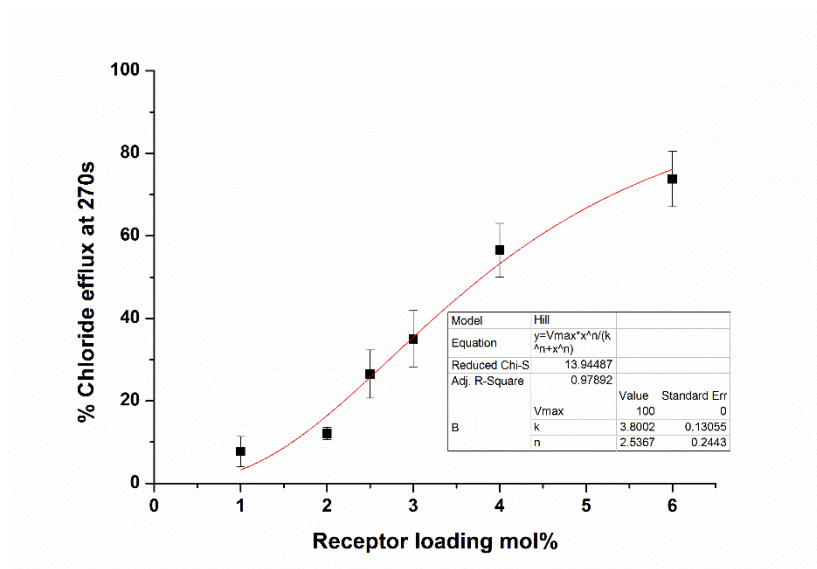


Figure S6.3.3- Hill plot for receptor **6**. $EC_{50}=3.8$ mol% $n=2.5$.

6.4 Cl^-/HCO_3^- Assay

POPC unilamellar vesicles containing NaCl (450 mM buffered to pH 7.2 using 20 mM sodium phosphate salts) were suspended in Na_2SO_4 (162 mM buffered to pH 7.2 using 20 mM sodium phosphate salts) to make a lipid concentration per sample of 1 mM. A DMSO solution of the receptor was added to commence the experiment, the chloride efflux was monitored using a chloride selective electrode. After 2 mins a $NaHCO_3$ solution was added to the sample giving an external $NaHCO_3$ concentration 40 mM. After 7 mins the vesicles were lysed using 50 μ L of polyoxyethylene (8) lauryl ether and after 9 mins a final chloride efflux reading was taken, this was used as 100 % chloride efflux and the rest of the readings were calibrated to this.

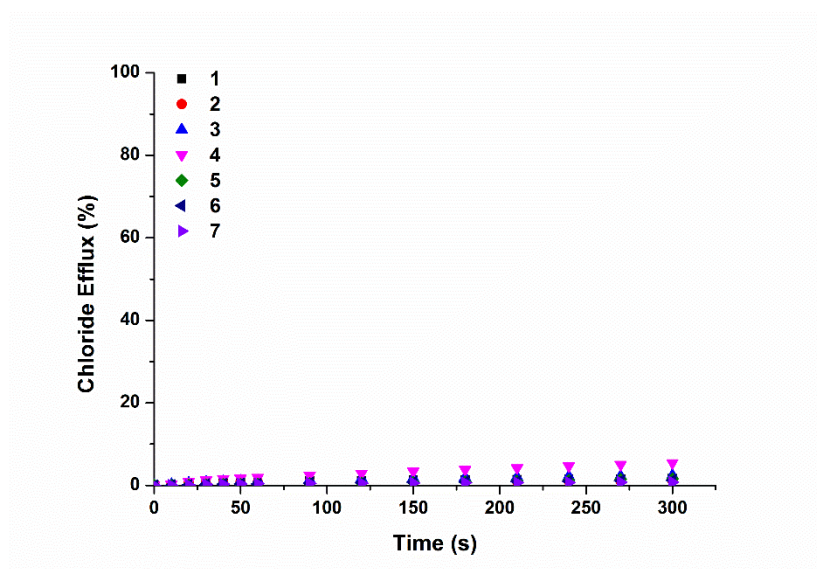


Figure S6.4.1- Chloride efflux facilitated by **1-7** at 2 mol% loading (with respect to lipid) from POPC vesicles containing 450 mM NaCl at pH 7.2 buffered with 20 mM sodium phosphate salts suspended in 162mM Na_2SO_4 at pH 7.2 buffered with sodium phosphate salts. To end the experiment detergent was added to lyse the vesicles and this final chloride efflux was used as 100 % to calibrate the ion selective electrode. Each point is an average of three runs.

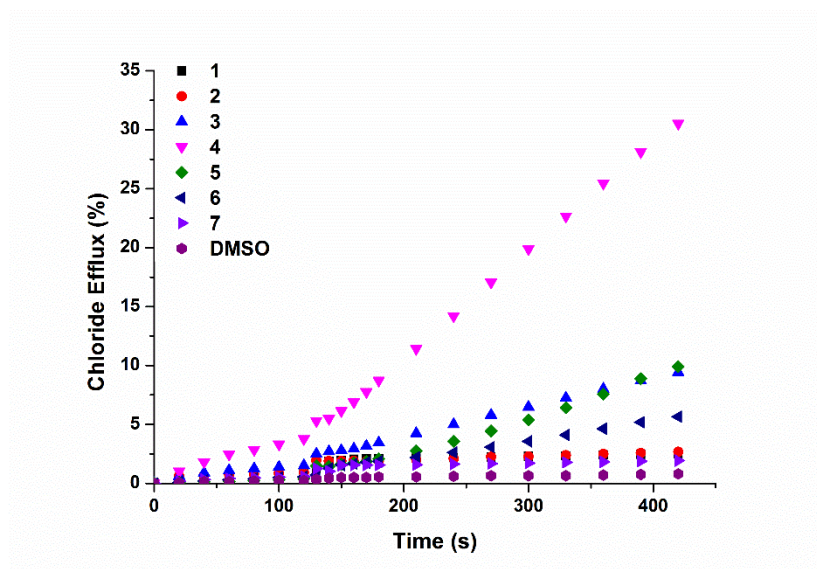


Figure S6.4.2- Chloride efflux facilitated by **1-7** at 2 mol% loading (with respect to lipid) from POPC vesicles containing 450 mM NaCl at pH 7.2 buffered with 20 mM sodium phosphate salts suspended in 162mM Na₂SO₄ at pH 7.2 buffered with sodium phosphate salts. At 120 s a NaHCO₃ solution was added to give a 40 mM external concentration. To end the experiment detergent was added to lyse the vesicles and this final chloride efflux was used as 100 % to calibrate the ion selective electrode. Each point is an average of three runs.

6.5 Cholesterol assay

This assay was done to probe the effect of modifying the viscosity of the membrane on the anion transport activity. Cl⁻/NO₃⁻ antiport assay repeated using unilamellar vesicles comprised of POPC:Cholesterol (7:3).

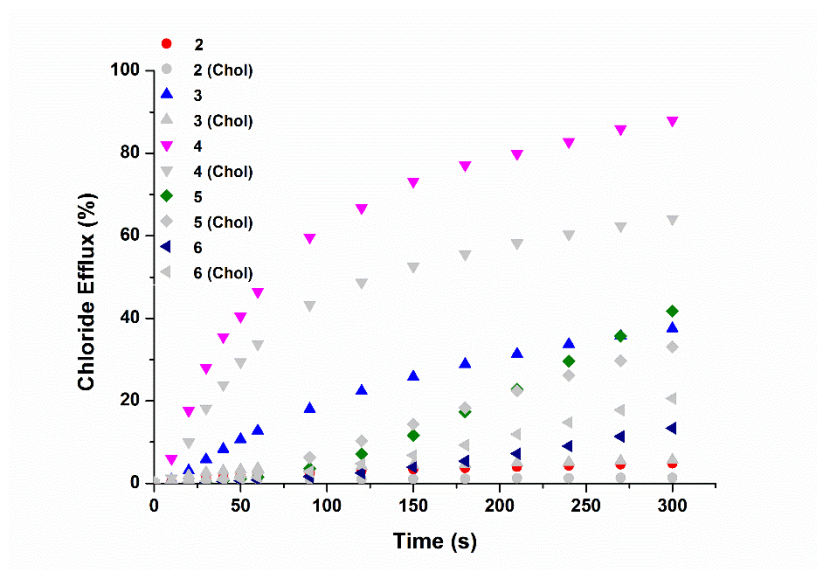


Figure S6.5.1- Chloride efflux facilitated by **2-6** at 2 mol% loading (with respect to lipid) from POPC:cholesterol (7:3) and POPC vesicles containing 489 mM NaCl at pH 7.2 buffered with 5 mM sodium phosphate salts suspended in 489mM NaNO₃ at pH 7.2 buffered with sodium phosphate salts. To end the experiment detergent was added to lyse the vesicles and this final chloride efflux was used as 100 % to calibrate the ion selective electrode. Each point is an average of three runs.

6.6 M⁺/Cl⁻ Symport assay

POPC unilamellar vesicles containing NaCl, KCl and CsCl (489 mM buffered to pH 7.2 using 5 mM sodium phosphate salts) were suspended in NaNO₃ (489 mM buffered to pH 7.2 using 5 mM sodium phosphate salts) to make a lipid concentration per sample of 1 mM. A DMSO solution of the receptor was added to commence the experiment, the chloride efflux was monitored using a chloride selective electrode. After 5 mins the vesicles were lysed using 50 μ L of polyoxyethylene (8) lauryl ether and after 7 mins a final chloride efflux reading was taken, this was used as 100 % chloride efflux and the rest of the readings were calibrated to this.

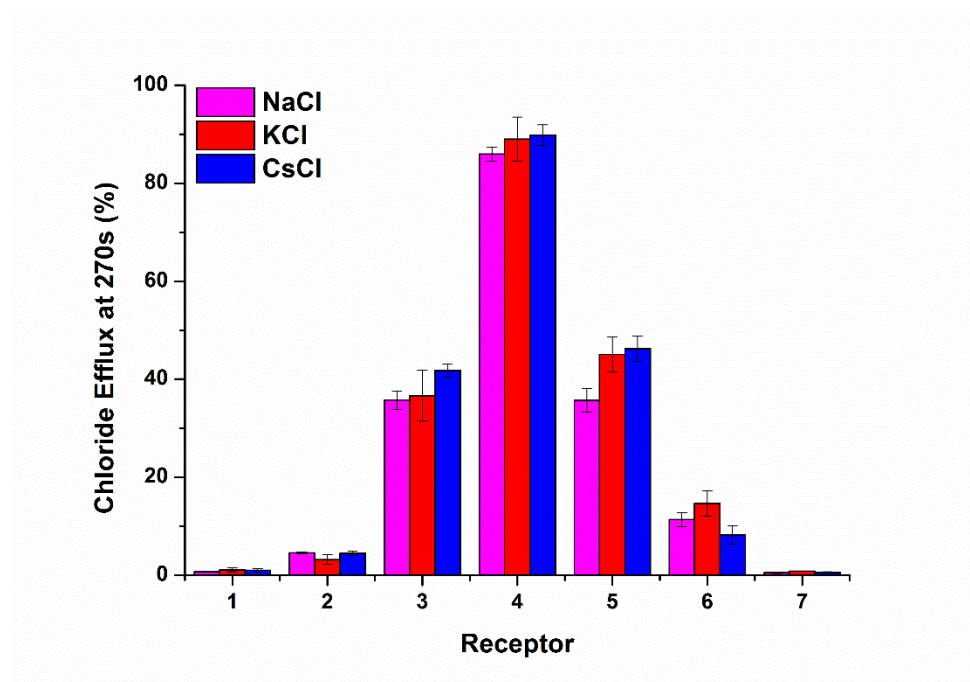


Figure S6.6.1- Chloride efflux promoted by 1-7 2 mol% loading (with respect to lipid) after 270 s from unilamellar POPC vesicles loaded with 489 mM MCl buffered to pH 7.2 with 5 mM sodium phosphate salts. The vesicles were dispersed in 489 mM NaNO₃ buffered to pH 7.2 with 5 mM sodium phosphate salts. To end the experiment detergent was added to lyse the vesicles and this final chloride efflux was used as 100 % to calibrate the ion selective electrode. Each point is an average of three runs. (Error bars represent the standard deviation).

6.7 U-tube Test

An organic phase was stirred between two aqueous phases (source and receiver) at room temperature and the chloride concentration of the receiver phase was determined using a chloride selective electrode. The chloride selective electrode was calibrated to enable the conversion of potential (mV) to chloride concentration (M). If chloride concentration in the receiver phase is observed to increase more than the control over the 8 days, it is likely that the receptors are using some form of mobile carrier mechanism, as ion channel formation is effectively impossible across this length of organic phase.

Source phase- 489 mM NaCl buffered to pH 7.2 with 5 mM sodium phosphate salts, 10 mL.

Receiver phase- 489 mM NaNO₃ buffered to pH 7.2 with 5 mM sodium phosphate salts, 10 mL.

Organic phase- 2mM TBA hexafluorophosphate (to provide counter ions and to aid solubility) in nitrobenzene with 1 mM receptor, 20mL.

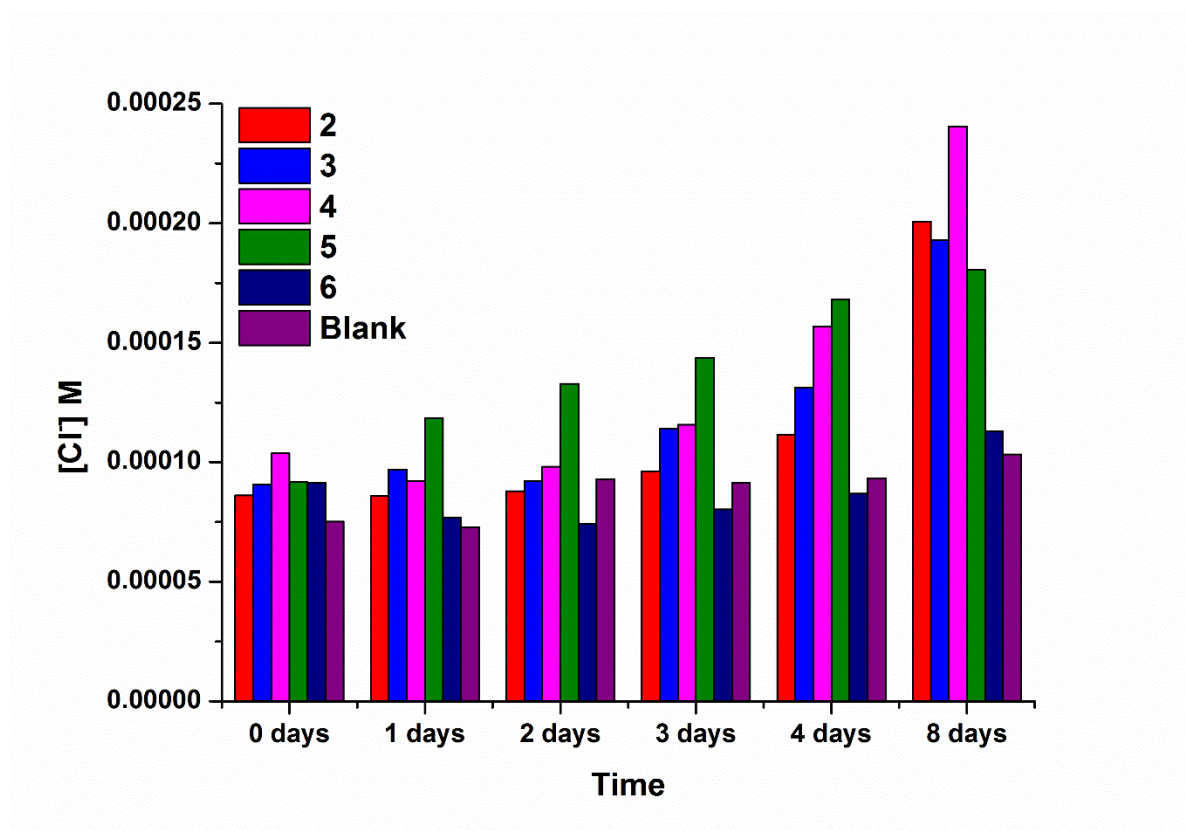


Figure S6.7.1- Change in the concentration (M) of chloride anions in the receiver phase of the U-tube facilitated by receptors 2-6. Some results from this test are reasonably unreliable due to observations of a small amount of precipitation of receptor 3.

After eight days all the receptors showed a greater level of chloride concentration in the receiver phase than the control, the small increase in chloride concentration in the control was attributed to the interaction of TBA^+ with chloride. Receptor 4 showed the greatest activity, which was expected as this was also the most effective lipid bilayer transporter.

6.8 Electrode calibration and conversion of raw data

Calibration of the Accumet Chloride Ion Selective Electrode used for the anion transport tests was performed prior to the vesicle assays. The electrode was placed into a series of NaCl solutions of known concentrations for five min at a time and the electrode potential (mV) was recorded. These values were plotted vs the NaCl concentration (M) and the plot was fitted to Equation 1 a simplified version of the Nernst Equation.

$$y = (P_1 \log_{10} x) + P_2 \quad (1)$$

The parameters P_1 and P_2 are then calculated and from these calibration parameters the raw potential data recorded for the transport assays can be converted into chloride concentrations. Using equation 1 and solving for x gives you the chloride concentration at any time point in the assay, subtracting the initial chloride concentration from this value gives the total chloride concentration released from the vesicle at any one time point. Using the value from 100 % chloride efflux ($t = 420/540\text{s}$) the percentage chloride efflux can be calculated for all time points.

7.0 Proton NMR titrations

7.1 Titrations in DMSO- d_6 /0.5% H₂O

Proton NMR titrations were performed via addition of aliquots of the guest anion in the tetrabutylammonium form (0.1 M) dissolved in a 0.005 M solution of receptor in DMSO- d_6 / 0.5 % water, to a 0.005 M solution of receptor in DMSO- d_6 / 0.5 %. Salts used were dried under high vacuum overnight before use. Spectra were recorded using a Bruker AVII400 spectrometer and calibrated to the solvent residual peak at $\delta = 2.50$ ppm (DMSO- d_6). Titration data was fitted using WinEQNMR2.⁷

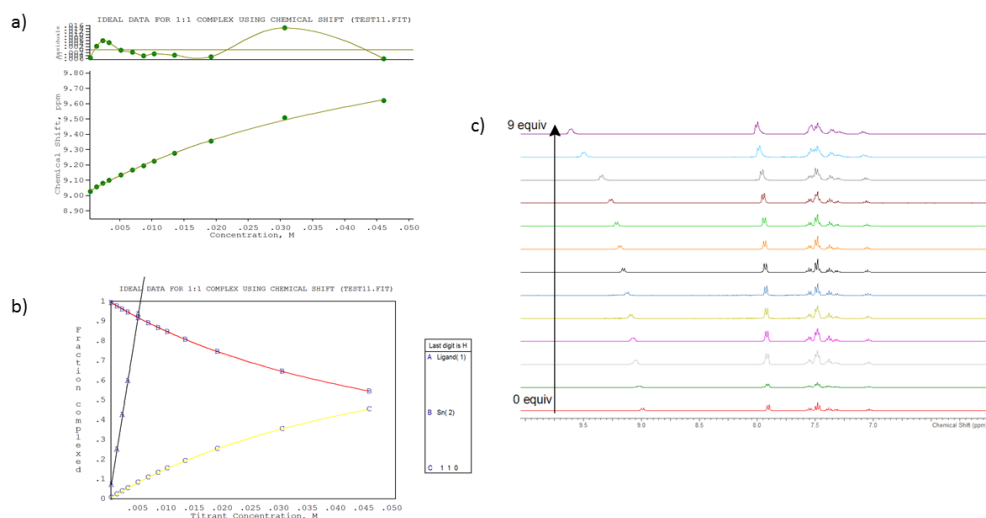


Figure S7.1.1- a) Titration curve of receptor **1** with tetrabutylammonium chloride in DMSO- d_6 /0.5 % H₂O at 298K. b) Species concentration plot of receptor **1** with tetrabutylammonium chloride in DMSO- d_6 /0.5 % H₂O at 298K. A-Guest concentration, B-Uncomplexed host concentration, C- Complex concentration. c) Stack plot of NMR spectra.

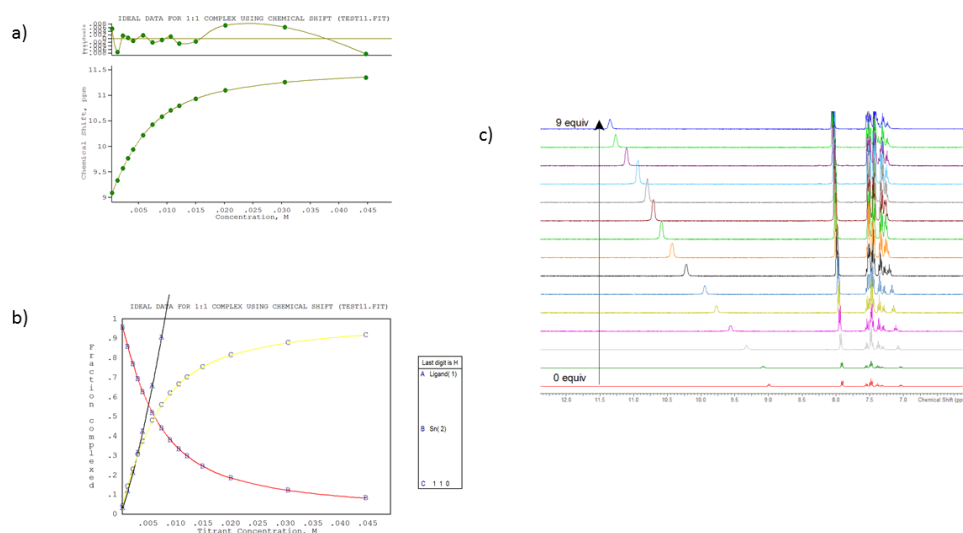


Figure S7.1.2- a) Titration curve of receptor **1** with tetraethylammonium bicarbonate in DMSO- d_6 /0.5 % H₂O at 298K. b) Species concentration plot of receptor **1** with tetraethylammonium bicarbonate in DMSO- d_6 /0.5 % H₂O at 298K. A-Guest concentration, B-Uncomplexed host concentration, C- Complex concentration. c) Stack plot of NMR spectra.

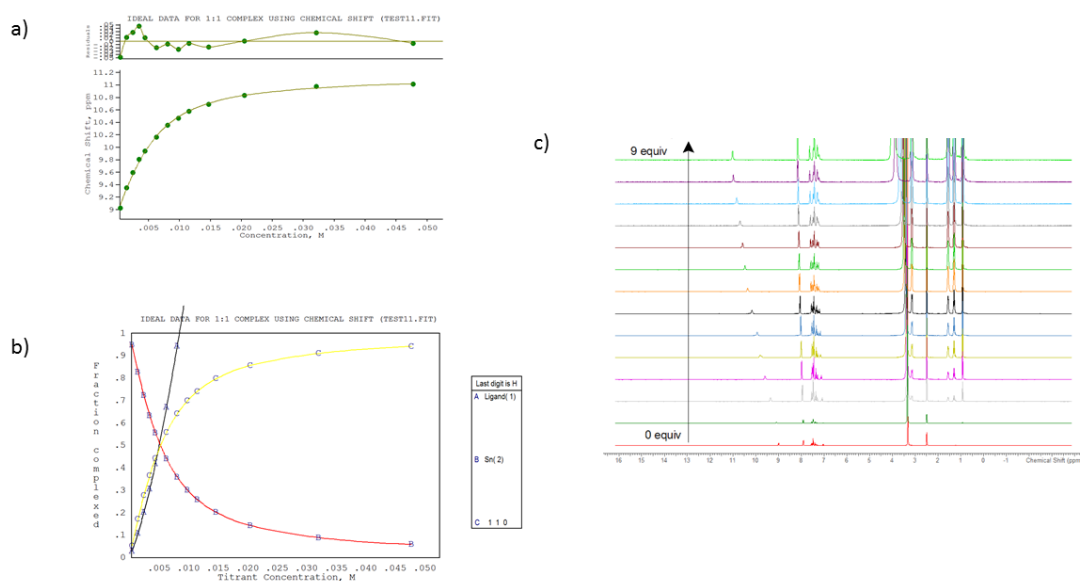


Figure S7.1.3- a) Titration curve of receptor **1** with tetrabutylammonium dihydrogen phosphate in DMSO- δ_6 /0.5 % H₂O at 298K. b) Species concentration plot of receptor **1** with tetrabutylammonium dihydrogen phosphate in DMSO- δ_6 /0.5 % H₂O at 298K. A-Guest concentration, B-Uncomplexed host concentration, C- Complex concentration. c) Stack plot of NMR spectra.

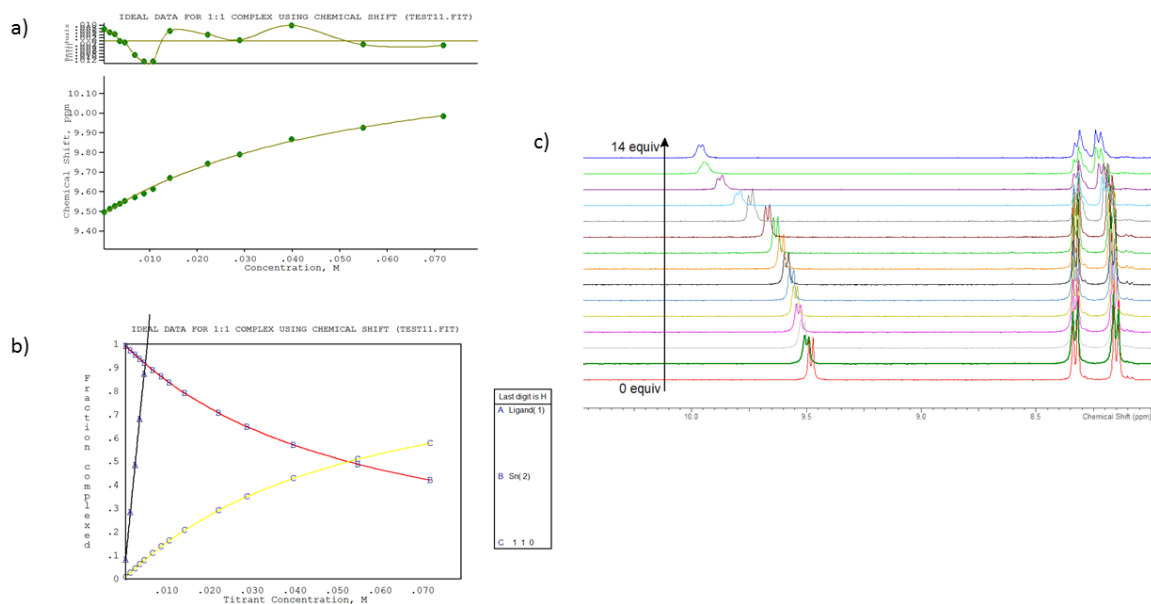


Figure S7.1.4- a) Titration curve of receptor **2** with tetrabutylammonium chloride in DMSO- δ_6 /0.5 % H₂O at 298K. b) Species concentration plot of receptor **2** with tetrabutylammonium chloride in DMSO- δ_6 /0.5 % H₂O at 298K. A-Guest concentration, B-Uncomplexed host concentration, C- Complex concentration. c) Stack plot of NMR spectra.

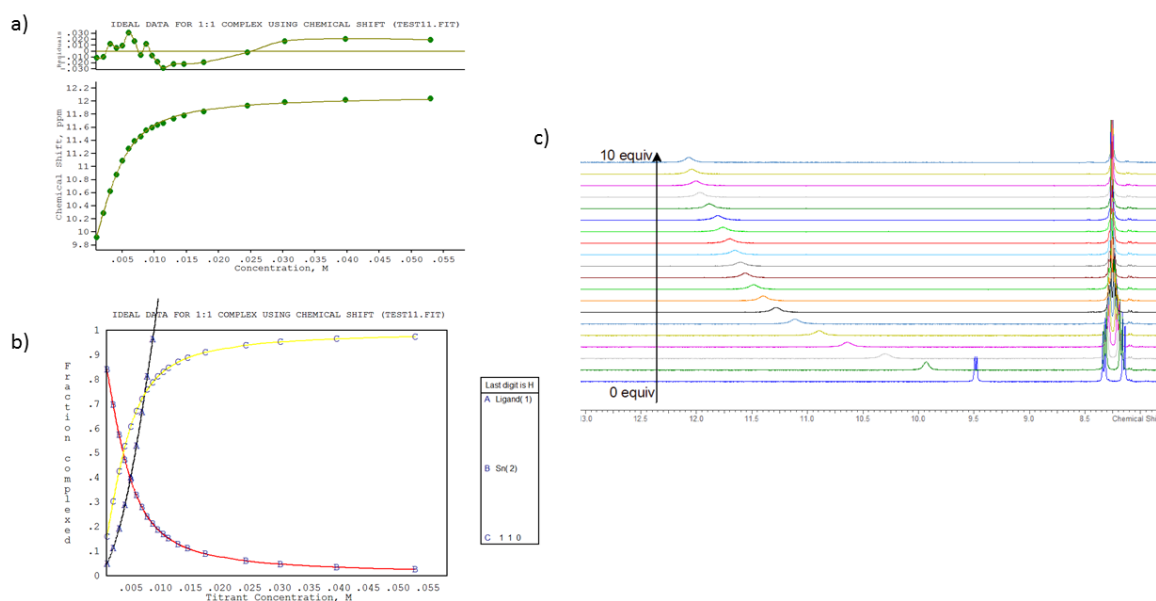


Figure S7.1.5- a) Titration curve of receptor 2 with tetraethylammonium bicarbonate in DMSO- δ_6 /0.5 % H₂O at 298K. b) Species concentration plot of receptor 2 with tetraethylammonium bicarbonate in DMSO- δ_6 /0.5 % H₂O at 298K. A-Guest concentration, B-Uncomplexed host concentration, C- Complex concentration. c) Stack plot of NMR spectra.

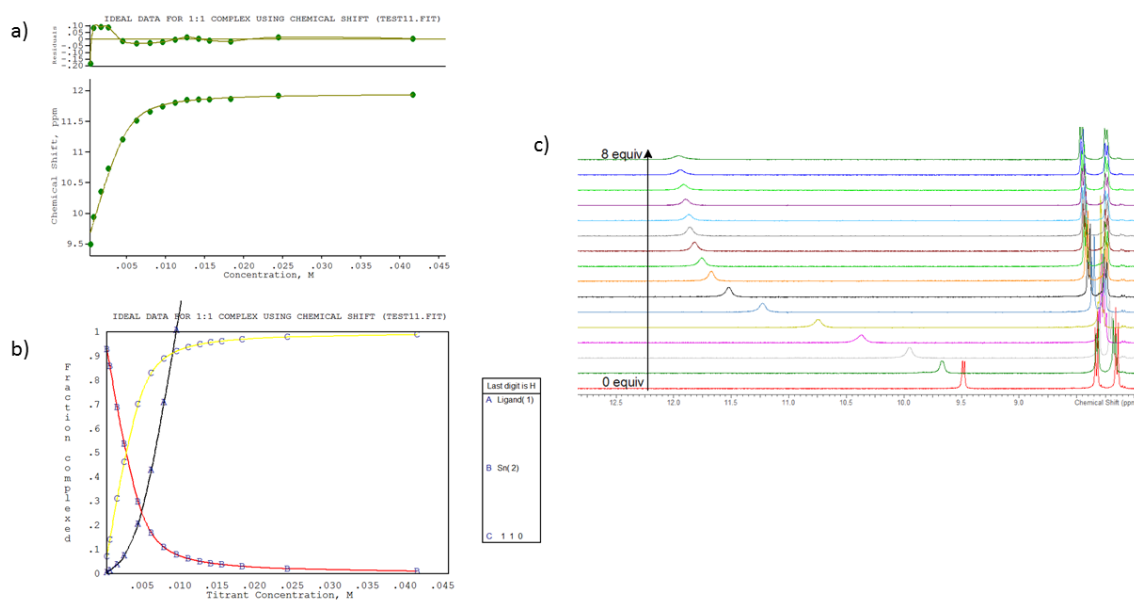


Figure S7.1.6- a) Titration curve of receptor 2 with tetrabutylammonium dihydrogen phosphate in DMSO- δ_6 /0.5 % H₂O at 298K. b) Species concentration plot of receptor 2 with tetrabutylammonium dihydrogen phosphate in DMSO- δ_6 /0.5 % H₂O at 298K. A-Guest concentration, B-Uncomplexed host concentration, C- Complex concentration. c) Stack plot of NMR spectra.

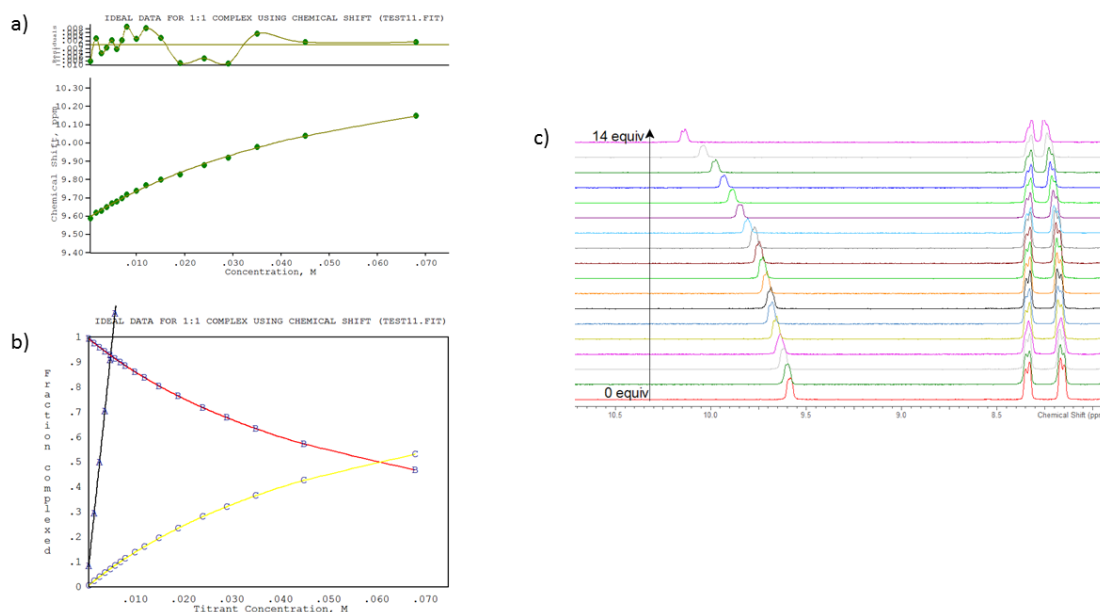


Figure S7.1.7- a) Titration curve of receptor 3 with tetrabutylammonium chloride in DMSO- δ_6 /0.5 % H₂O at 298K. b) Species concentration plot of receptor 3 with tetrabutylammonium chloride in DMSO- δ_6 /0.5 % H₂O at 298K. A-Guest concentration, B-Uncomplexed host concentration, C- Complex concentration. c) Stack plot of NMR spectra.

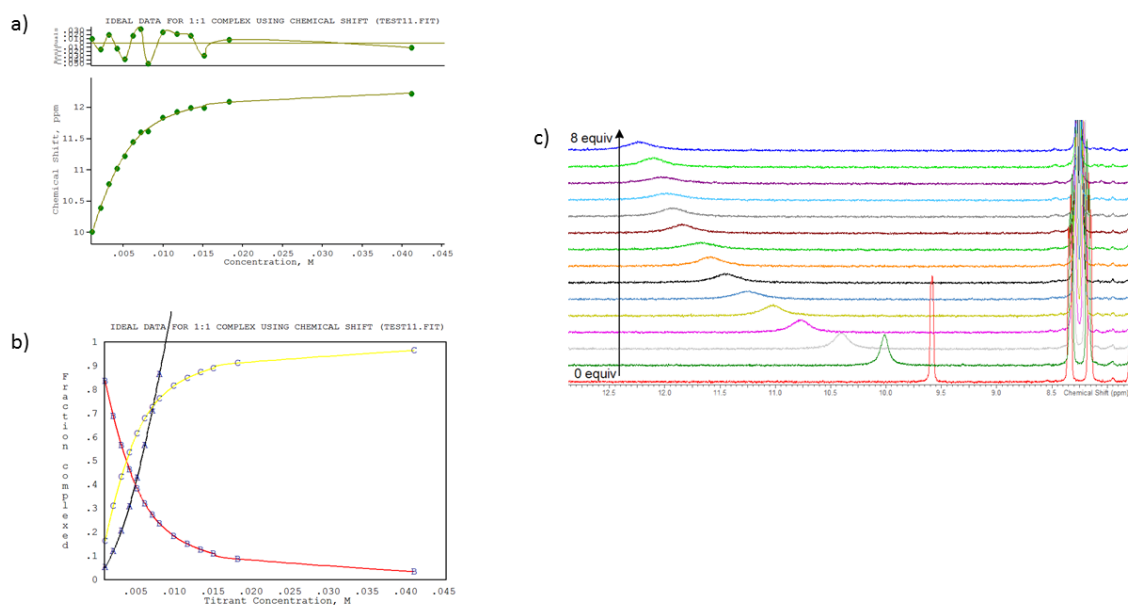


Figure S7.1.8- a) Titration curve of receptor 3 with tetraethylammonium bicarbonate in DMSO- δ_6 /0.5 % H₂O at 298K. b) Species concentration plot of receptor 3 with tetraethylammonium bicarbonate in DMSO- δ_6 /0.5 % H₂O at 298K. A-Guest concentration, B-Uncomplexed host concentration, C- Complex concentration. c) Stack plot of NMR spectra.

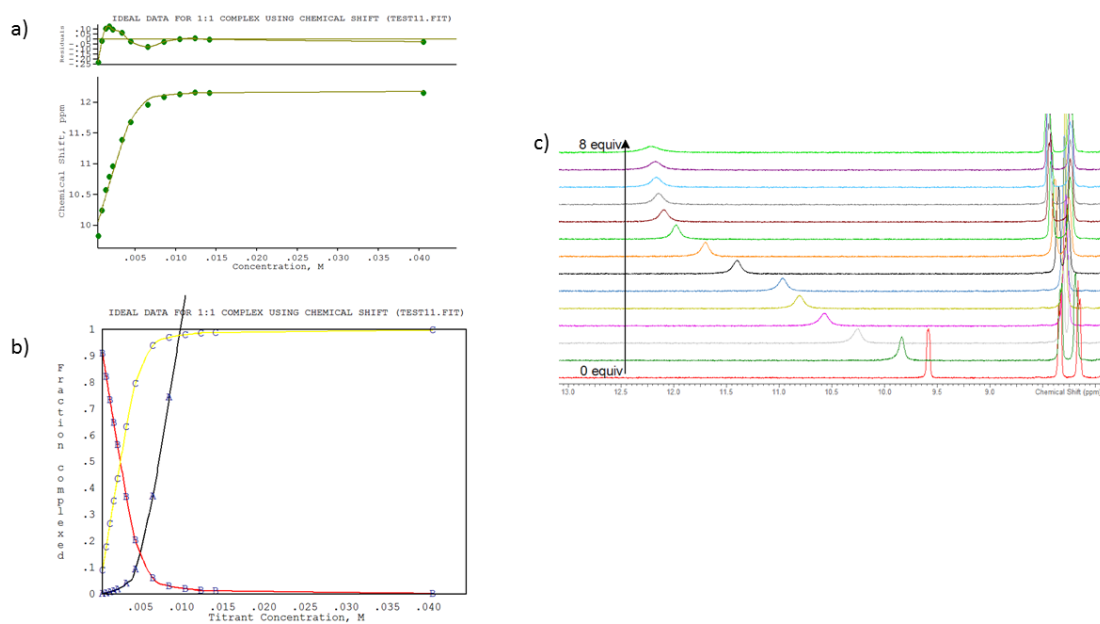


Figure S7.1.9- a) Titration curve of receptor 3 with tetrabutylammonium dihydrogen phosphate in DMSO- δ_6 /0.5 % H₂O at 298K. b) Species concentration plot of receptor 3 with tetrabutylammonium dihydrogen phosphate in DMSO- δ_6 /0.5 % H₂O at 298K. A-Guest concentration, B-Uncomplexed host concentration, C- Complex concentration. c) Stack plot of NMR spectra.

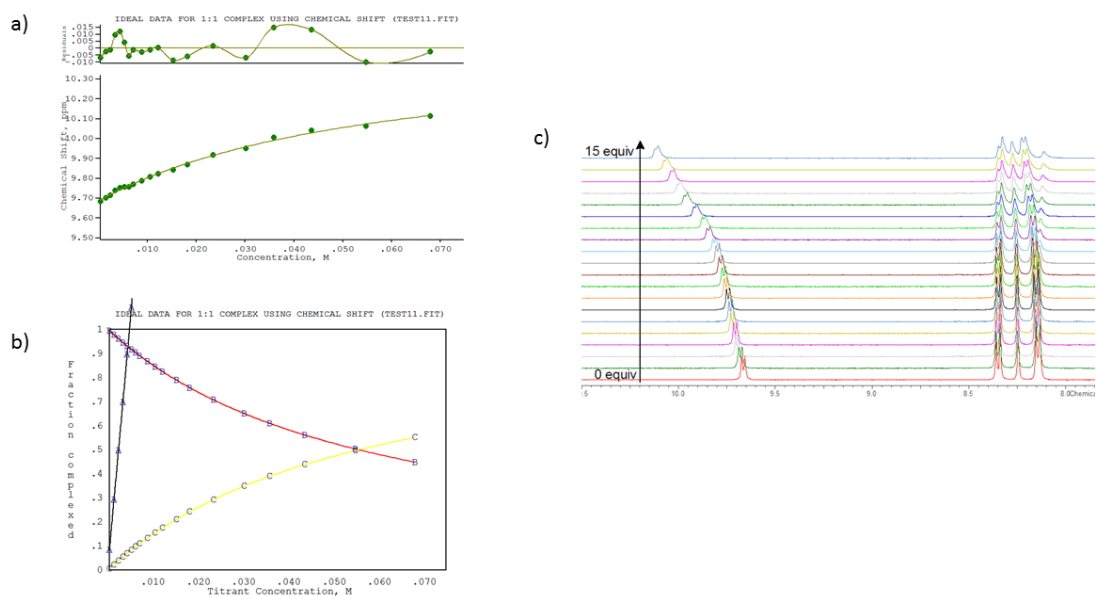


Figure S7.1.10- a) Titration curve of receptor 4 with tetrabutylammonium chloride in DMSO- δ_6 /0.5 % H₂O at 298K. b) Species concentration plot of receptor 4 with tetrabutylammonium chloride in DMSO- δ_6 /0.5 % H₂O at 298K. A-Guest concentration, B-Uncomplexed host concentration, C- Complex concentration. c) Stack plot of NMR spectra.

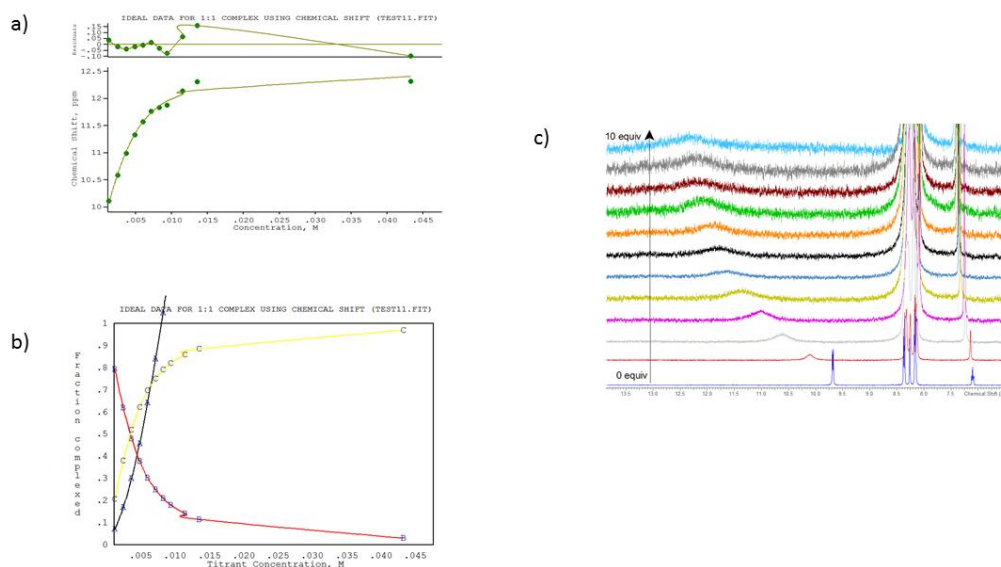


Figure S7.1.11- a) Titration curve of receptor 4 with tetraethylammonium bicarbonate in DMSO- δ_6 /0.5 % H₂O at 298K. b) Species concentration plot of receptor 2 with tetraethylammonium bicarbonate in DMSO- δ_6 /0.5 % H₂O at 298K. A-Guest concentration, B-Uncomplexed host concentration, C- Complex concentration. c) Stack plot of NMR spectra.

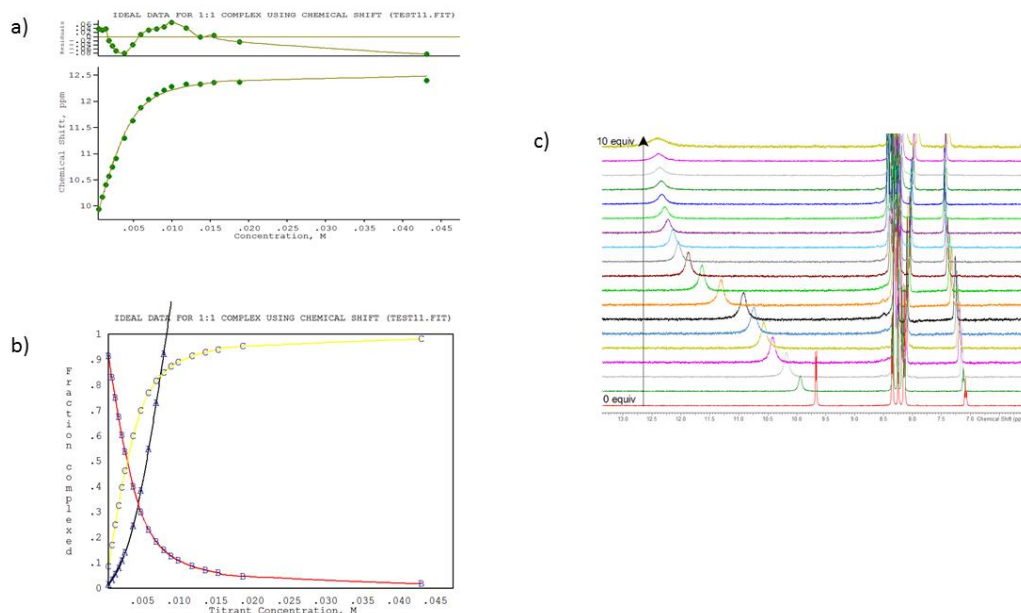


Figure S7.1.12- a) Titration curve of receptor 4 with tetrabutylammonium dihydrogen phosphate in DMSO- δ_6 /0.5 % H₂O at 298K. b) Species concentration plot of receptor 4 with tetrabutylammonium dihydrogen phosphate in DMSO- δ_6 /0.5 % H₂O at 298K. A-Guest concentration, B-Uncomplexed host concentration, C- Complex concentration. c) Stack plot of NMR spectra.

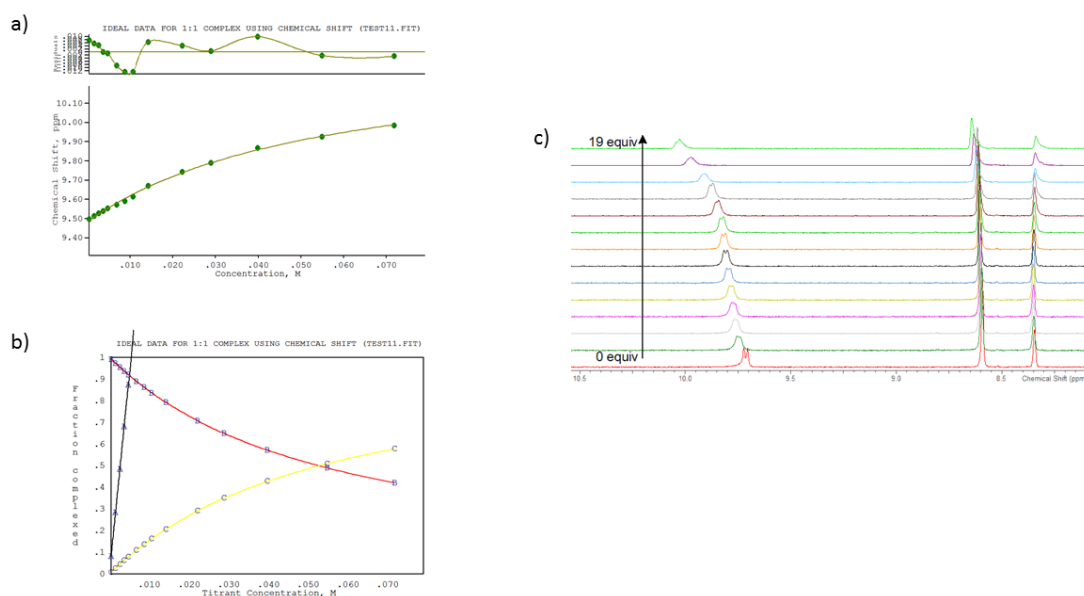


Figure S7.1.13- a) Titration curve of receptor 5 with tetrabutylammonium chloride in DMSO- δ_6 /0.5 % H₂O at 298K. b) Species concentration plot of receptor 5 with tetrabutylammonium chloride in DMSO- δ_6 /0.5 % H₂O at 298K. A-Guest concentration, B-Uncomplexed host concentration, C- Complex concentration. c) Stack plot of NMR spectra.

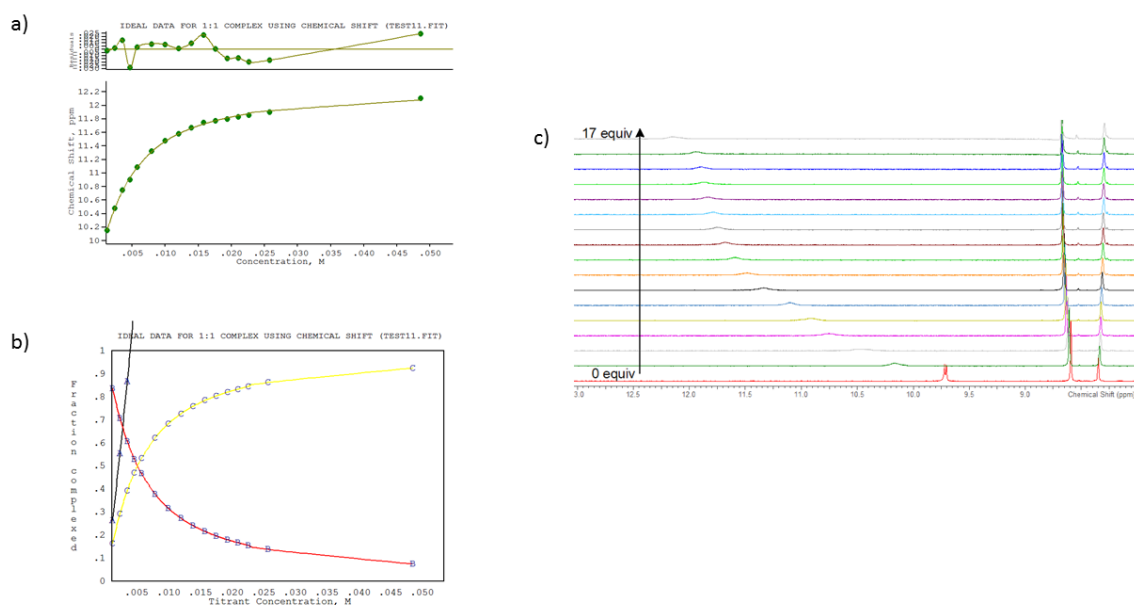


Figure S7.1.14- a) Titration curve of receptor 5 with tetraethylammonium bicarbonate in DMSO- δ_6 /0.5 % H₂O at 298K. b) Species concentration plot of receptor 5 with tetraethylammonium bicarbonate in DMSO- δ_6 /0.5 % H₂O at 298K. A-Guest concentration, B-Uncomplexed host concentration, C- Complex concentration. c) Stack plot of NMR spectra.

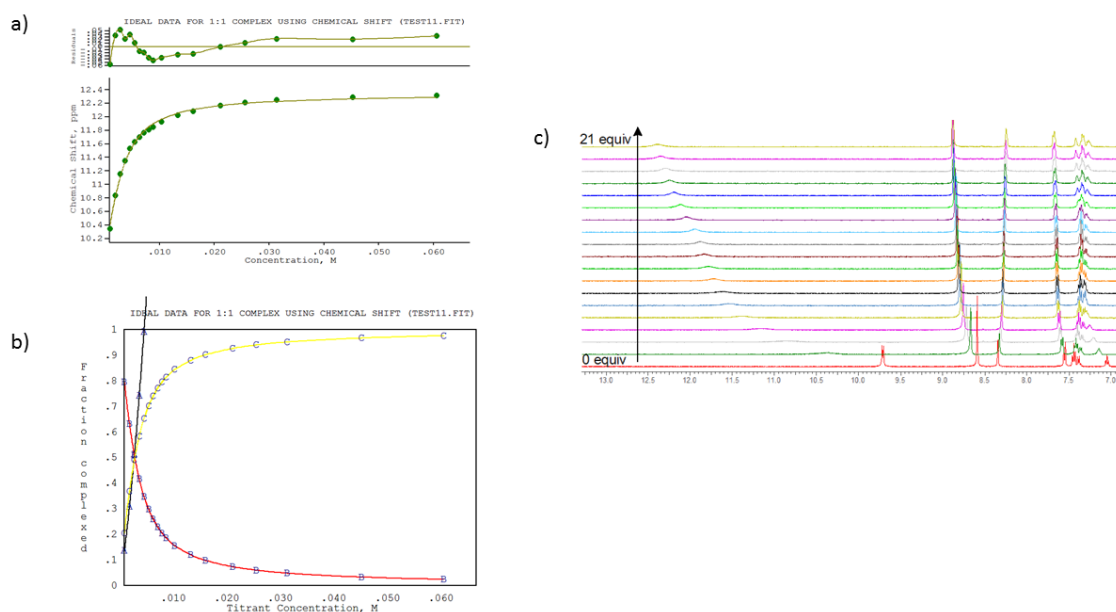


Figure S7.1.15- a) Titration curve of receptor 5 with tetrabutylammonium dihydrogen phosphate in DMSO- δ_6 /0.5 % H₂O at 298K. b) Species concentration plot of receptor 5 with tetrabutylammonium dihydrogen phosphate in DMSO- δ_6 /0.5 % H₂O at 298K. A-Guest concentration, B-Uncomplexed host concentration, C- Complex concentration. c) Stack plot of NMR spectra.

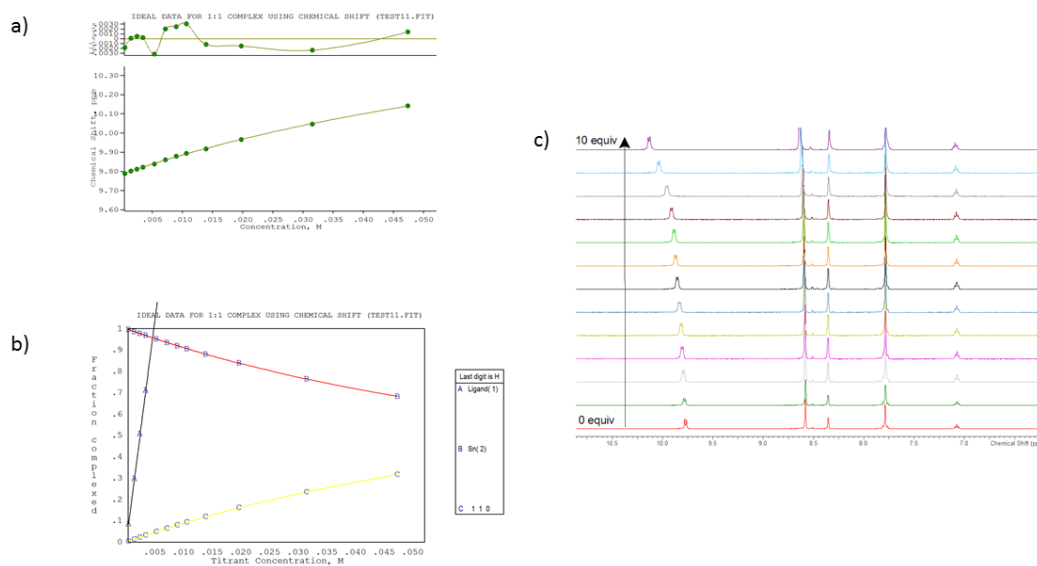


Figure S7.1.16- a) Titration curve of receptor 6 with tetrabutylammonium chloride in DMSO- δ_6 /0.5 % H₂O at 298K. b) Species concentration plot of receptor 6 with tetrabutylammonium chloride in DMSO- δ_6 /0.5 % H₂O at 298K. A-Guest concentration, B-Uncomplexed host concentration, C- Complex concentration. c) Stack plot of NMR spectra.

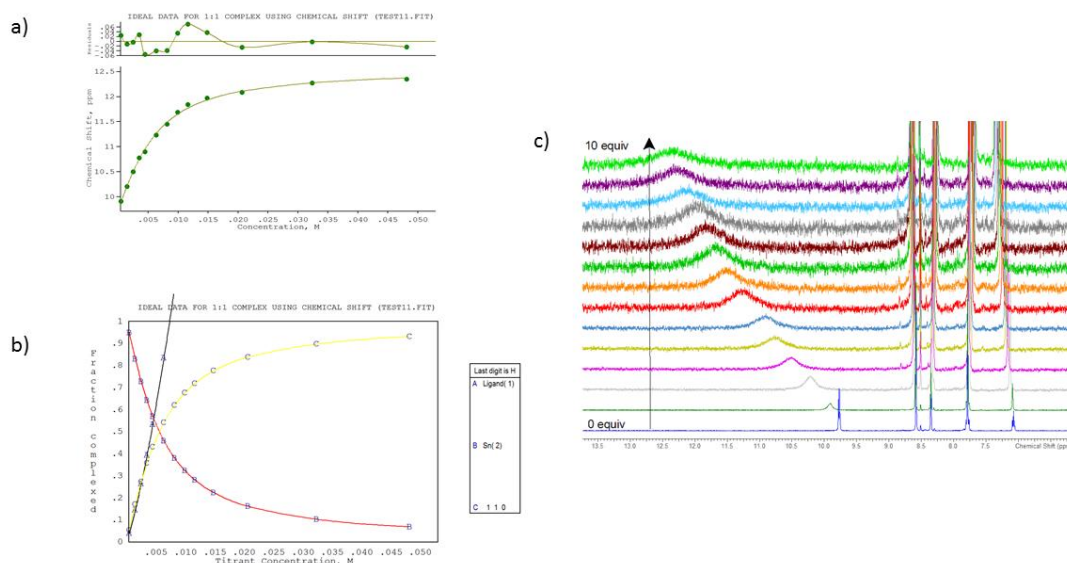


Figure S7.1.17- a) Titration curve of receptor 6 with tetraethylammonium bicarbonate in DMSO- δ_6 /0.5 % H₂O at 298K. b) Species concentration plot of receptor 6 with tetraethylammonium bicarbonate in DMSO- δ_6 /0.5 % H₂O at 298K. A-Guest concentration, B-Uncomplexed host concentration, C- Complex concentration. c) Stack plot of NMR spectra.

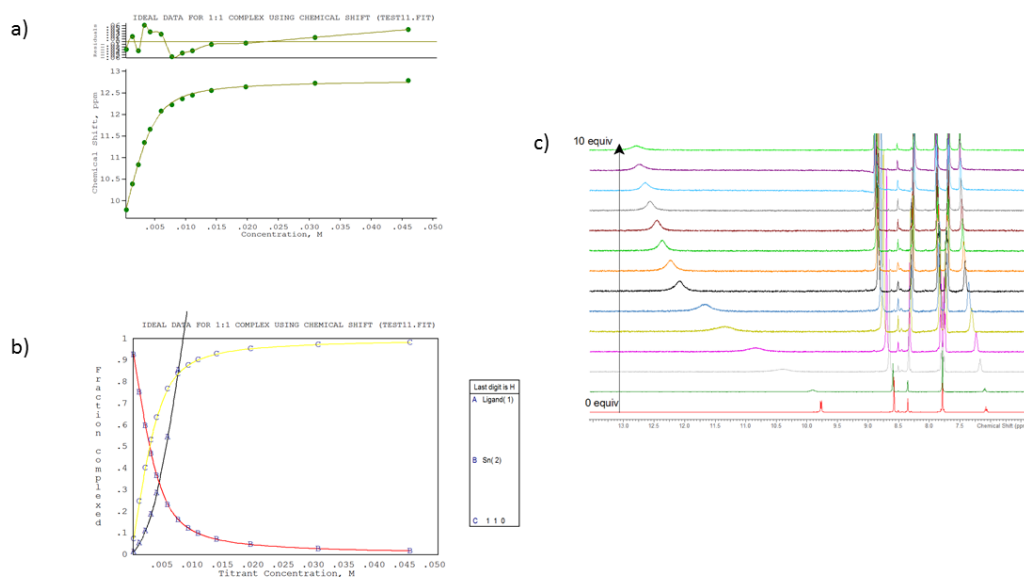


Figure S7.1.18- a) Titration curve of receptor 6 with tetrabutylammonium dihydrogen phosphate in DMSO- δ_6 /0.5 % H₂O at 298K. b) Species concentration plot of receptor 6 with tetrabutylammonium dihydrogen phosphate in DMSO- δ_6 /0.5 % H₂O at 298K. A-Guest concentration, B-Uncomplexed host concentration, C- Complex concentration. c) Stack plot of NMR spectra.

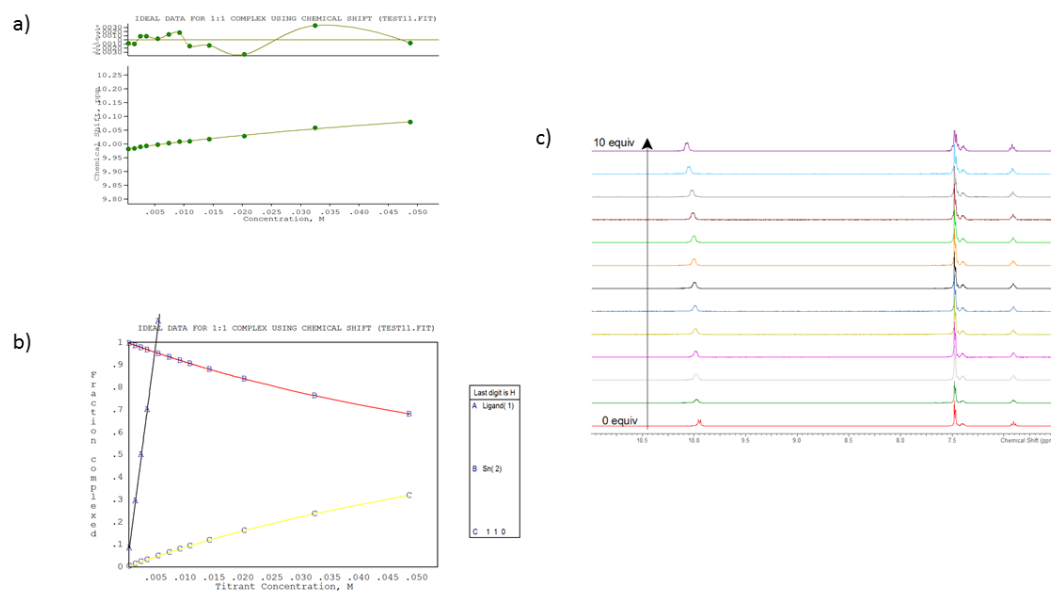


Figure S7.1-19- a) Titration curve of receptor 7 with tetrabutylammonium chloride in DMSO- δ_6 /0.5 % H₂O at 298K. b) Species concentration plot of receptor 7 with tetrabutylammonium chloride in DMSO- δ_6 /0.5 % H₂O at 298K. A-Guest concentration, B-Uncomplexed host concentration, C- Complex concentration. c) Stack plot of NMR spectra.

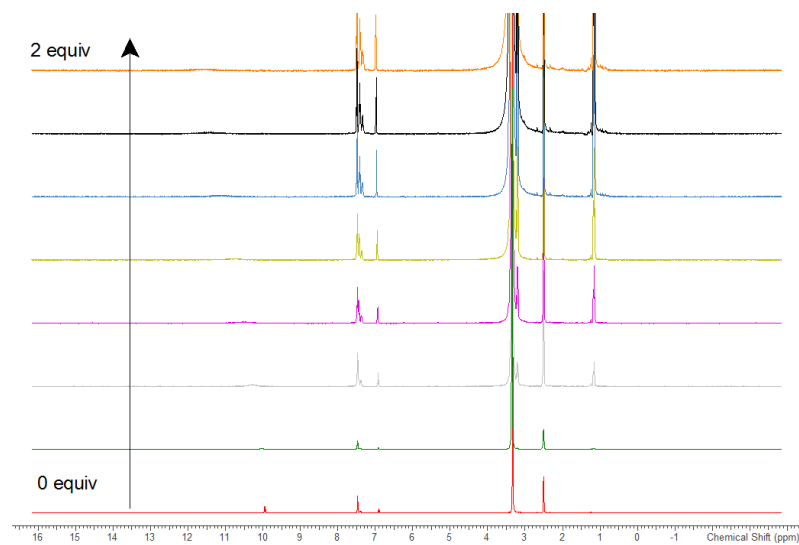


Figure S7.1-20- Stack plot of NMR spectra of receptor 7 titrated with tetraethylammonium bicarbonate in DMSO- δ_6 /0.5 % H₂O at 298K. No titration curve plotted, data could not be fitted using winEQNMR2 due to disappearance of the NH peak.

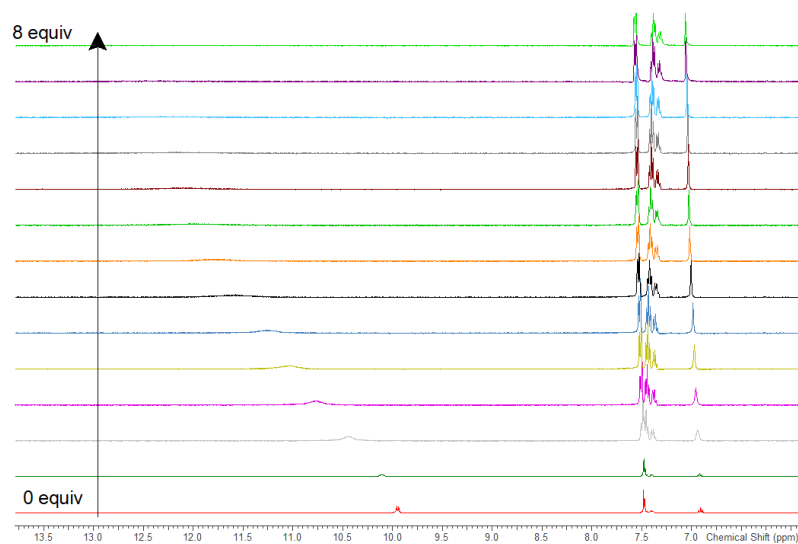


Figure S7.1.21- Stack plot of NMR spectra of receptor 7 titrated with tetrabutylammonium dihydrogen phosphate in DMSO- δ_6 /0.5 % H₂O at 298K. No titration curve plotted, data could not be fitted using winEQNMR2 due to disappearance of the NH peak.

7.2 Titrations in 59.75% MeCN-*d*₃/ 39.75% DMSO-*d*₆/0.5% H₂O

¹H NMR titrations were performed via addition of aliquots of the guest anion in the tetrabutylammonium form (0.1 M) dissolved in a 0.005 M solution of receptor in 59.75% MeCN-*d*₃/ 39.75% DMSO-*d*₆/0.5% H₂O, to a 0.005 M solution of receptor in 59.75% MeCN-*d*₃/ 39.75% DMSO-*d*₆/0.5% H₂O. Salts used were dried under high vacuum overnight before use. Spectra were recorded using a Bruker AVII400 spectrometer and calibrated to the solvent residual peak at $\delta = 1.94$ ppm (MeCN-*d*₃). Titration data was fitted using Win EQNMR2.⁷

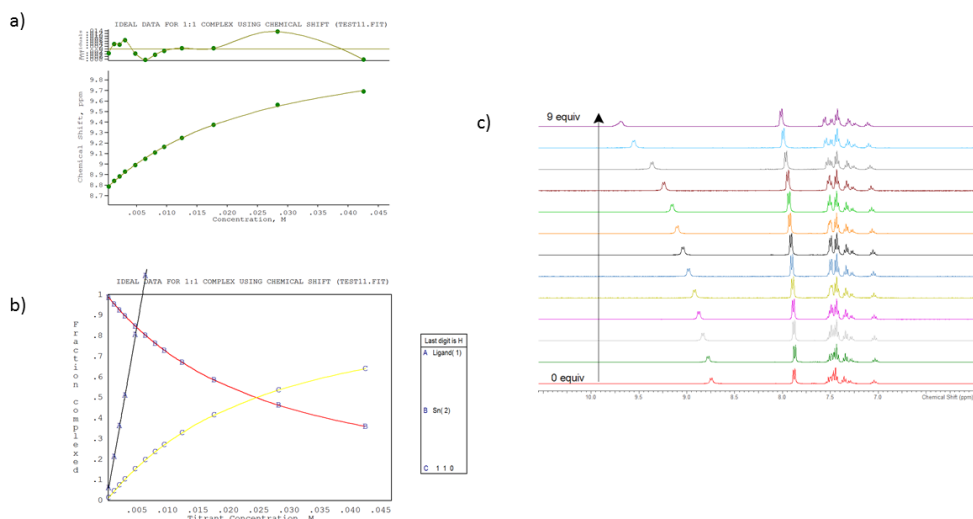


Figure S7.2.1- a) Titration curve of receptor 1 with tetrabutylammonium chloride in 59.75% MeCN-*d*₃/ 39.75% DMSO-*d*₆/0.5% H₂O at 298K. b) Species concentration plot of receptor 1 with tetrabutylammonium chloride in 59.75% MeCN-*d*₃/ 39.75% DMSO-*d*₆/0.5% H₂O at 298K. A-Guest concentration, B-Uncomplexed host concentration, C- Complex concentration. c) Stack plot of NMR spectra.

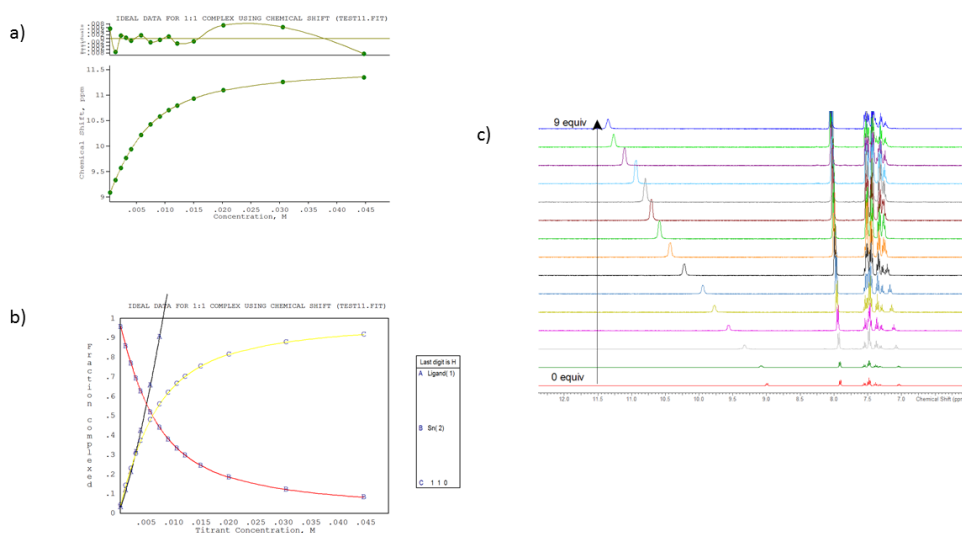


Figure S7.2.2- a) Titration curve of receptor 1 with tetraethylammonium bicarbonate in 59.75% MeCN-*d*₃/ 39.75% DMSO-*d*₆/0.5% H₂O at 298K. b) Species concentration plot of receptor 1 with tetraethylammonium bicarbonate 59.75% MeCN-*d*₃/ 39.75% DMSO-*d*₆/0.5% H₂O at 298K. A-Guest concentration, B-Uncomplexed host concentration, C- Complex concentration. c) Stack plot of NMR spectra.

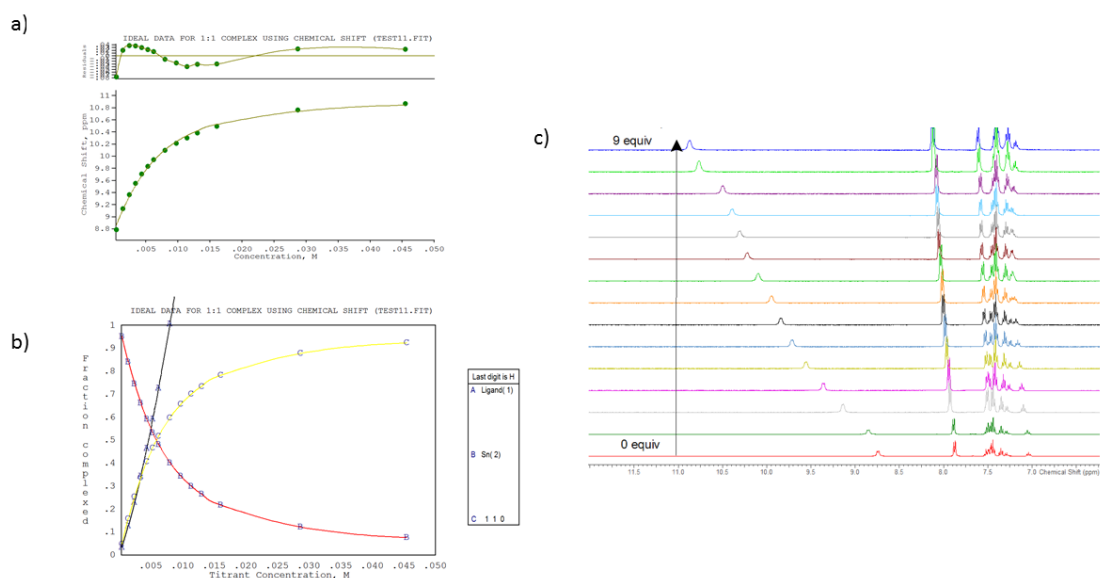


Figure S7.2.3- a) Titration curve of receptor 1 with tetrabutylammonium dihydrogen phosphate in 59.75% MeCN- d_3 /39.75% DMSO- d_6 /0.5% H₂O at 298K. b) Species concentration plot of receptor 1 with tetrabutylammonium dihydrogen phosphate in 59.75% MeCN- d_3 /39.75% DMSO- d_6 /0.5% H₂O at 298K. A-Guest concentration, B-Uncomplexed host concentration, C- Complex concentration. c) Stack plot of NMR spectra.

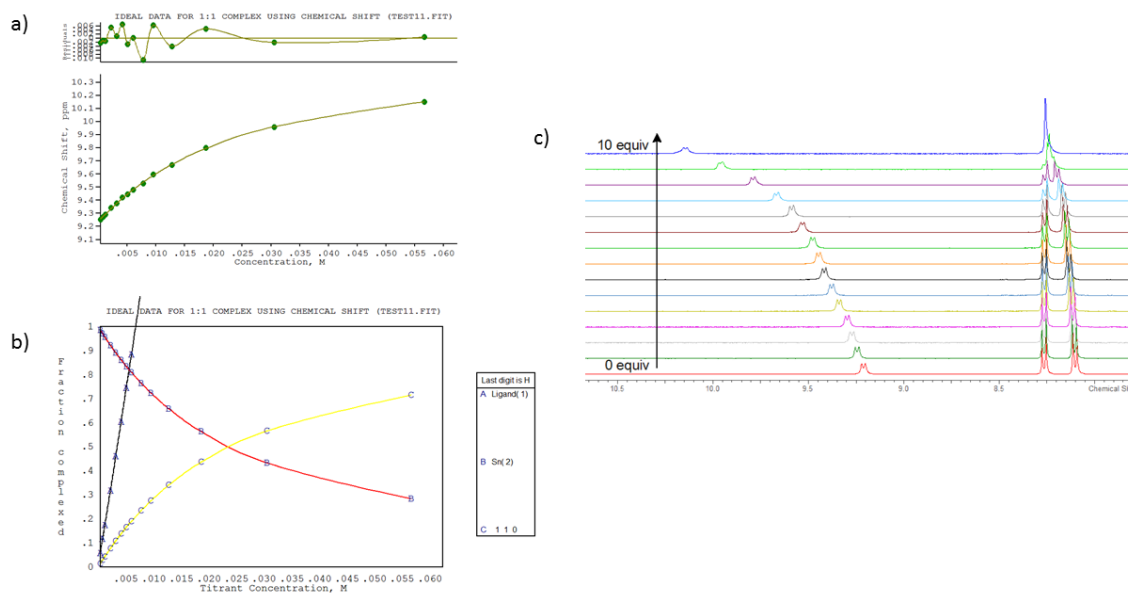


Figure S7.2.4- a) Titration curve of receptor 2 with tetrabutylammonium chloride in 59.75% MeCN- d_3 /39.75% DMSO- d_6 /0.5% H₂O at 298K. b) Species concentration plot of receptor 2 with tetrabutylammonium chloride in 59.75% MeCN- d_3 /39.75% DMSO- d_6 /0.5% H₂O at 298K. A-Guest concentration, B-Uncomplexed host concentration, C- Complex concentration. c) Stack plot of NMR spectra.

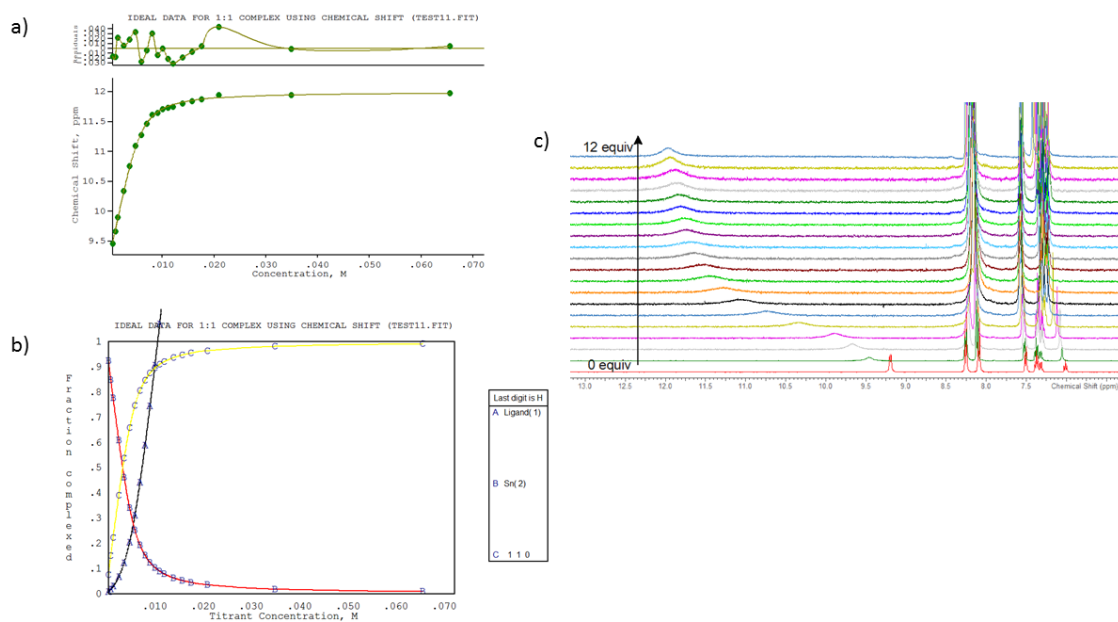


Figure S7.2.5- a) Titration curve of receptor 2 with tetraethylammonium bicarbonate in 59.75% MeCN- d_3 /39.75% DMSO- d_6 /0.5% H₂O at 298K. b) Species concentration plot of receptor 2 with tetraethylammonium bicarbonate in 59.75% MeCN- d_3 /39.75% DMSO- d_6 /0.5% H₂O at 298K. A-Guest concentration, B-Uncomplexed host concentration, C- Complex concentration. c) Stack plot of NMR spectra.

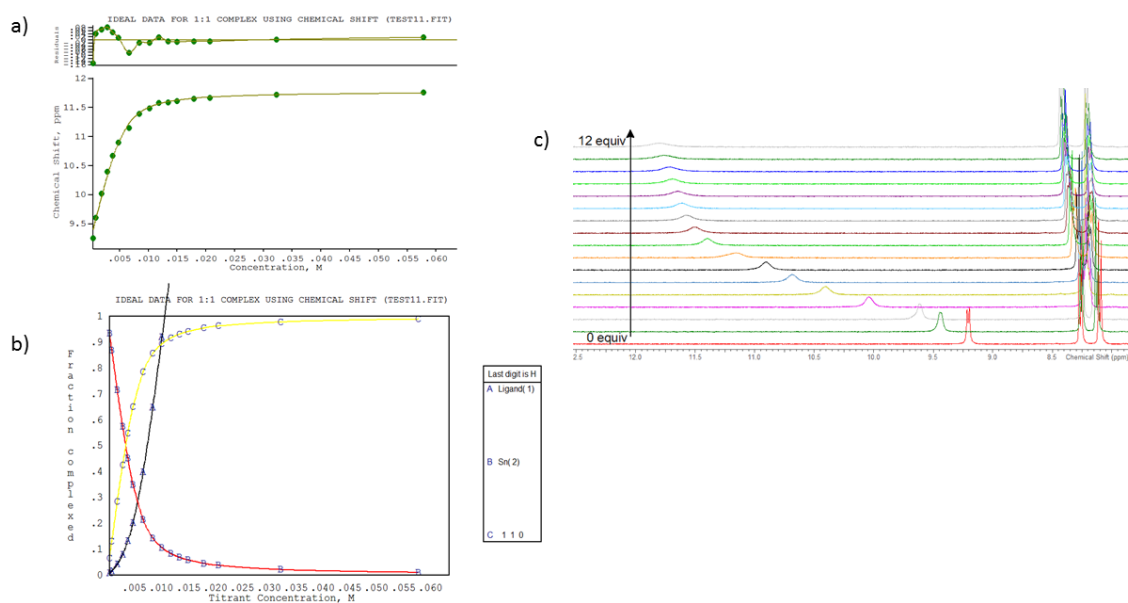


Figure S7.2.6- a) Titration curve of receptor 2 with tetrabutylammonium dihydrogen phosphate in 59.75% MeCN- d_3 /39.75% DMSO- d_6 /0.5% H₂O at 298K. b) Species concentration plot of receptor 2 with tetrabutylammonium dihydrogen phosphate in 59.75% MeCN- d_3 /39.75% DMSO- d_6 /0.5% H₂O at 298K. A-Guest concentration, B-Uncomplexed host concentration, C- Complex concentration. c) Stack plot of NMR spectra.

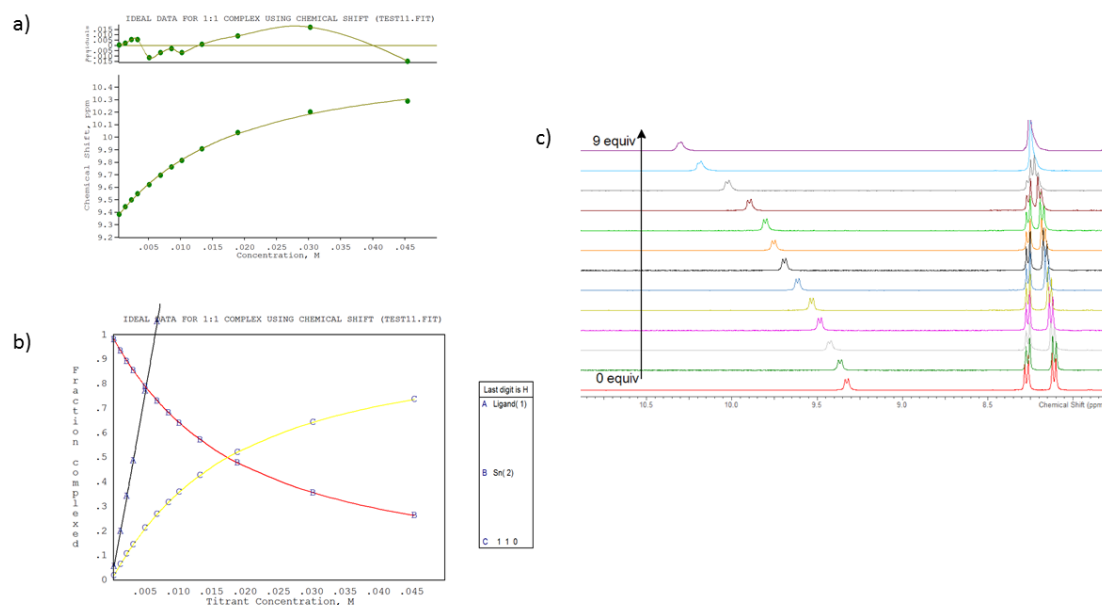


Figure S7.2.7- a) Titration curve of receptor 3 with tetrabutylammonium chloride in 59.75% MeCN- d_3 /39.75% DMSO- d_6 /0.5% H₂O at 298K. b) Species concentration plot of receptor 3 with tetrabutylammonium chloride in 59.75% MeCN- d_3 /39.75% DMSO- d_6 /0.5% H₂O at 298K. A-Guest concentration, B-Uncomplexed host concentration, C- Complex concentration. c) Stack plot of NMR spectra.

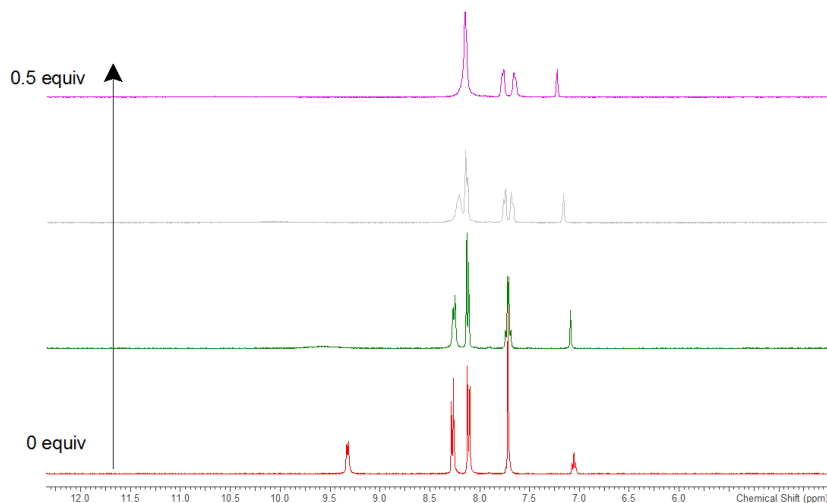


Figure S7.2.8- Stack plot of NMR spectra of receptor 3 titrated with tetraethylammonium bicarbonate in 59.75% MeCN- d_3 /39.75% DMSO- d_6 /0.5% H₂O at 298K. No titration curve plotted, data could not be fitted using winEQNMR2 due to disappearance of the NH peak.

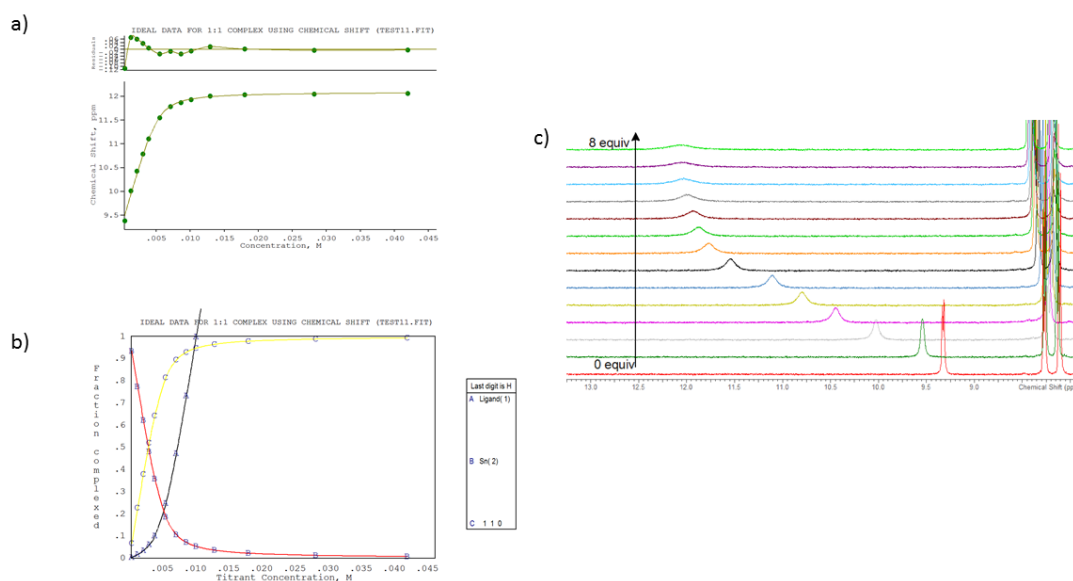


Figure S7.2.9- a) Titration curve of receptor 3 with tetrabutylammonium dihydrogen phosphate in 59.75% MeCN- d_3 / 39.75% DMSO- d_6 /0.5% H₂O at 298K. b) Species concentration plot of receptor 3 with tetrabutylammonium dihydrogen phosphate in 59.75% MeCN- d_3 / 39.75% DMSO- d_6 /0.5% H₂O at 298K. A-Guest concentration, B-Uncomplexed host concentration, C- Complex concentration. c) Stack plot of NMR spectra.

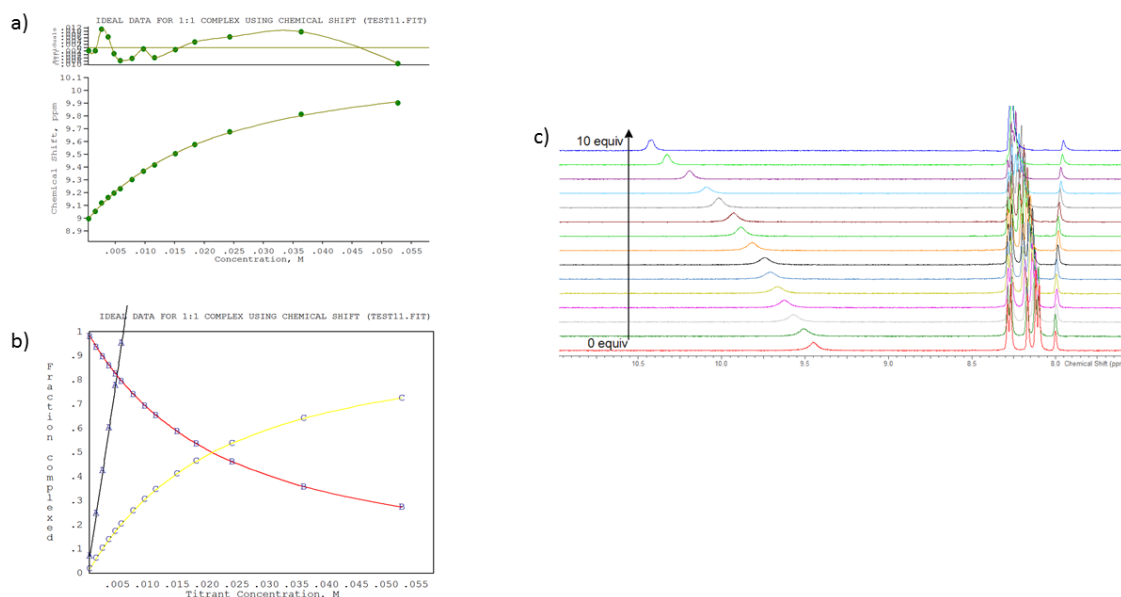


Figure S7.2.10- a) Titration curve of receptor 4 with tetrabutylammonium chloride in 59.75% MeCN- d_3 / 39.75% DMSO- d_6 /0.5% H₂O at 298K. b) Species concentration plot of receptor 4 with tetrabutylammonium chloride in 59.75% MeCN- d_3 / 39.75% DMSO- d_6 /0.5% H₂O at 298K. A-Guest concentration, B-Uncomplexed host concentration, C- Complex concentration. c) Stack plot of NMR spectra.

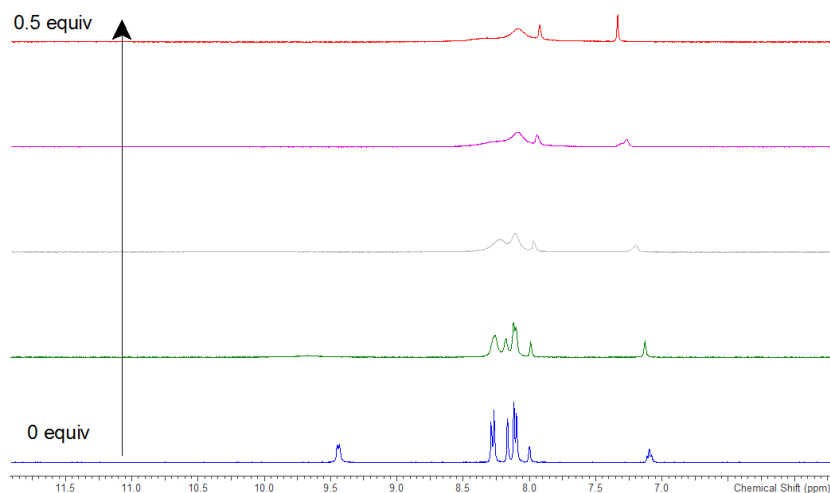


Figure S7.2.11- a) Stack plot of NMR spectra of receptor 4 titrated with tetraethylammonium bicarbonate in 59.75% MeCN- d_3 / 39.75% DMSO- d_6 /0.5% H₂O at 298K. No titration curve plotted, data could not be fitted using winEQNMR2 due to disappearance of the NH peak.

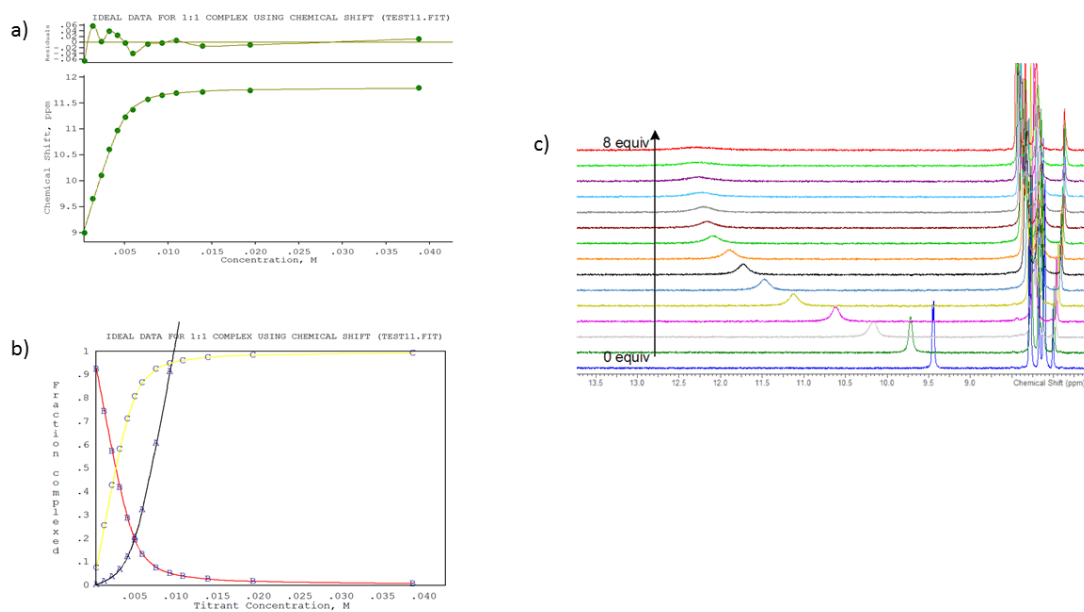


Figure S7.2.12- a) Titration curve of receptor 4 with tetrabutylammonium dihydrogen phosphate in 59.75% MeCN- d_3 / 39.75% DMSO- d_6 /0.5% H₂O at 298K. b) Species concentration plot of receptor 4 with tetrabutylammonium dihydrogen phosphate in 59.75% MeCN- d_3 / 39.75% DMSO- d_6 /0.5% H₂O at 298K. A-Guest concentration, B-Uncomplexed host concentration, C- Complex concentration. c) Stack plot of NMR spectra.

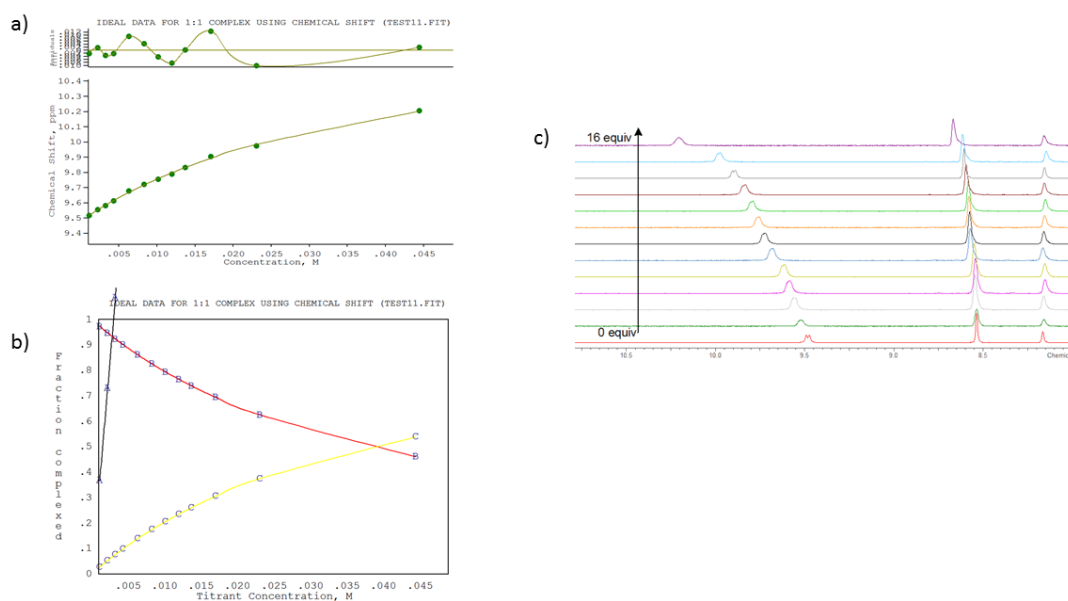


Figure S7.2.13- a) Titration curve of receptor 5 with tetrabutylammonium chloride in 59.75% MeCN- d_3 /39.75% DMSO- d_6 /0.5% H₂O at 298K. b) Species concentration plot of receptor 5 with tetrabutylammonium chloride in 59.75% MeCN- d_3 /39.75% DMSO- d_6 /0.5% H₂O at 298K. A-Guest concentration, B-Uncomplexed host concentration, C- Complex concentration. c) Stack plot of NMR spectra.

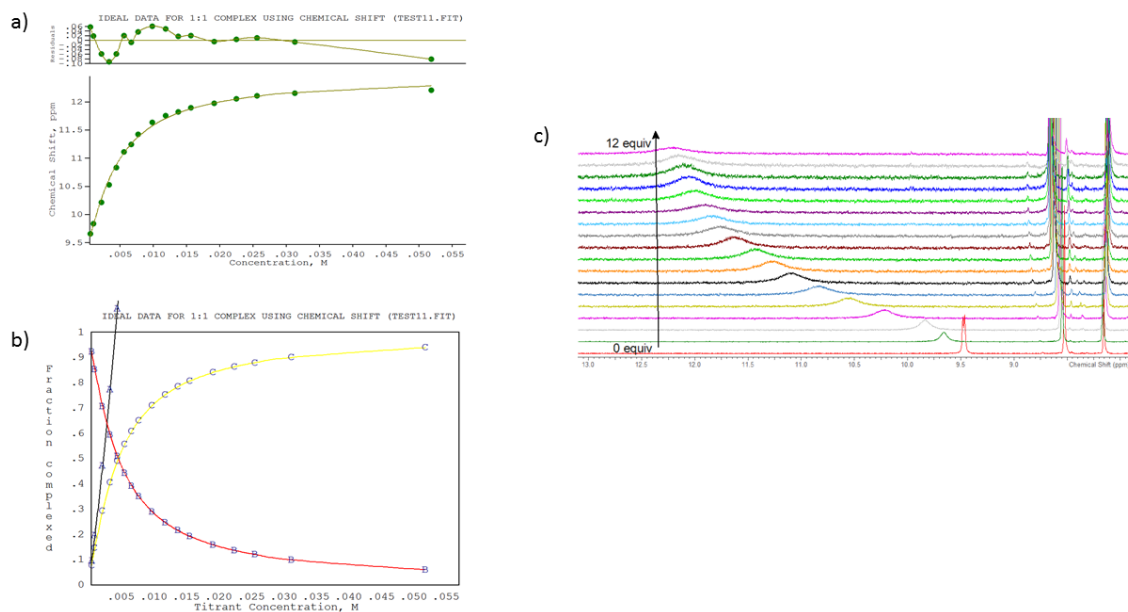


Figure S7.2.14- a) Titration curve of receptor 5 with tetraethylammonium bicarbonate in 59.75% MeCN- d_3 /39.75% DMSO- d_6 /0.5% H₂O at 298K. b) Species concentration plot of receptor 5 with tetraethylammonium bicarbonate in 59.75% MeCN- d_3 /39.75% DMSO- d_6 /0.5% H₂O at 298K. A-Guest concentration, B-Uncomplexed host concentration, C- Complex concentration. c) Stack plot of NMR spectra.

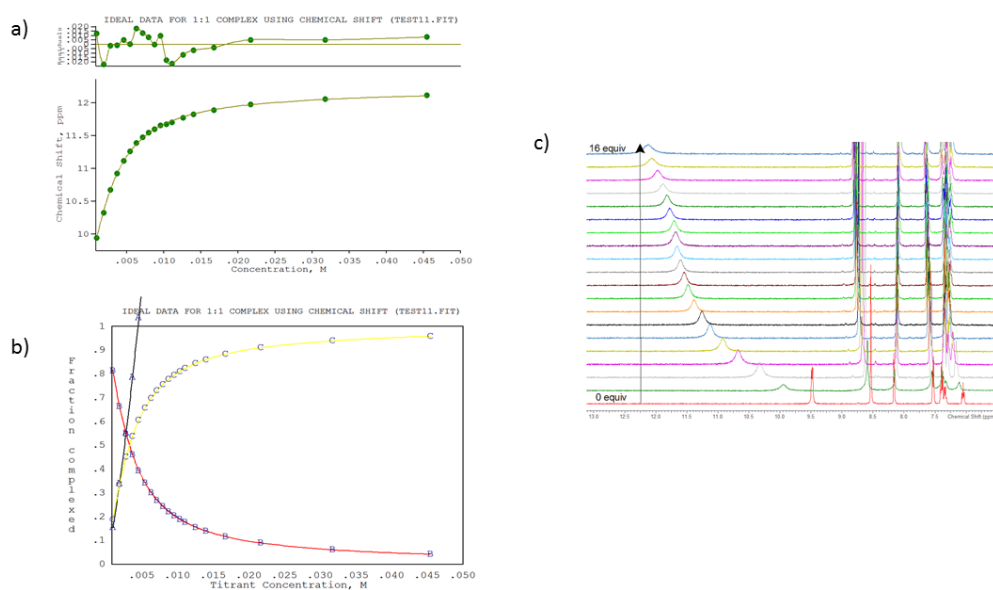


Figure S7.2.15- a) Titration curve of receptor 5 with tetrabutylammonium dihydrogen phosphate in 59.75% MeCN- d_3 /39.75% DMSO- d_6 /0.5% H $_2$ O at 298K. b) Species concentration plot of receptor 5 with tetrabutylammonium dihydrogen phosphate 59.75% MeCN- d_3 /39.75% DMSO- d_6 /0.5% H $_2$ O at 298K. A-Guest concentration, B-Uncomplexed host concentration, C- Complex concentration. c) Stack plot of NMR spectra.

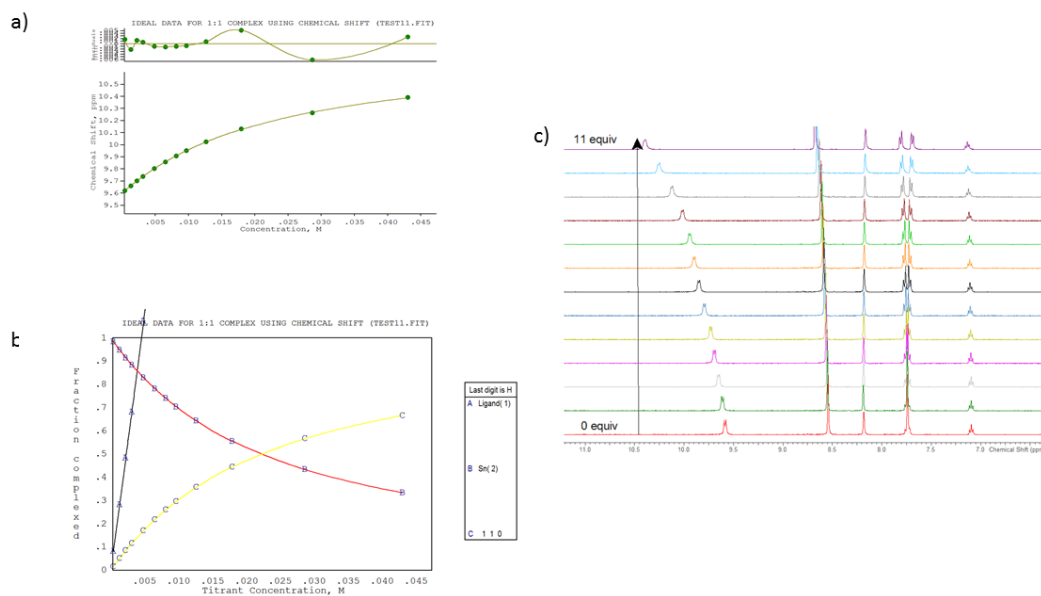


Figure S7.2.16- a) Titration curve of receptor 6 with tetrabutylammonium chloride in 59.75% MeCN- d_3 /39.75% DMSO- d_6 /0.5% H $_2$ O at 298K. b) Species concentration plot of receptor 6 with tetrabutylammonium chloride in 59.75% MeCN- d_3 /39.75% DMSO- d_6 /0.5% H $_2$ O at 298K. A-Guest concentration, B-Uncomplexed host concentration, C- Complex concentration. c) Stack plot of NMR spectra.

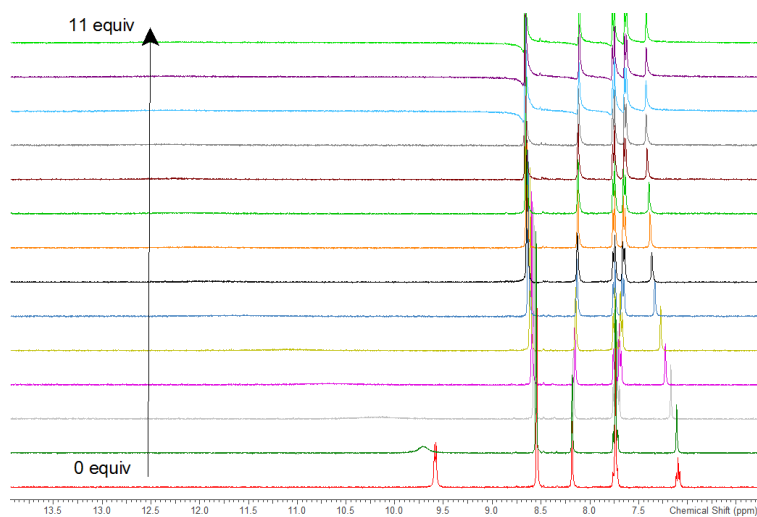


Figure S7.2.17- Stack plot of NMR spectra of receptor 6 titrated with tetraethylammonium bicarbonate in 59.75% MeCN- d_3 / 39.75% DMSO- d_6 /0.5% H₂O at 298K. No titration curve plotted, data could not be fitted using winEQNMR2 due to disappearance of the NH peak.

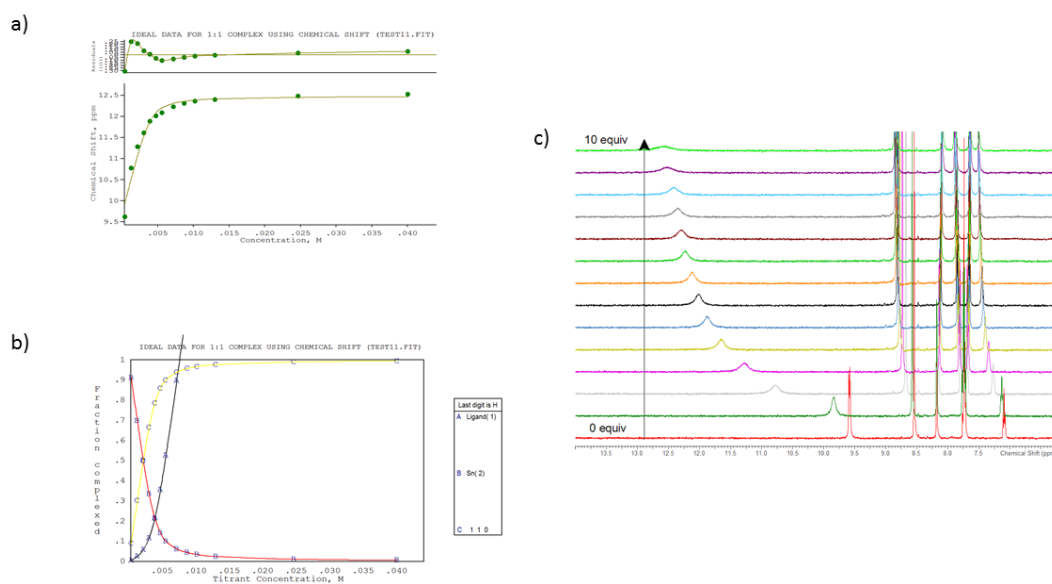


Figure S7.2.18- a) Titration curve of receptor 6 with tetrabutylammonium dihydrogen phosphate in 59.75% MeCN- d_3 / 39.75% DMSO- d_6 /0.5% H₂O at 298K. b) Species concentration plot of receptor 6 with tetrabutylammonium dihydrogen phosphate in 59.75% MeCN- d_3 / 39.75% DMSO- d_6 /0.5% H₂O at 298K. A-Guest concentration, B-Uncomplexed host concentration, C- Complex concentration. c) Stack plot of NMR spectra.

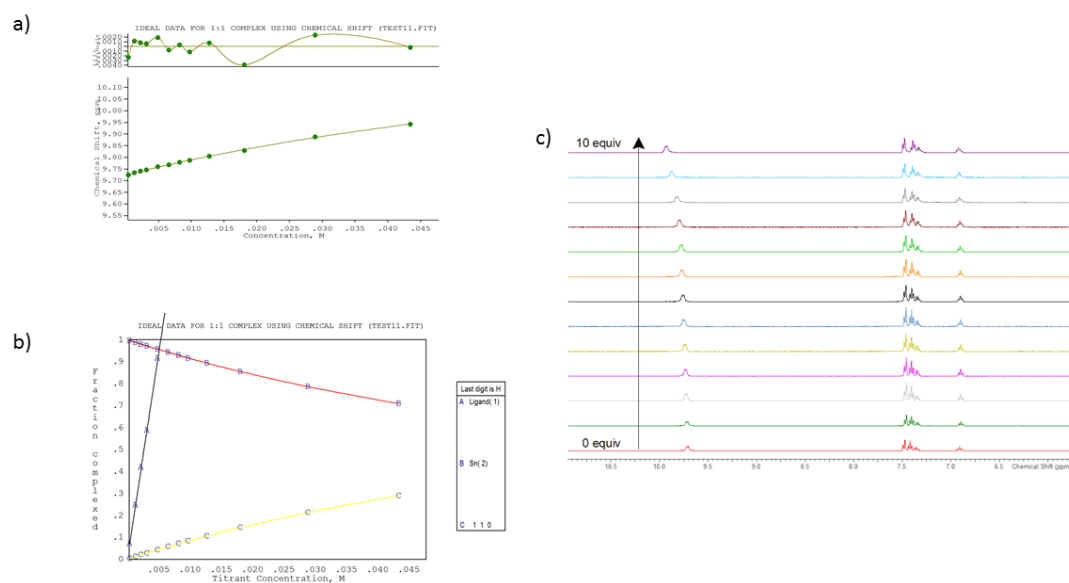


Figure S7.2.19- a) Titration curve of receptor 7 with tetrabutylammonium chloride 59.75% MeCN- d_3 /39.75% DMSO- d_6 /0.5% H₂O at 298K. b) Species concentration plot of receptor 7 with tetrabutylammonium chloride in 59.75% MeCN- d_3 /39.75% DMSO- d_6 /0.5% H₂O at 298K. A-Guest concentration, B-Uncomplexed host concentration, C- Complex concentration. c) Stack plot of NMR spectra.

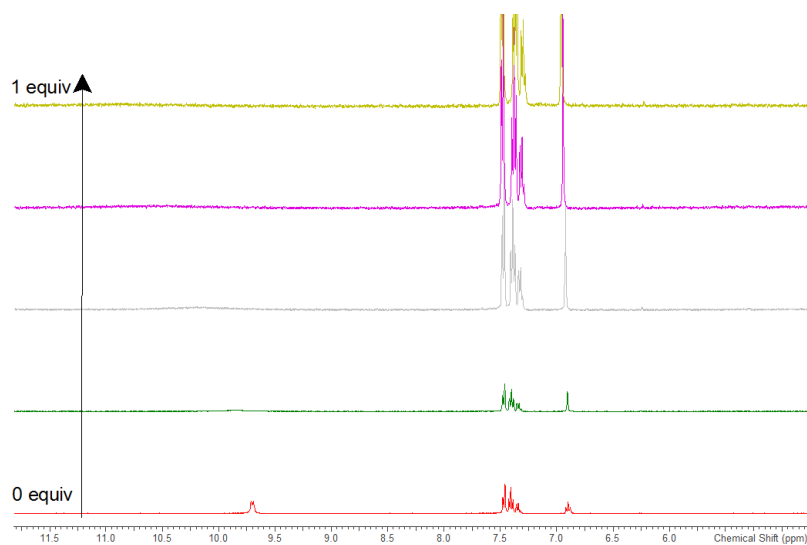


Figure S7.2.20- Stack plot of NMR spectra of receptor 7 titrated with tetraethylammonium bicarbonate in 59.75% MeCN- d_3 /39.75% DMSO- d_6 /0.5% H₂O at 298K. No titration curve plotted, data could not be fitted using winEQNMR2 due to disappearance of the NH peak.

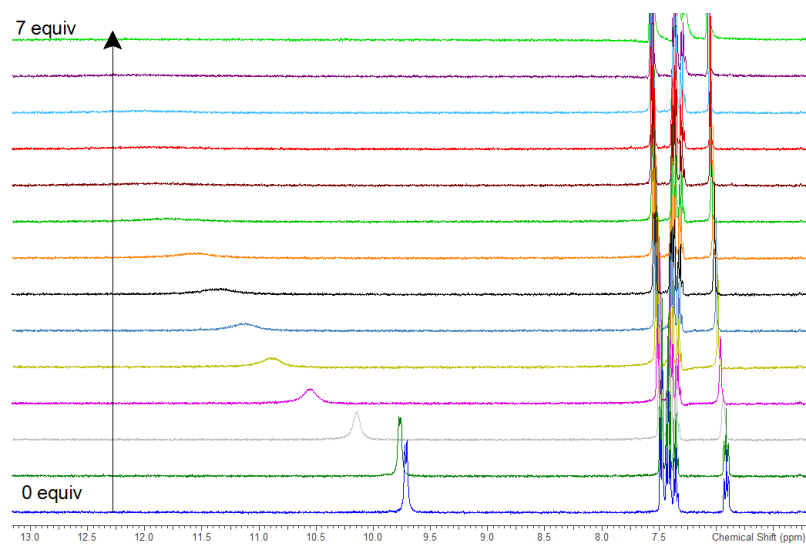


Figure S7.2.21- a) Stack plot of NMR spectra of receptor 7 titrated with tetrabutylammonium dihydrogen phosphate in 59.75% MeCN- d_3 / 39.75% DMSO- d_6 /0.5% H₂O at 298K. No titration curve plotted, data could not be fitted using winEQNMR2 due to disappearance of the NH peak.

8.0 NMR dilution studies

A series of ^1H NMR spectra were acquired at a range of concentrations 1–100 mM in $\text{DMSO-}d_6$ for each receptor. Small changes in chemical shift were observed to for specific proton signals most notably the NH signal and the middle proton between the two amide groups, this supported the indication of the formation of hydrogen bonds between the amide motif on adjacent molecules.

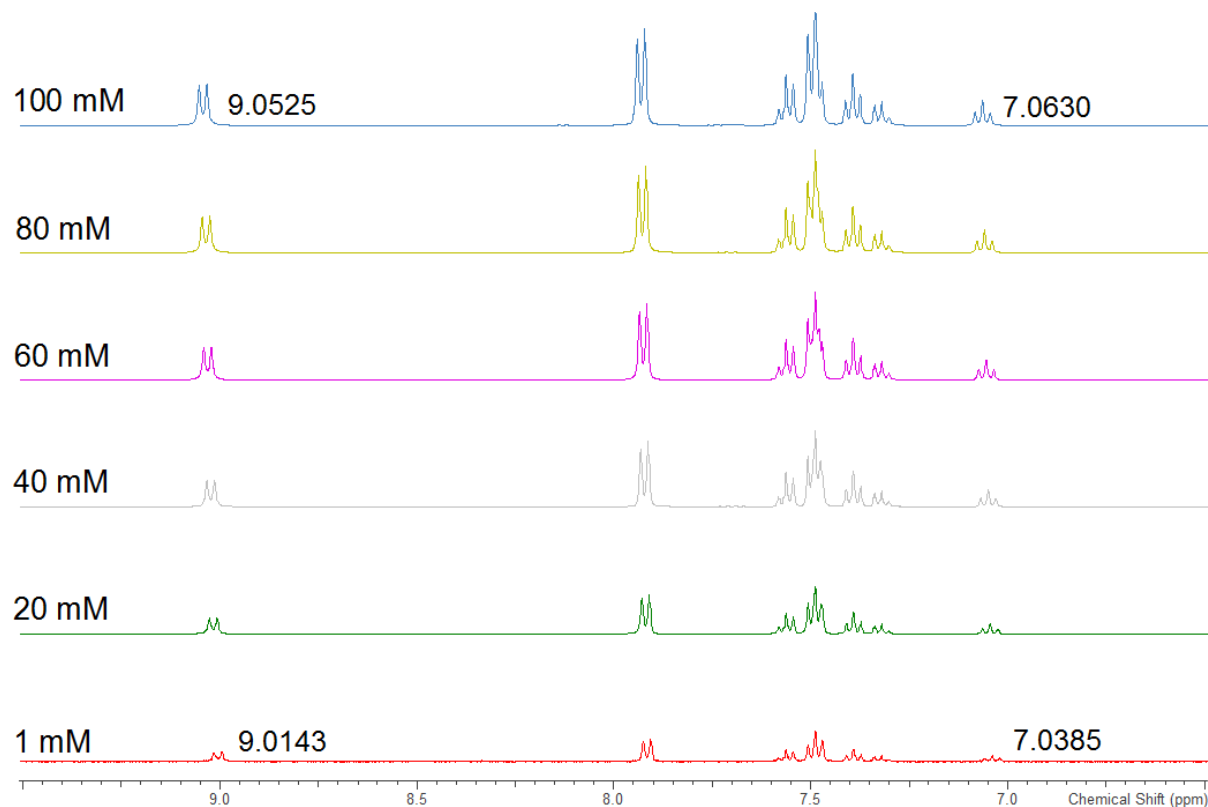


Figure S8.1- NMR dilution stack plot for receptor **1**.

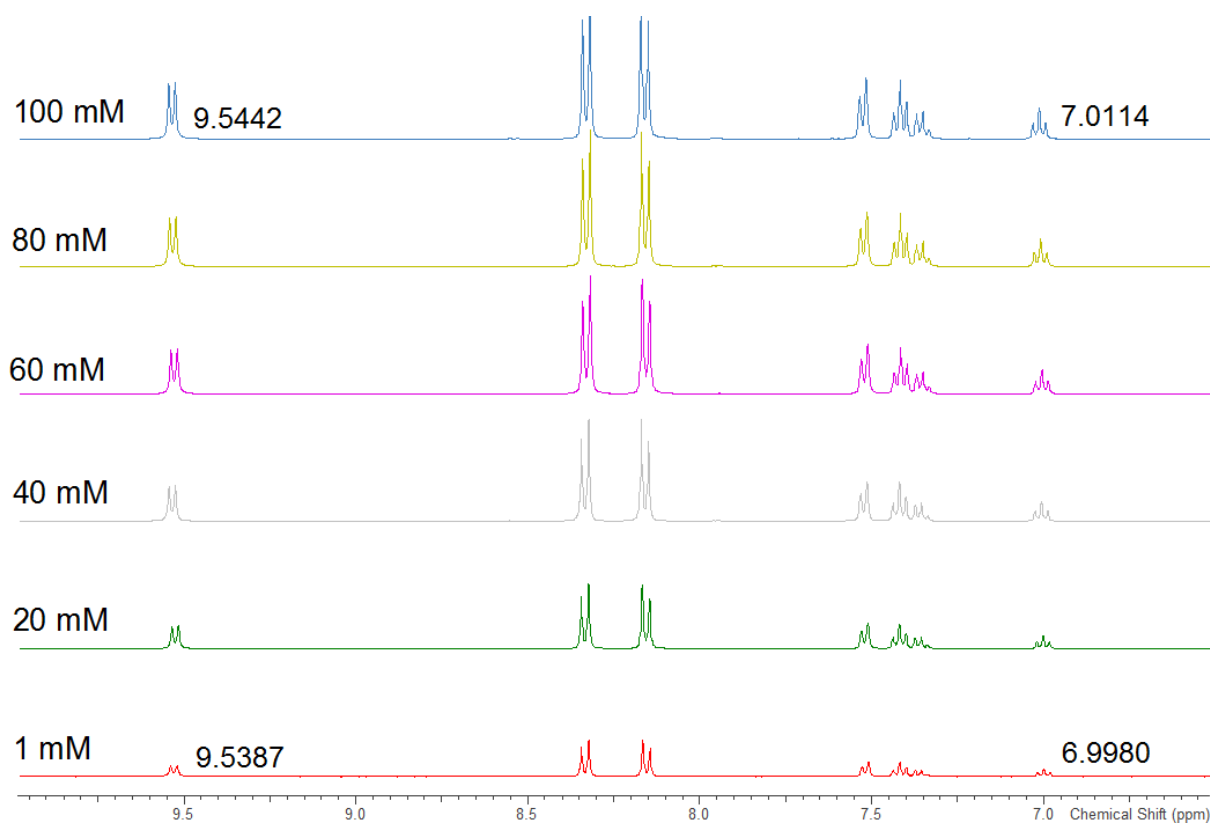


Figure S8.2- NMR dilution stack plot for receptor **2**.

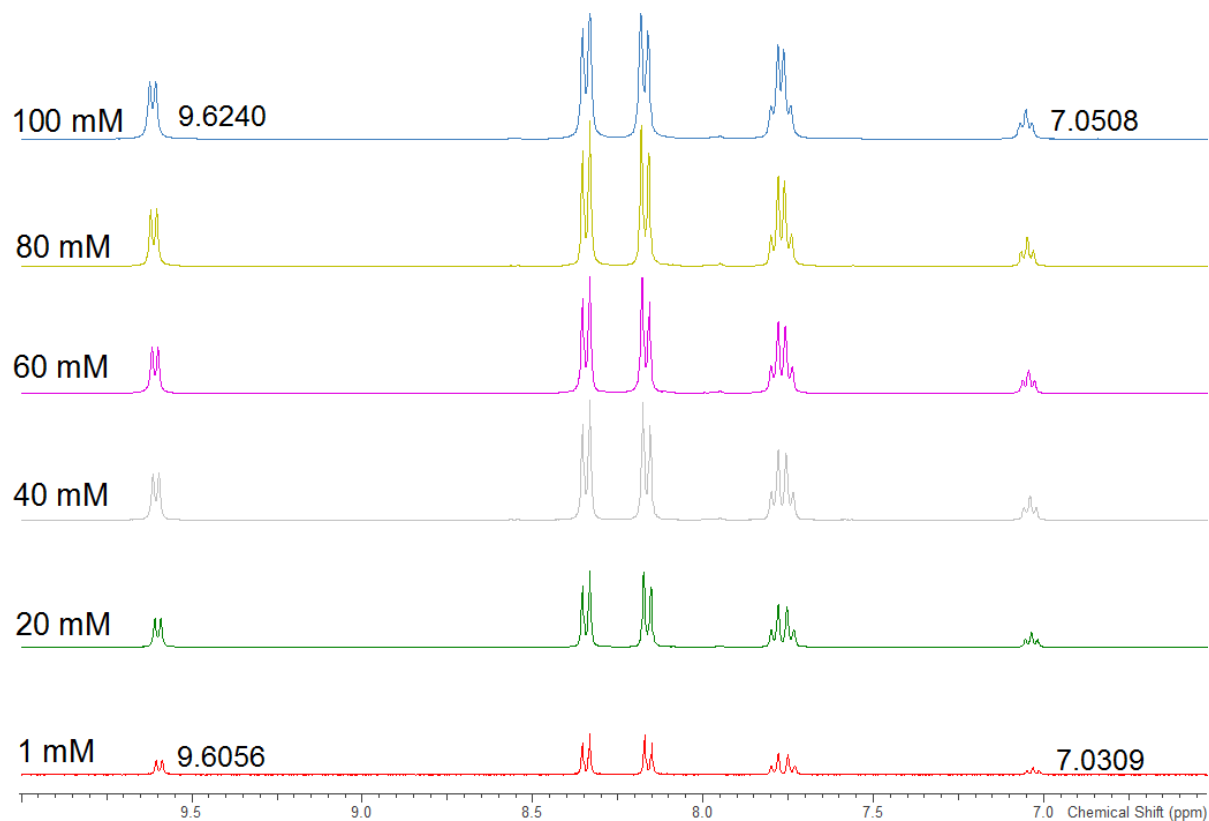


Figure S8.3- NMR dilution stack plot for receptor **3**.

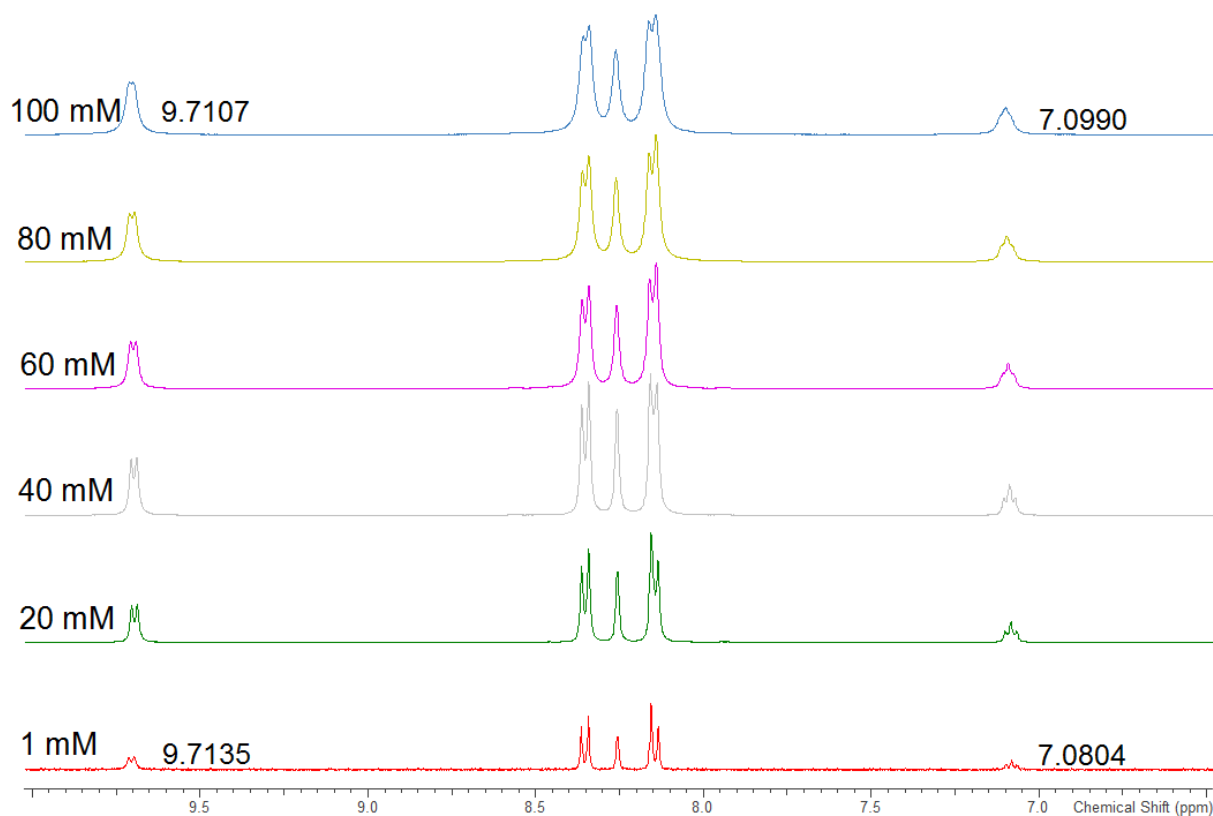


Figure S8.4- NMR dilution stack plot for receptor 4.

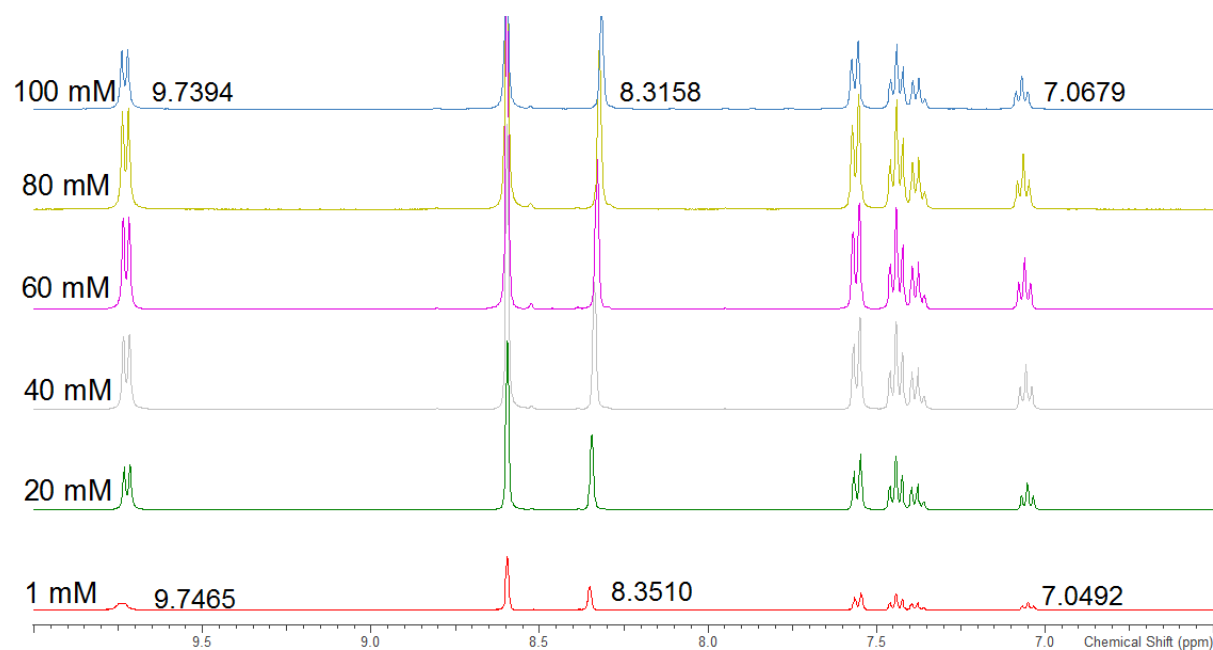


Figure S8.5- NMR dilution stack plot for receptor 5.

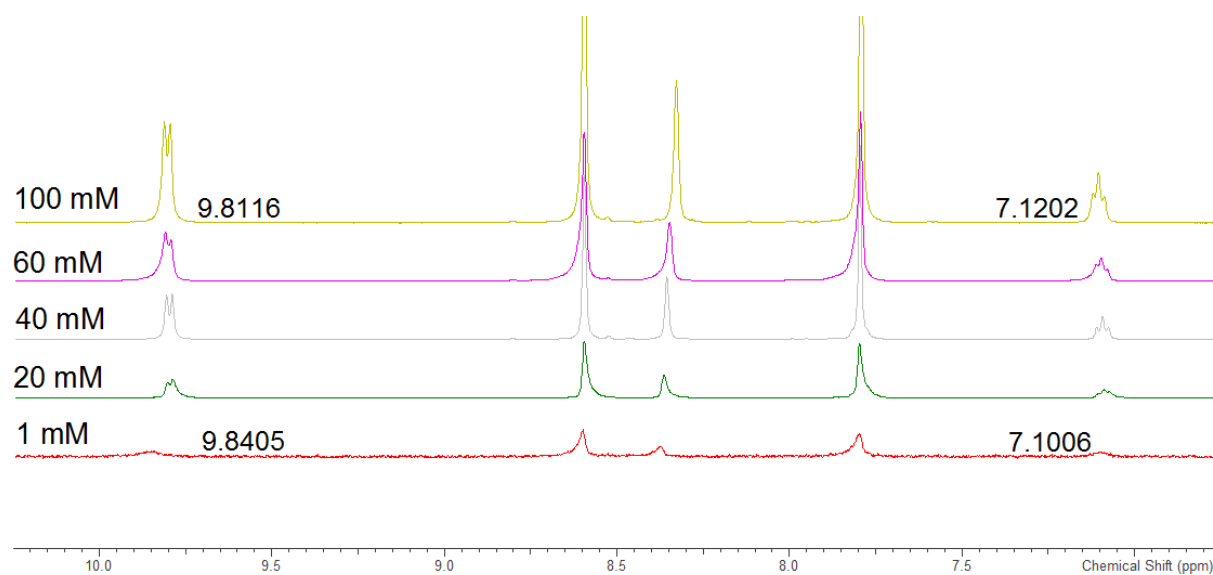


Figure S8.6- NMR dilution stack plot for receptor **6**, limited by amount of receptor.

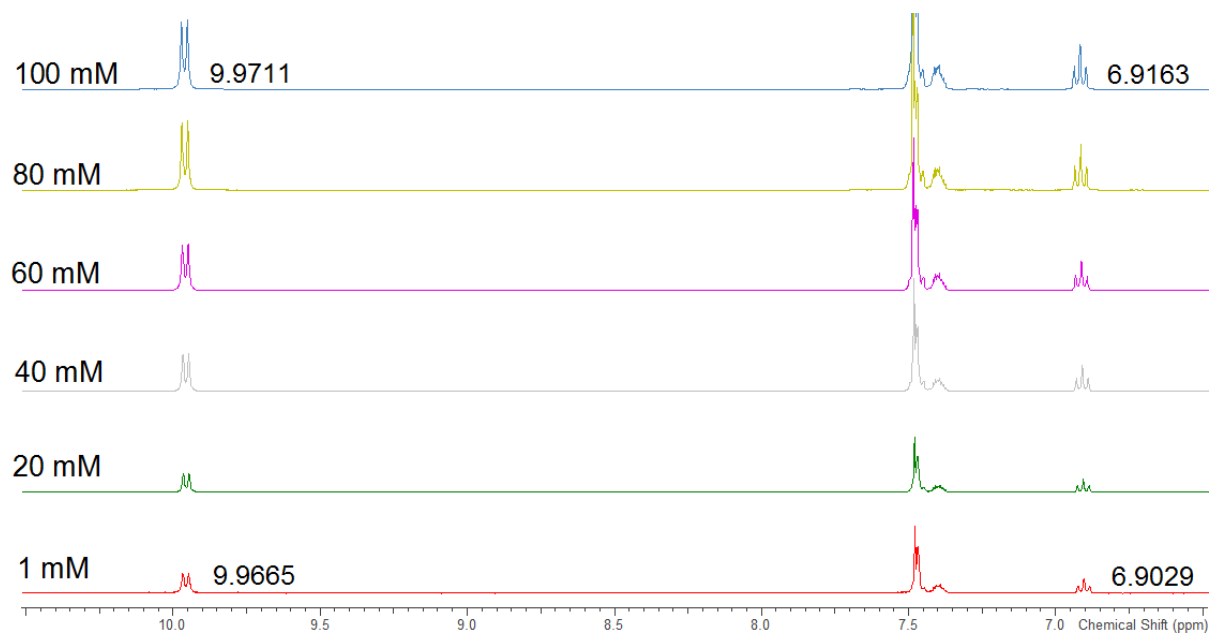


Figure S8.7- NMR dilution stack plot for receptor **7**.

9.0 References

- (1) Coles, S. J.; Gale, P. A. *Chem. Sci.* **2012**, 3, 683–689.
- (2) Yang, P.; Myint, K.; Tong, Q.; Feng, R.; Cao, H.; Gao, Y.; Gertsch, J.; Teramachi, J.; Kurihara, N.; Roodman, G. D. *J. Med. Chem.* **2012**, 55, 9973–9987.
- (3) Koulov, A. V.; Lambert, T. N.; Shukla, R.; Jain, M.; Boon, J. M.; Smith, B. D.; Li, H.; Sheppard, D. N.; Joos, J.-B.; Clare, J. P.; Davis, A. P. *Angew. Chem. Int. Ed. Engl.* **2003**, 42, 4931–4933.
- (4) Smith, B. D.; Lambert, T. N. *Chem. Commun. (Camb)*. **2003**, 2261–2268.
- (5) Macdonald, R. C.; Macdonald, R. I.; Menco, B. P. M.; Takeshita, K.; Subbarao, N. K.; Hu, L. *Biochim. Biophys. Acta*. **1991**, 1061, 297–303.
- (6) Hill, A. V. *Biochem. J.* **1913**, 7, 471–480.
- (7) Hynes, M. J. *J. Chem. Soc. Dalt. Trans.* **1993**, 311–312.